BILINGUAL PUBLISHING CO.
Pioneer of Global Academics Since 1984

Journal of Marine Science

Volume 3 | Issue 3 | July 2021 | ISSN 2661-3239(Online)

Volume 3 Issue 3 • July 2021 • ISSN 2661-3239 (Online)

Journal of Marine Science

BILINGUAL PUBLISHING CO.
Pioneer of Global Academics Since 1984

BILINGUAL PUBLISHING CO.
Pioneer of Global Academics Since 1984

Volume 3 | Issue 3 | July 2021 | Page1-49
Journal of Marine Science

Contents

Editorial

Articles

Review

BILINGUAL PUBLISHING CO.
Pioneer of Global Academics Since 1984

Journal of Marine Science
https://ojs.bilpublishing.com/index.php/jms

ARTICLE

Biofilm Formation by Marine *Cobetia marina* alex and *Pseudoalteromonas* spp: Development and Detection of Quorum Sensing N-Acyl Homoserine Lactones (AHLs) Molecules

Samia S. Abouelkheir[1*] Eman A. Abdelghany[2] Soraya A. Sabry[2] Hanan A. Ghozlan[2]

1. National Institute of Oceanography and Fisheries (NIOF), Marine Environment Division, Marine Microbiology Laboratory, Egypt
2. Botany and Microbiology Department, Faculty of Science, Alexandria University, Alexandria, 21321, Egypt

ARTICLE INFO

Article history
Received: 24 June 2021
Accepted: 9 July 2021
Published Online: 20 July 2021

Keywords:
Quorum sensing
Biofilm
Pseudoalteromonas prydzensis alex
Pseudoalteromonas sp. alex
Cobetia marina alex
Extracellular polymeric substance (EPS)

ABSTRACT

Surfaces submerged in seawater are colonized by various microorganisms, resulting in the formation of heterogenic marine biofilms. This work aims to evaluate the biofilm formation by *Cobetia marina* alex and doing a comparative study between this promising strain with the two bacterial strains isolated previously from the Mediterranean seawater, Alexandria, Egypt. Three strains; *Cobetia marina* alex, *Pseudoalteromonas* sp. alex, and *Pseudoalteromonas prydzensis* alex were screened for biofilm formation using the crystal violet (CV) quantification method in a single culture. The values of biofilm formed were OD_{600}= 3.0, 2.7, and 2.6, respectively leading to their selection for further evaluation. However, factors affecting biofilm formation by *C. marina* alex were investigated. Biofilm formation was evaluated in single and multispecies consortia. Synergistic and antagonistic interactions proved in this work lead to the belief that these bacteria have the capability to produce some interesting signal molecules N-acyl Homoserine Lactones (AHLs).

1. Introduction

In marine environments, bacteria play roles that include driving biogeochemical cycles [1] and supplying materials and energy to higher trophic levels [2]. Although genotypic evolution may contribute a significant selective advantage to environmental stimuli, phenotypic plasticity allows bacteria to grow and thrive under fluctuating, challenging conditions [3]. In addition, bacterial biofilm forms a highly structured community of cells that are attached to each other and/or on a surface through the production of an extracellular polymeric substance (EPS) matrix that enable bacteria to colonize different habitats [4,5]. Biofilms have several terms, including periphytons and Microphytobenthos [6].

The cell-to-cell communication process between bacteria, generally known as quorum sensing (QS), controls several vital features of biofilm development between other phenomena [7]. The bacterial cell envelope plays a crucial role in the intercellular signalling as well as communication between neighbouring cells in small microcolonies that help in decision-making processes. Part

**Corresponding Author:*
Samia S. Abouelkheir,
National Institute of Oceanography and Fisheries (NIOF), Marine Environment Division, Marine Microbiology Laboratory, Egypt;
Email: ss.elkheir@niof.sci.eg

 DOI: https://doi.org/10.30564/jms.v3i3.3397

of this communication occurs through quorum sensing (QS), a phenomenon that involves cell density-dependent control of gene expression. For QS to be possible, a minimum number of bacteria must be aggregated within a specific volume sensed by increasing the concentration of autoinducers [8].

Cobetia marina is a Gram-negative, aerobic, slightly halophilic, rod-shaped bacterium extensively used as a model in marine biofouling research and as multi-species biofilm formation in natural seawater [9]. It is distinct from the genus *Halomonas* and is one of eleven genera of the family Halomonadaceae [10]. Historically, *Cobetia marina* was first described as *Arthrobacter marinus* by Cobet et al. (1970) [11], but was later identified as *Pseudomonas marina* [12]. Almost 10 years later, it was reclassified once again within the genus *Deleya* [13] and then transferred to the genus *Halomonas* [14]. Delineation of the species in this genus was performed based on 16S and 23S rRNA sequence similarities and additional phenotypic evidence that supported the inclusion of *Halomonas marina* in the novel genus *Cobetia* as *Cobetia marina* [15,16]. On the other hand, *Pseudoalteromonas* is a genus of Gammaproteobacteria present in various marine habitats that is widespread in the world's ocean [17]. Many strains of this genus are surface colonizers on marine eukaryotes and produce a wide range of pigments and bioactive compounds that inhibit settling of several fouling invertebrates and algae during biofilm formation [18].

Therefore, it was thus aimed in this study to explore and identify biofilm-forming bacteria attached to rock surfaces in seawater. It was also aimed to evaluate whether synergistic or competitive interactions occur during multispecies biofilm formation. Moreover, some factors affecting biofilm formation by *C. marina* alex were studied.

2. Materials & Methods

2.1 Media

Seawater (SW), Modified Väätänen Nine Salts Solution (VNSS), Luria Bertani medium (LB) and Synthetic medium (SM) used to evaluate the biofilm formation and to explore the role of nutritional status were prepared as previously described by Abouelkheir et al. (2020) [19]. YMG Medium [20] used for screening for EPS production contained in g/L: glucose, 10; yeast extract, 3; malt extract, 3; peptone, 5. All components were dissolved in 500 ml distilled water and 500 ml aged seawater (ASW), pH adjusted to 7.0.

2.2 Identification of Bacterial Isolate

Isolate ER7 was selected for phylogenetic analysis using 16SrRNA in addition to phenotypic characterization.

2.3 Bacterial Strains

Cobetia marina alex used in this study was isolated from rock surface submerged in Mediterranean seawater, Alexandria, Egypt and identified by 16SrRNA. *Pseudoalteromonas prydzensis* alex with accession number JF965506 and *Pseudoalteromonas* sp. JN592714 were isolated and identified in a previous work [19]. *Agrobacterium tumefaciens* was secured from the faculty of Agriculture, Alexandria University. *Escherichia coli*, *Pseudomonas sp.*, *Staphylococcus sp.*, *Bacillus* sp., *Vibrio* sp. N1, *Vibrio* sp. N2, *Streptococcus* sp., and *Candida albicans* were obtained from Department of Botany and Microbiology, Faculty of Science, Alexandria University and National Institute of Oceanography and Fisheries, Alexandria branch.

2.4 Biofilm Development and Assessment in Glass Tubes

Biofilm formation technique was adopted after Hassan et al. (2011) [21] and quantification of biofilm was performed using the method described by Haney et al., (2018) [22] based on staining the biofilm with crystal violet (Figure 1).

2.5 Factors Affecting Biofilm Formation by *C. marina* alex

Effect of pH on biofilm formation was examined by adjusting portions of SW medium to different pHs from 5 to 7. Simultaneously, biofilm formation was evaluated at different temperatures (20, 30, and 37 °C). The role of NaCl concentration on biofilm formation was examined by supplementing the SW medium with different concentrations (5, 10, 15, 20 and 25%). Carbon sources (glucose, lactose, galactose, maltose or sucrose) were separately added to SW medium at two different concentrations (0.25 and 0.5 g/L) to elucidate their effect on biofilm formation.

2.6 Progression of Biofilm Formation

The biofilm formed in test tubes was quantified at different time intervals from 1 to 4 days. Biofilm formation was also monitored microscopically by examining cell attachment to glass coverslips as described by Walker & Horswill (2012) [23].

2.7 EPS Production

The ability of bacterial strains to produce EPS was

DOI: https://doi.org/10.30564/jms.v3i3.3397

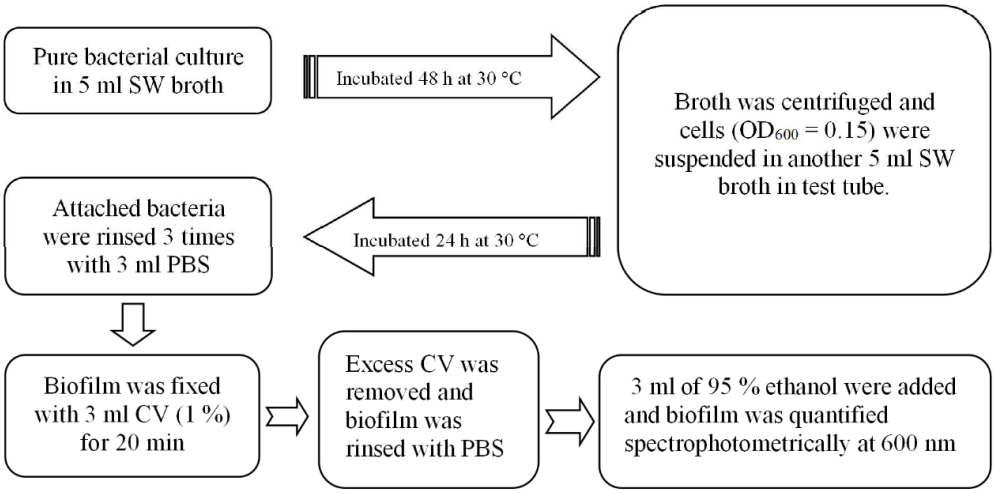

Figure 1. A schematic diagram shows the formation and quantification of biofilm using the test tube method

investigated by the method adopted by Casillo et al., (2018) [24]. Each bacterial strain was grown in 50 ml YMG broth and incubated at 25 ºC for 24 h. 200 µl were used to inoculate 50 ml of the same medium and incubated at 25ºC for 5 days at 120 rpm. Cells were removed by centrifugation at 10000x g for 20 min. Cold ethyl alcohol (3 ml) was added to cell free supernatant and left overnight at 10 °C. The precipitated EPS was air dried and weighed.

2.8 Bioassay for Acyl Homoserine Lactone (AHL) Production by Agar-plate

Agrobacterium tumefaciens was used as a reporter strain to screen for AHL- like signalling molecules [25]. Agar plate-based bioassay was carried out by streaking 50 µl of the reporter strain on the surface of LB medium supplemented with 50 µl X-Gal (5-Bromo-4-Chloro-3-Indolyl-D-Galactopyranoside) solution (Appli Chem. GmbH, Darmstadt, Germany) prepared by dissolving 20 mg of X-Gal in 1ml of 100 % dimethylformamide (DMF) and stored at -20 °C in the dark. 50 µl of each tested strain were spotted on top of the plates. Plates were checked after incubation at 28 °C for 48 h. The development of blue colour (catabolism of X-Gal) in the plates indicated the presence of AHL like substances.

2.9 Biofilm Formation by Multispecies Consortia

Species interaction was studied in single species using one bacterium, in dual combination of two strains or triple combination of the three strains (*Cobetia marina* alex, *Pseudoalteromonas prydzensis* alex, and *Pseudoalteromonas* sp. alex). This was performed by mixing equal inoculum of each organism and allowing the biofilm to be formed and quantified. Biofilm formation was also assessed in a consortia of *Cobetia marina* alex and one of several marine bacteria. These included 3 Gram +ve (*Staphylococcus* sp., *Streptococcus* sp., and *Bacillus* sp.) and 4 Gram-ve (*E. coli*, *Pseudomonas* sp., *Vibrio* sp. N1, and *Vibrio* sp. N2), as well as *Candida* sp. In mixed species consortia, equal cell densities were used. Biofilm was measured as previously described.

2.10 Data Analysis

All investigations were performed in triplicates. The results were statistically analyzed and accomplished by using Past3 software and Origin Pro 8.1. The data were expressed by means ± SE and ± SD. The significant values were determined at P-value < 0.05.

3. Results and Discussion

3.1 Biofilm Formation

Pseudoalteromonas sp. alex, *P. prydzensis* alex, and *Cobetia marina* alex (ER7) were screened for biofilm formation in single culture [26]. The values of biofilm formed in test tubes ranged from $OD6_{00}$ 0.5 to 3 which are in good agreement with those reported by other investigators in natural environments [27]. The highest value (OD_{600}= 3.0) was recorded for isolate ER7 leading to its selection for further evaluation.

3.2 Phylogenetic Analysis of ER7

The partial sequence of amplified 16SrRNA gene of isolate ER7 was aligned with closest relatives of sequences on NCBI database and showed 99% similarity to several sequences of *Cobetia marina* strains (Figure 2). *Cobetia marina* is a member of the family Halomonodaceae, Gammaproteobacteria together with eight other genera [28].

 DOI: https://doi.org/10.30564/jms.v3i3.3397

Its ecophysiological diversity was studied by Tang et al. (2018) [29]. The sequence was deposited in GenBank with accession number JF965505. It was thus designated as *Cobetia marina* alex. Members of Gammaproteobacteria are the most abundant group of readily cultivable heterotrophs in the marine environment [30].

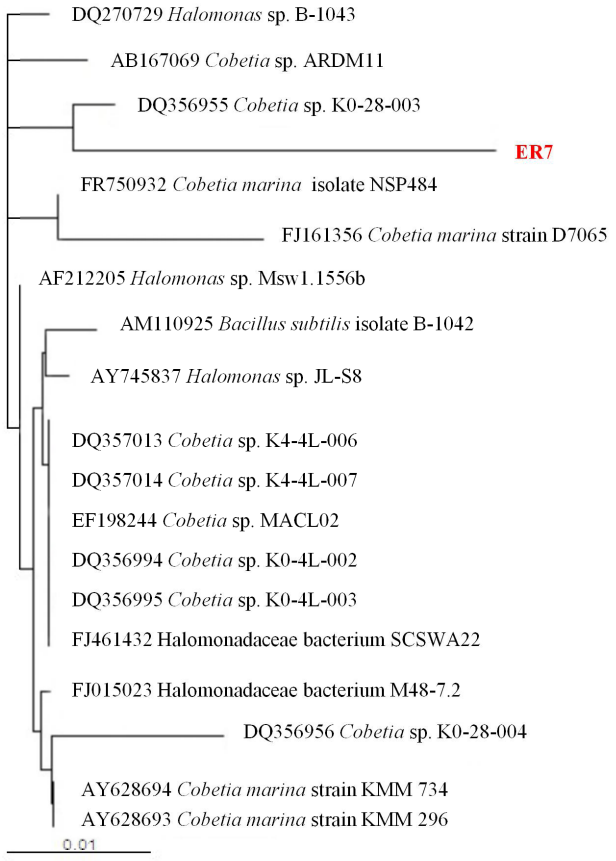

Figure 2. Phylogenetic tree of ER7, the dendrogram based on partial 16S rRNA gene sequencing shows the phylogenetic position of ER7 among representatives of related bacterial species

3.3 Phenotypic Characterization

The three bacterial strains formed off-white mucoid colonies on seawater agar plates. Cells were Gram negative, non sporulating short rods (arranged in pairs for *Cobetia marina*) and unable to grow in absence of seawater referring to their halophilic nature. All strains tolerated up to 10% NaCl in the medium. Only *C. marina* alex grew at 10 ºC indicating its psychrotolerant nature. All were catalase and oxidase positive except for *C. marina* alex (oxidase negative). Although strains of *Pseudoalteromonas* produced hydrolytic enzymes and degraded several substrates such as cellulose, carboxymethyl−cellulose (CMC), xylan, pectin, and soluble starch, *C. marina* alex did not show any degradative capability to the same substrates.

All strains showed variability to utilize different carbon sources and sensitivity to the tested antibiotics (Figure 3). In this context, the phenotypic features of *C. marina* alex isolated from the Mediterranean Sea, and Alexandria were compared to other *C. marina* strains isolated from other habitats. Strains used for comparison were *C. marina* LMG2217T (type strain) isolated from seawater, Atlantic Ocean, *C. marina* KMM296 isolated from Mussel (*Grenomytilus grayanus*), the Sea of Japan, Pacific Ocean and five strains isolated from brown alga (*Fucus evanescens*), the Sea of Okhotsk, Pacific Ocean. Data used for comparison were all taken from Ivanova et al. (2005) [31].

Data given in Figure 4 depict a number of phenotypic characteristics that distinguish the Mediterranean Sea strain from other *Cobetia* strains. Sodium ion was required for growth in all except for *C.* sp. KMM296. They all shared the property of reducing NO_3 and inability to produce lipase. Only *C. marina* alex could not grow in 20% NaCl, whereas LMG2217 and KMM734 grew at this level. Our strain shared the ability to grow at 10 °C together with KMM296. Maltose was used as a carbon source by *C. marina* alex only.

3.4 Factors Affecting Biofilm Formation by *C. marina* alex

3.4.1 Effect of pH and Temperature

The psychrotolerant, moderate halophilic bacterium was allowed to grow stagnant on portions of SW medium adjusted to different pHs from 5 to 10 and incubated under static conditions at 20, 30 and 37°C; biofilm was measured after 24h.

Figure 5a reveals that the biofilm values formed at neutral or slightly alkaline pH were comparable (OD ~ $_{600}$ 4.5) but a higher value (OD ~ $_{600}$ 7.6) was recorded at alkaline pH. Similar data were obtained with *Stenotrophomonas maltophilia* [32]. On the contrary, optimal biofilm formation by *Cobetia crustatorum* sp. nov was recorded at pH 5.0-6.0. However, it was observed that biofilm formation was sensitive to pH changes with *Streptococcus gordonii* and *S. meliloti* [33]. Taken together, these results suggest that pH effect in terms of establishing a biofilm, may differ from one bacterial species to another, thereby, enabling each bacterial species to efficiently colonize its preferred environment.

Moreover, Anderson (2016) [34] examined the effect of increasing temperatures on biofilms in coastal waters and reported that the increase in water temperature enhanced biofilms at the warmer station compared to the colder one.

DOI: https://doi.org/10.30564/jms.v3i3.3397

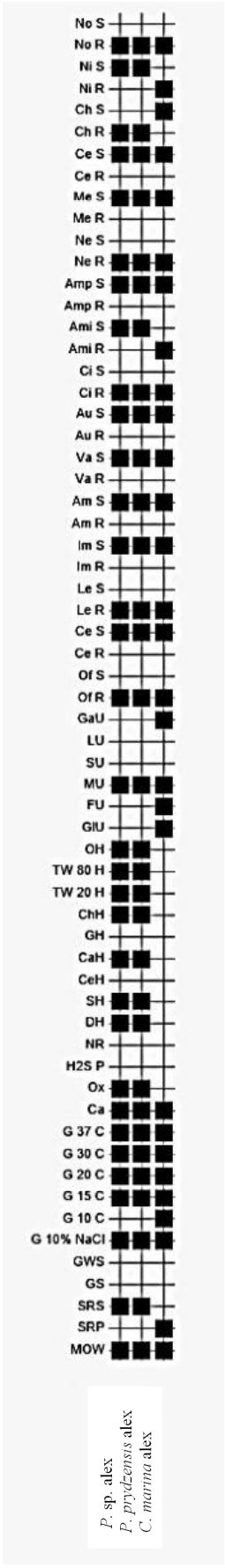

Figure 3. Differential characteristics of the three biofilm-forming bacterial strains used in this study, presence (■) and absence (|)
MOW: Off-white mucoid, SRP: Short rods arranged in pairs, GS: Cells were Gram-negative, GWS: Unable to grow in absence of seawater

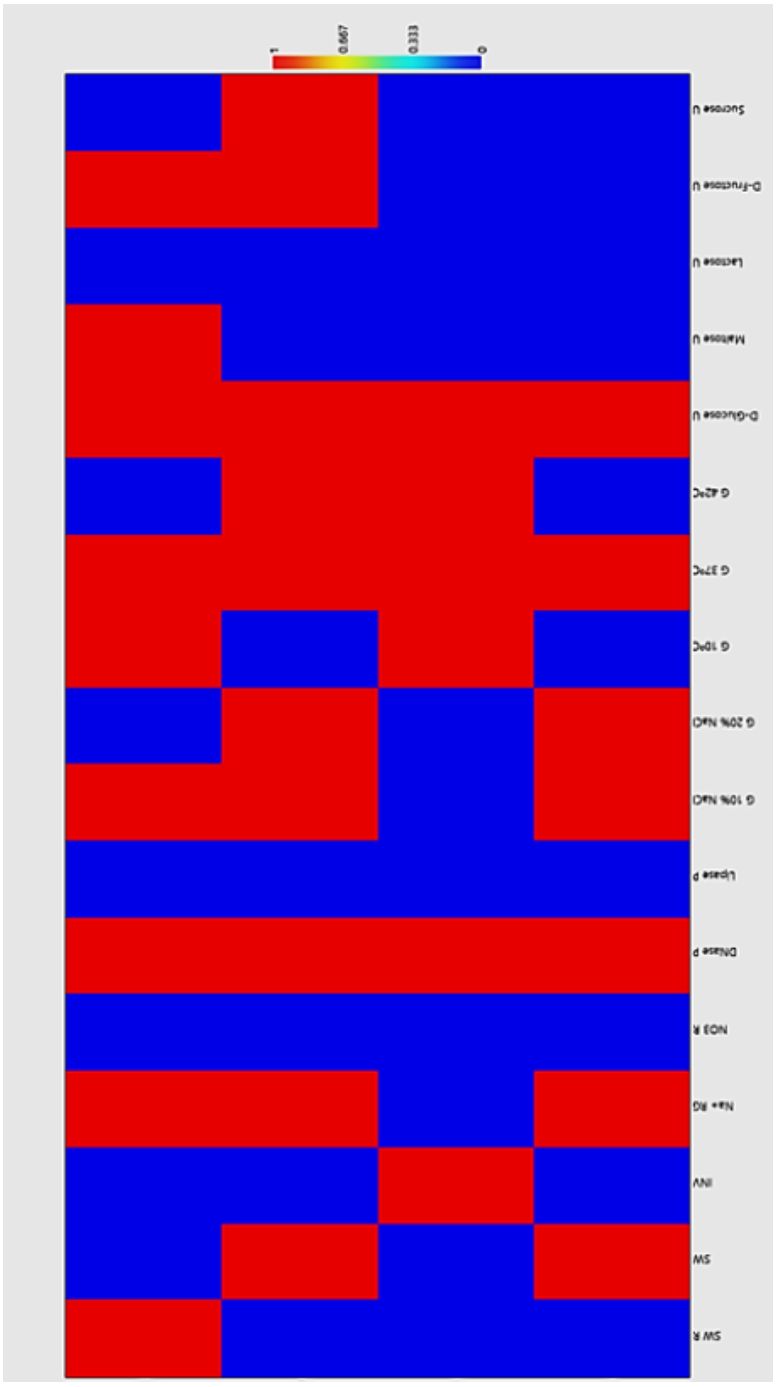

Figure 4. Plot matrix chart showing comparative phenotypic features (presence (red) and absence (blue)) of *C. marina* alex isolated in this study and other strains isolated from different ecological habitats [31]

In general, effective temperature is dependent on bacterial strain [35].

3.4.2 Effect of Osmolarity

The present investigation was undertaken to study the effect of adding different concentrations of NaCl to the culture medium on biofilm formation. Data provided in Figure 5b show that biofilm formation by *C. marina* alex was dramatically affected by osmolarity. The value was doubled upon the addition of 5 % NaCl in the medium compared to medium with seawater only. Moreover, supplementing the medium with 10% NaCl caused an almost 1.5 fold increase in biofilm value. Further increase in NaCl concentration was obviously deleterious to biofilm formation. Osmolarity was reported to clearly influence *P. flourescens* biofilm formation by Kimkes & Heinemann (2020) [36]. Similarly, Amaya-Gómez et al. (2015) [35] found that growth at high osmolarity inhibited biofilm formation. Biofilm formation by *Cobetia crustatorum* sp. nov was best in presence of 6.5 % (w/v) NaCl [10].

3.4.3 Effect of Carbon Source

Data given in Figure 5c show that among tested carbon sources, only maltose (0.25 g/L) enhanced biofilm formation with an increase of about 30 % compared to SW medium free from the carbon source. However, glucose addition did not significantly improve biofilm formation.

3.5 Single Species Biofilm Progression

Biofilm development was monitored in test tubes of a monoculture of *Cobetia marina* alex, *P. prydzensis* alex, and *P.* sp. alex. A similar pattern for biofilm development was observed for all strains. Cells began to attach to substratum after inoculation and well developed as indicated by OD_{600} values (7.9, 7.2 and 6.9, respectively) after 12 h of incubation and remained stable till 18h. Detachment of cells from biofilm was clearly observed by the drop in OD_{600} values after 16h (Figure 6).

The attachment and colonization experiments conducted to monitor biofilm formation microscopically on glass coverslips depicted that cells of *C. marina* alex formed a well-defined spherical microcolony after 6 h and was well developed after 12 h (Figure 7). The same pattern was characterized for the marine bacterium *Vibrio cholerae* which also formed microcolony [37]. On the other hand, it was observed that *P. prydzensis* alex and *P.* sp. alex cells were not randomly scattered but rather distributed in batches after 6 h of attachment. Similar observations were reported for *P. tunicola* [38,39]. The biofilm formation by *P. spongiae* was performed in static

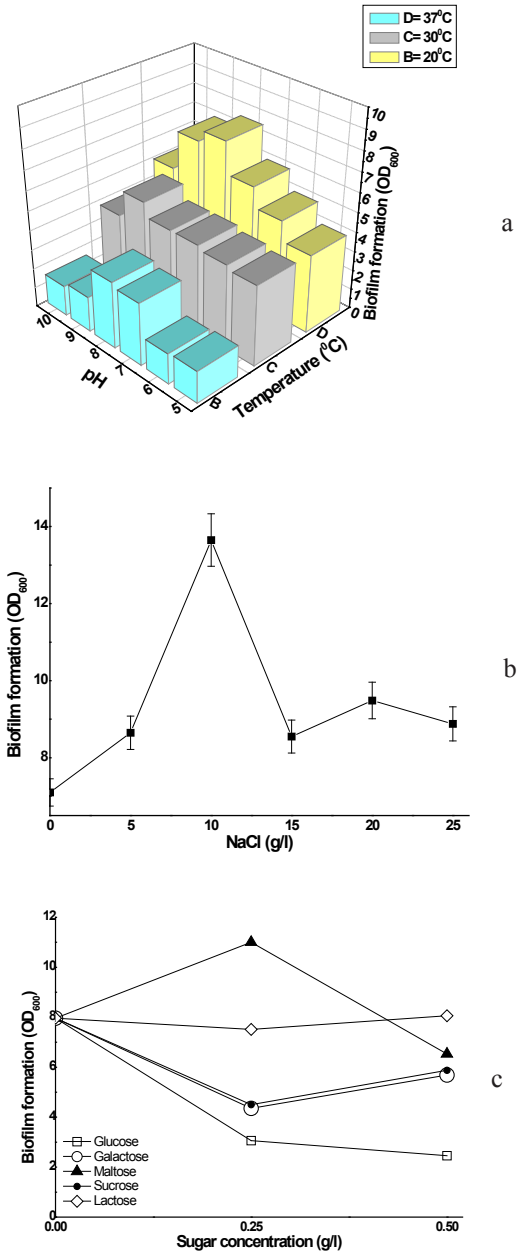

Figure 5. Effect of temperature and pH on biofilm formation by *C. marina* alex. (a), Effect of NaCl concentration on biofilm formation by *C. marina* alex on seawater medium at 30 °C for 24 h. The error bars represent the standard error of the means (SEMs) and the null hypothesis of the analysis of result; the samples came from the same population and biofilm formation at the 0.05 level is not significantly different. Statistics were achieved by a Kruskal-Wallis ANOVA test (b), Values of OD_{600} as a measure of biofilm formation by *C. marina* alex grown on seawater medium supplemented with different carbon sources at 30 °C for 24 h (c); The error bars represent the standard error of the means (SEMs)

DOI: https://doi.org/10.30564/jms.v3i3.3397

condition for a short period of time (10 h) [40].

3.6 Extracellular Polysaccharides (EPS) Production

EPS is produced as a secondary metabolite that plays a role in biofilm formation [41]. The amount of EPS produced is determined by the biomass yield beside other factors, therefore, the amount of EPS produced per unit biomass (productivity) varied among the tested strains (Figure 8). Under our experimental condition, *C. marina* alex produced equal amounts of dry weight and EPS (0.26 g/100 ml) and therefore exhibited the highest productivity (1.0 g/cells) compared to other tested species. The two *Pseudoalteromonas* species gave almost the same amount of dry weight but *P. prydzensis* alex produced a higher amount of EPS (0.34 g/100 ml) compared to *P.* sp. alex (0.24 g/100 ml) and consequently, the EPS productivity of *P. prydzensis* alex was 50% higher than that of *P.* sp. alex. Same observation was reported by Al- Nahas et al. (2011) [42] for *Pseudoalteromonas* species.

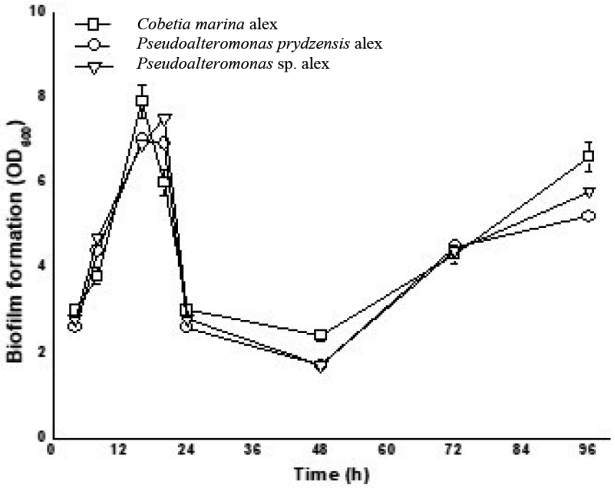

Figure 6. Single species biofilm progression on seawater medium at 30 °C at different time intervals; The error bars represent the standard error of the means (SEMs)

3.7 Quorum Sensing Molecules

A variety of different molecules can be used as signals. Common classes of signalling molecules are oligopeptides in Gram-positive bacteria, N-Acyl Homoserine Lactones (AHLs) in Gram-negative bacteria and a family of autoinducers known as AI-2 in both Gram-negative and Gram-positive bacteria. AHLs signals are involved in the regulation of a range of important biological functions, including luminescence, antibiotic production, plasmid

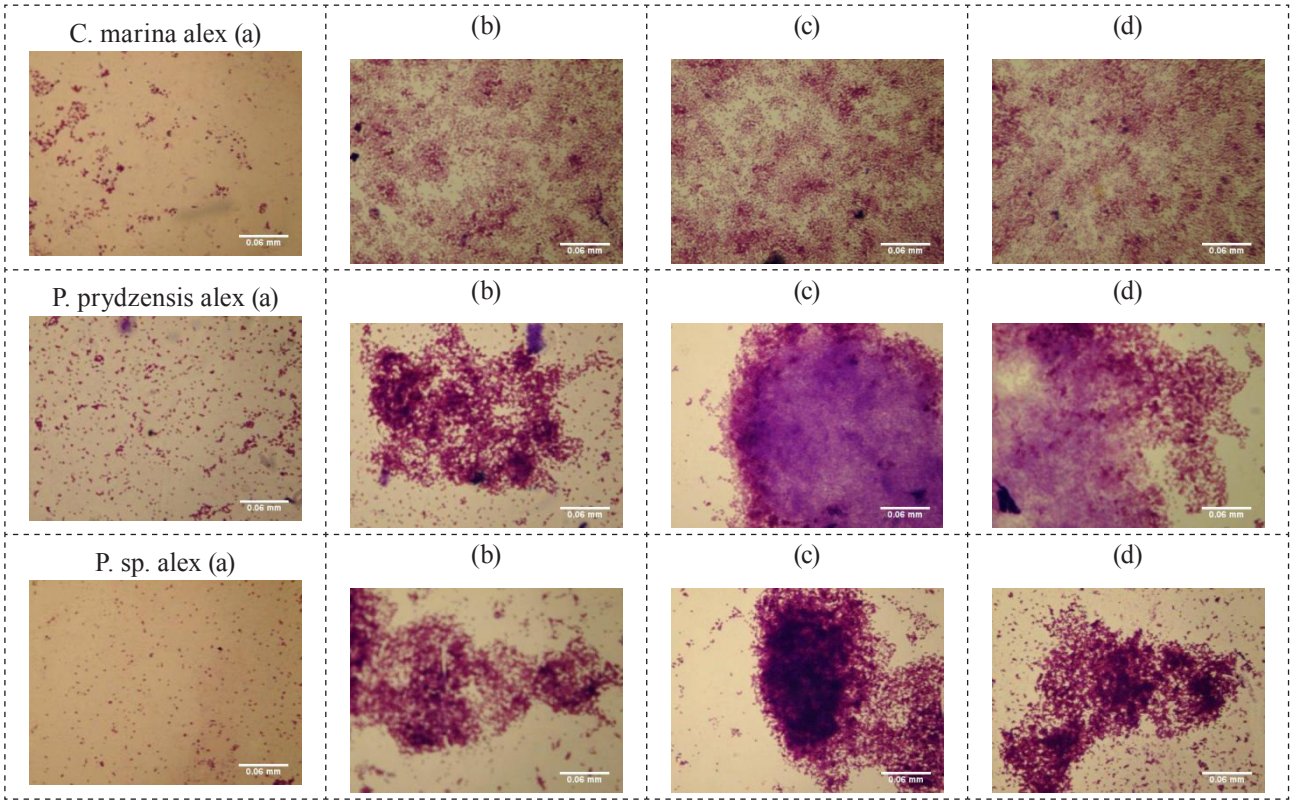

Figure 7. Biofilm development of *C. marina* alex, *P. prydzensis* alex, and *P.* sp. alex grew on cover slide as observed by Phase-contrast light microscope (x1000) with scale bar of 0.06. (a) Planktonic cells and biofilm development after (b) 6 h (c) 12 h and (d) 24 h incubation

 DOI: https://doi.org/10.30564/jms.v3i3.3397

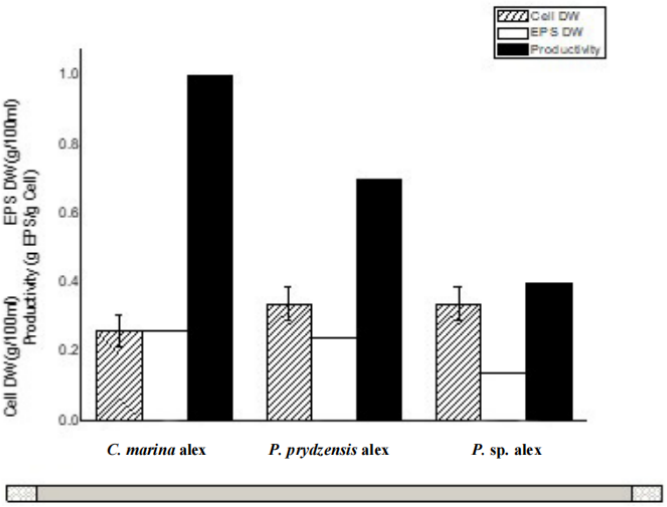

Figure 8. Cell mass, EPS mass, and EPS productivity after incubation on YMG broth at 25 ºC for 5 days at 120 rpm; the error bars represent the standard deviation of the means (SDMs)

transfer, motility, virulence and biofilm formation [43]. In the present study as a sequential step to EPS production, detection of quorum sensing molecules was essential. The reporter strain (*Agrobacterium tumefaciens*) was used in order to test the production of AHL signalling molecules. The strain produces a blue colour in the presence of 5-bromo-4-chloro-3-indolyl-b-D-galactopyranoside (X-Gal) in response to a wide range of AHLs [44]. Positive results were obtained with the three tested bacterial strains as indicated by the appearance of blue colour surrounding the colonies (Figure 9). This only occurs as a response to the production of AHLs as quorum sensing molecules. Our data are in agreement with other data which indicate that most AHL-producing bacteria belong to *Vibrio* and *Pseudoalteromonas* species and Rhodobacteraceae family [25] frequently found to be dominant in early marine biofilm communities [45]. Moreover, Dobretsov et al. (2009) [46] screened about forty-three bacterial isolates from marine snow and associated planktonic diatoms, for production of AHLs in the laboratory using *Agrobacterium tumefaciens* as bacterial reporter strain. Ibacache-Quiroga et al. (2013) [47] used *Agrobacterium tumefaciens* NTL4 as a biosensor in which a blue colour indicated X-gal hydrolysis was recorded as positive for presence of HSL in cell-free supernatant of *A. salmonicida*. Our results indicate that quorum sensing molecules may play a role in biofilm formation by the tested strains.

3.8 Interspecies Interaction

The interspecies interactions in dual, triple and mixed species biofilms were investigated to find out whether synergistic interactions occur during multispecies biofilm formation and whether multispecies biofilms offer enhanced fitness compared to single-species biofilm. Therefore, this approach was an attempt to get closer to the reality of naturally occurring biofilms. Each of the three strains was grown as single-species biofilm and in a possible combination of two or three species biofilm consortia in replicates of four. The results obtained reveal that when the three species (*C. marina* alex, *P. prydzensis*

Figure 9. Screening for AHL molecule in *C. marina* alex (a), *P. prydzensis* alex (b) and *P.* sp. alex (c) grown on LB agar plates-based bioassay. Blue color refers to the presence of quorum sensing molecule (AHL)

DOI: https://doi.org/10.30564/jms.v3i3.3397

alex, and *P.* sp. alex) coexisted in a biofilm, the value of biofilm after 24h increased by more than three-fold compared to the value of each single species (Figure 10). A surprising result was that a mixed culture of *C. marina* alex and *P.* sp. alex yielded a biofilm of a value similar to that of the triple biofilm. It also observed that dual-species biofilms were of more or less similar values and higher than those of single species (Figure 10).

The previously obtained data refer to the presence of synergism between the three marine bacterial species and between *C. marina* alex and *P.* sp. alex. No antagonistic interaction was observed among the tested strains. These data are in agreement with that obtained by Rao et al., (2010) [48] who suggested that *Pseudolateromonas tunicata* required the presence of diverse bacteria for effective colonization. The phenomenon of cooperative biofilm formation in mixed consortia has been described [49]. Synergy between species present in dual-or multispecies biofilms has been reported several times, mostly in description of biofilm-forming bacterial isolates from the oral cavity [50]. Guillonneau et al. (2018) [51] interestingly found that the two strains *Persicivirga mediterranea* TC4 and *Shewanella* sp. TC10 produced a newly secreted compound when grown in dual species versus mono-species biofilms. Moreover, the roles played by multispecies biofilms in resistance to disinfectants due to more EPS secretion compared with mono species biofilms was reviewed by Reuben et al. (2019) [52].

In an extension to the species interaction investigation, an experiment was conducted to evaluate the possible

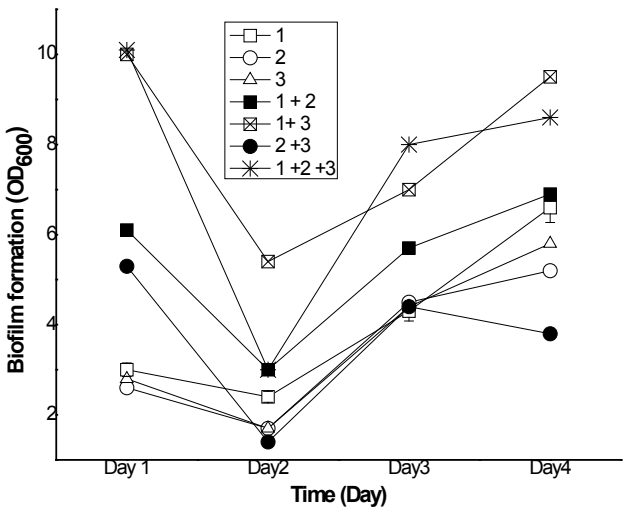

Figure 10. Interaction between the three marine bacteria in single, dual and triple biofilms; (1) *C. marina* alex, (2) *P. prydzensis* alex, and (3) *P.* sp. alex. The error bars represent the standard error of the means (SEMs)

interaction that might exist between *C. marina* alex and some marine bacteria in addition to a clinical isolate of *Candida* sp. *C. marina* alex was allowed to form single and dual biofilms with each of the tested organisms. Data in Figure 11 indicate that a negative effect (antagonism) was observed with all strains. The most notably antagonism was recorded in the dual combination of *C. marina* alex and *Vibrio* spp. where almost 90-100 % inhibition in biofilm formation was found compared to the single biofilm of *C. marina* alex.

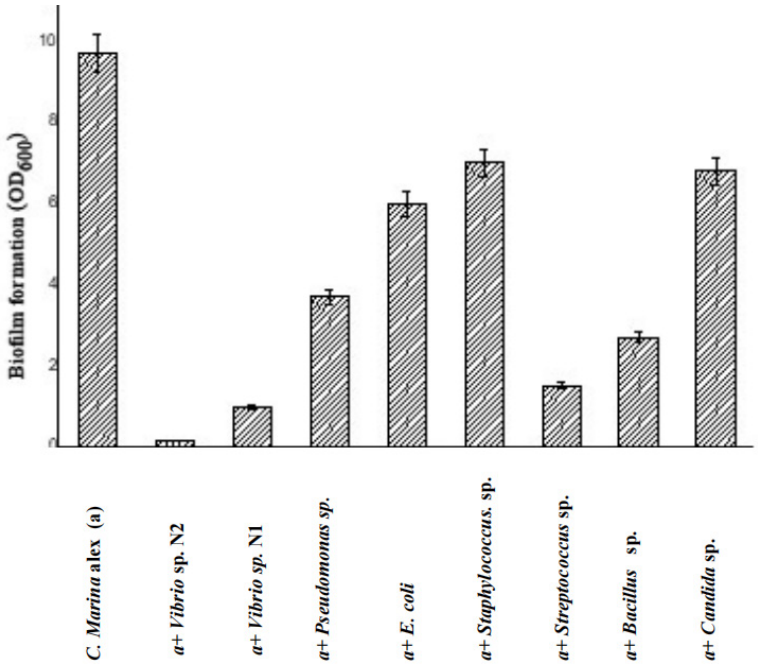

Figure 11. Antagonism in biofilms formed by *C. marina* alex as a control and in dual combinations with some marine bacteria. The error bars represent the standard error of the means (SEMs)

 DOI: https://doi.org/10.30564/jms.v3i3.3397

Percentages decreases of 60 and 40% were recorded with *Pseudomonas* sp. and *E. coli*, respectively. Same observation was found with the Gram- positive bacteria. Although 35% biofilm inhibition was recorded with *Staphylococcus* sp., much more existed with *Streptococcus* sp. and *Bacillus* sp. (almost 90 and 75%, respectively). Biofilm formed in a dual combination of *C. marina* alex and *Candida* sp. was 35% less than that formed by *C. marina* alex. The antagonistic interaction found in this work is surprising because all tested microorganisms were able to form biofilms in single culture. Therefore, more detailed studies are still needed to provide more explanation to such interaction.

4. Conclusions

There is widespread occurrence of microbial biofilms in marine ecosystems, but the factors that affect the configuration of these microbial communities are still a matter of current consideration. This study highlights the biofilm-forming bacteria in the Mediterranean seawater, Alexandria, Egypt as well as cell-to-cell communication and interactions among species which will provide a clearer picture that could improve current understanding of these microbial structures inhabited the Mediterranean seawater in Alexandria, Egypt. Biofilm forming bacteria have gained a great attention due to the recent biotechnological applications of biofilms in wastewater treatment, bioremediation technology, and enzyme function.

Author Contributions

S.S.A. conceived the idea conducted the experiments, analyzed and interpreted the data, wrote the manuscript, performed the statistical analysis, designed and constructed figures and charts; E.A.A. proposed the research concept, conceived & conducted the experiments; H.A.G. and S.A.S. conceived the research idea, analyzed the data, and edited the manuscript.

Competing Interests

The authors declare no competing interests.

Data Availability Statement

Correspondence and requests for materials should be addressed to S.S.A. The datasets generated and analyzed during the current study are available from the corresponding author on reasonable request.

References

[1] Hawley AK, Nobu MK, Wright JJ, Durno WE, Morgan-Lang C, Sage B, Schwientek P, Swan BK, Rinke C, Torres-Beltrán, M. et al. 2017. Diverse Marinimicrobia bacteria may mediate coupled biogeochemical cycles along eco-thermodynamic gradients. Nat. Commun. 8: 1507.
DOI: 10.1038/s41467-017-01376-9.

[2] de Carvalho CCCR, Caramujo M.J. 2012. Lipids of prokaryotic origin at the base of marine food webs. Mar. Drugs. 10: 2698-2714.
DOI: 10.3390/md10122698de.

[3] Brooks AN, Turkarslan S, Beer KD, Lo FY, Baliga NS. 2011. Adaptation of cells to new environments. Wiley Interdiscip. Rev. Syst. Biol. Med. 3: 544-561.
DOI: 10.1002/wsbm.136.

[4] Tahrioui, A. Duchesne R, Bouffartigues E, Rodrigues S, Maillot O, Tortuel D, Hardouin J, Taupin L, Groleau, M-C, Dufour, A. et al. 2019. Extracellular DNA release, quorum sensing, and PrrF1/ F2 small RNAs are key players in *Pseudomonas aeruginosa* to bramycin-enhanced biofilm formation. npj Biofilms Microbiomes. 5 (15): 1-10.

[5] Caruso G. 2020. Microbial Colonization in Marine Environments: Overview of Current Knowledge and Emerging Research Topics. J. Mar. Sci. Eng. 8: 78.
DOI: 10.3390/jmse8020078.

[6] de Carvalho CCCR. 2018. Marine Biofilms: A Successful Microbial Strategy With Economic Implications. Front. Mar. Sci. 5: 126.
DOI: 10.3389/fmars.2018.00126.

[7] Antunes LC, Ferreira RB, Buckner MM, Finlay BB. 2010. Quorum sensing in bacterial virulence. Microbiology. 156: 2271-2282.

[8] Khatoon Z, McTiernan CD, Suuronen EJ, Mah T, Alarcon EI. 2018. Bacterial biofilm formation on implantable devices and approaches to its treatment and prevention. Heliyon. 4: 1-36.

[9] Akuzov D, Franca L, Grunwald I, Vladkova T. 2018. Sharply Reduced Biofilm Formation from *Cobetia marina* and in Black Sea Water on Modified Siloxane Coatings. Coat. 8: 136.
DOI: 10.3390/coatings8040136.

[10] Kim M-S, Roh SW, Bae J-W. 2010. *Cobetia crustatorum* sp. nov, a novel slightly halophilic bacterium isolated from traditional fermented seafood in Korea. Int. J. Syst. Evol. Microbiol. 60: 620-626.
DOI: 10.1099/ijs.0.008847-0.

[11] Cobet AB, Wirsen C, Jones GE. 1970. The effect of nickel on a marine bacterium, *Arthrobacter marinus* sp. nov J. Gen. Microbiol. 62: 159-169.

[12] Baumann L, Baumann P, Mandel M, Allen RD. 1972. Taxonomy of aerobic marine eubacteria. J. Bacteriol. 110: 402-429.

DOI: https://doi.org/10.30564/jms.v3i3.3397

[13] Baumann L, Bowditch RD, Baumann P. 1983. Description of Deleya gen. nov created to accommodate the marine species *Alcaligenes aestus, A. pacificus, A. cupidus, A. venustus*, and *Pseudomonas marina*. Int. J. Syst. Bacteriol. 33: 793-802.

[14] Dobson SJ, Franzmann PD. 1996. Unification of the genera *Deleya* (Baumann et al. 1983), *Halomonas* (Vreeland et al. 1980), and *Halovibrio* (Fendrich 1988) and the species *Paracoccus halodenitrificans* (Robinson and Gibbons 1952) into a single genus, *Halomonas*, and placement of the genus *Zymobacter* in the family Halomonadaceae. Int. J. Syst. Bacteriol. 46: 550-558.

[15] Arahal DR, Castillo AM, Ludwig W, Schleifer KH, Ventosa A. 2002a. Proposal of *Cobetia marina* gen. nov, comb. nov, within the family Halomonadaceae, to include the species *Halomonas marina*. Syst. Appl. Microbiol. 25: 207-211.

[16] Arahal DR, Ludwig W, Schleifer KH, Ventosa A. 2002b. Phylogeny of the family Halomonadaceae based on 23S and 16S rDNA sequence analyses. Int. J. Syst. Evol. Microbiol. 52: 241-249.

[17] Zeng Z, Cai X, Wang P, Guo Y, Liu X, Li B, Wang X. 2017. Biofilm Formation and Heat Stress Induce Pyomelanin Production in Deep-Sea *Pseudoalteromonas* sp. SM9913. Front. Microbiol. 8: 1822. DOI: 10.3389/fmicb.2017.01822.

[18] Ballestriero F, Thomas T, Burke C, Egan S, Kjelleberg S. 2010. Identification of compounds with bioactivity against the nematode Caenorhabditis elegans by a screen based on the functional genomics of the marine bacterium *Pseudoalteromonas tunicata* D2. Appl. Environ. Microbiol. 76: 5710-5717. DOI: 10.1128/Aem.00695-10.

[19] Abouelkheir SS, Abdelghany EA, Ghozlan HA, Sabry SA. 2020. Characterization of Biofilm Forming Marine *Pseudoalteromonas* spp. J. Mar. Sci. 2 (1): 31-37. DOI: https://doi.org/10.30564/jms.v2i1.1412.

[20] Kumar MA, Anandapandian KTK, Parthiban K. 2011. Production and characterization of exopolysaccharides (EPS) from biofilm forming marine bacterium. Braz. Arch. Biol. Technol. 54 (2): 259-265.

[21] Hassan, A. Usman J, Kaleem F, Omair M, Khalid A, Iqbal M. 2011. Evaluation of different detection methods of biofilm formation in the clinical isolates. Braz. j. infect. dis. 15 (4): 305-311.

[22] Haney EF, Trimble MJ, Cheng JT, Vallé Q, Hancock REW. 2018. Critical Assessment of Methods to Quantify Biofilm Growth and Evaluate Antibiofilm Activity of Host Defence Peptides. Biomolecules. 8 (29): 1-22.

[23] Walker JN, Horswill AR. 2012. A coverslip-based technique for evaluating *Staphylococcus aureus* biofilm formation on human plasma. Front. Cell. Infect. Microbiol. 2 (39): 1-5.

[24] Casillo A, Lanzetta R, Parrilli M, Corsaro MM. 2018. Exopolysaccharides from Marine and Marine Extremophilic Bacteria: Structures, Properties, Ecological Roles and Applications. Mar. Drugs. 16 (69): 1-34.

[25] Liu J, Fu K, Wang Y, Wu C, Li F, Shi L, Ge Y, Zhou L. 2017. Detection of Diverse N-Acyl-Homoserine Lactones in *Vibrio alginolyticus* and Regulation of Biofilm Formation by N-(3-Oxodecanoyl) Homoserine Lactone In vitro. Front. Microbiol. 8: 1097. https://doi.org/10.3389/fmicb.2017.01097.

[26] Simões M, Simões LC, Vieira MJ. 2010. A review of current and emergent biofilm control strategies. LWT - Food Sci Technol. 43: 4: 573-583. http://dx.doi.org/10.1016/j.lwt.2009.12.008.

[27] Jasper A, Menegat R, Guerrasommer M, Cazzuloklepzig M, Souza PA. 2006. Depositional cyclicity and paleoecological variability in Quitéria outcrop Rio Bonito Formation, Paraná basin, Brazil. J. South Amer Earth Scienc. 21: 34:276-293.

[28] De La Haba RR, Arahal DR, Marquez MC, Ventosa A. 2010. Phylogenetic relationships within the family Halomonadaceae based on comparative 23S and 16S rRNA gene sequence analysis. Int. J. Syst. Evol. Microbiol. 60: 737-748.

[29] Tang X, Xu K, Han X, Mo Z, Mao Y. 2018. Complete genome of *Cobetia marina* JCM 21022T and phylogenomic analysis of the family Halomonadaceae. J. Oceanol. Limnol. 36: 528-536.

[30] Franco DC, Signori CN, Duarte RTD, Nakayama CR, Campos LS, Pellizari VH. 2017. High Prevalence of Gammaproteobacteria in the Sediments of Admiralty Bay and North Brans field Basin, Northwestern Antarctic Peninsula. Front. Microbiol. 8: 1-9.

[31] Ivanova EP, Zhukova NV, Lysenko AM, Gorshkova NM, Sergeev AF, Mikhailov VV, John P Bowman JP. 2005. *Loktanella agnita* sp. nov and *Loktanella rosea* sp. nov, from the north-west Pacific Ocean. Int. J. Syst. Evol. Microbiol. 55: 2203-2207.

[32] Flores-Treviño S, Bocanegra-Ibarias P, Camacho-Ortiz A, Morfín-Otero R, Salazar-Sesatty HA, Garza-González E. 2019. *Stenotrophomonas maltophilia* biofilm: its role in infectious diseases. Expert Rev. Anti. Infect. Ther. 17: 11: 877-893.

[33] Domenech M, García E, Moscoso M. 2012. Biofilm formation in *Streptococcus pneumoniae*. Microb.

Biotechnol. 5 (4): 455-465.

[34] Anderson OR. 2016. Marine and estuarine natural microbial biofilms: ecological and biogeochemical dimensions. AIMS Microbiol. 2 (3): 304-331. DOI: 10.3934/microbiol.2016.3.304.

[35] Amaya-Gómez CV, Hirsch AM, Soto MJ. 2015. Biofilm formation assessment in *Sinorhizobium meliloti reveals* interlinked control with surface motility. BMC Microbiol. 15: 58. DOI: 10.1186/s12866-015-0390-z.

[36] Kimkes TEP, Heinemann M. 2020. How bacteria recognize and respond to surface contact. FEMS Microbiol. Rev. 44(1): 106-122. https://doi.org/10.1093/femsre/fuz029.

[37] Seper A, Pressler K, Kariis A, Haid AG, Roier S, Leitner DR, Reidl J, Tamayo R, Schilda S. 2014. Identification of genes induced in *Vibrio cholerae* in a dynamic biofilm system. Int. J. Med. Microbiol. 304 (5-6):749-763.

[38] Rao D, Webb JS, Kjelleberg S. (2005) Competitive interactions in mixed species biofilms containing the marine bacterium *Pseudoaltromonas tunicata*. Appl. Environ. Microbiol. 71: 1729-1736.

[39] Rao D, Webb JS, Kjelleberg S. 2006. Microbial colonisation and competition on the marine alga *Ulva australis*. Appl. Environ. Microbiol. 72: 5547-5555.

[40] Huang YL, Dobretsov S, Xiong H, Qian PY. 2007. Relevance of biofilm formation of *Pseudoalteromonas* spongiae for its inductiveness to larval settlement of the polychaete Hydroides elegans. Appl. Environ. Microbiol. 73: 6284-6288.

[41] Van Houdt R, Michiels CW. 2010. Biofilm formation and the food industry, a focus on the bacterial outer surface. J. Appl. Microbiol. 109: 1117-1131.

[42] Al-Nahas MO, Darwish MM, Ali AE, Amin MA. 2011. Characterization of an exopolysaccharide-producing marine bacterium, isolate *Pseudoalteromonas* sp. AM. Afr. J. Microbiol. Res. 5 (22): 3823-3831.

[43] Grandclément C, Tannières M, Moréra S, Dessaux Y, Faure D. 2016. Quorum quenching: role in nature and applied developments. FEMS Microbiol. Rev. 40 (1): 86-116.

[44] Gui M, Liu L, Wu R, Hu J, Wang S, Li P. 2018. Detection of New Quorum Sensing N-Acyl Homoserine Lactones From *Aeromonas veronii*. Front. Microbiol. 9: 1712. DOI: 10.3389/fmicb.2018.01712.

[45] Chi W, Zheng L, He C, Han B, Zheng M, Gao W, Sun C, Zhou G, Gao X. 2017. Quorum sensing of microalgae associated marine *Ponticoccus* sp. PD-2 and its algicidal function regulation. AMB Expr. 7: 59. DOI: 10.1186/s13568-017-0357-6.

[46] Dobretsov S, Teplitski M, Paul V. 2009. Mini-review: quorum sensing in the marine environment and its relationship to biofouling. J. Bioadhesion Biofilm Res. 25 (5): 413-427.

[47] Ibacache-Quiroga, C. Ojeda J, Espinoza-Vergara G, Olivero P, Cuellar M, Dinamarca MA. 2013. The hydrocarbon-degrading marine bacterium *Cobetia* sp. strain MM1IDA2H-1 produces a biosurfactant that interferes with quorum sensing of fish pathogens by signal hijacking. Microb. Biotechnol. 6 (4): 394-405. https://doi.org/10.1111/1751-7915.12016.

[48] Rao D, Skovhus T, Tujula N, Holmström C, Dahllöf I, Webb JS, Kjelleberg S. 2010. Ability of *Pseudoalteromonas tunicata* to colonize natural biofilms and its effect on microbial community structure. FEMS Microbiol. Ecol. 73 (3): 450-457.

[49] Elias S, Banin E. 2012. Multi-species biofilms: living with friendly neighbors. FEMS Microbiol. Rev. 36: 990-1004.

[50] Ren D, Madsen J, Sørensen S, Burmølle M. 2015. High prevalence of biofilm synergy among bacterial soil isolates in cocultures indicates bacterial interspecific cooperation. ISME J. 9: 81-89. https://doi.org/10.1038/ismej.2014.96.

[51] Guillonneau R, Baraquet C, Bazire A, Molmeret M. 2018. Multispecies Biofilm Development of Marine Bacteria Implies Complex Relationships Through Competition and Synergy and Modification of Matrix Components. Front. Microbiol. 9: 1960. DOI: 10.3389/fmicb.2018.01960.

[52] Reuben RC, Roy PC, Sarkar SL, Ha S-D, Jahid IK. 2019. Multispecies Interactions in Biofilms and Implications to Safety of Drinking Water Distribution System. Microbiol. Biotechnol. Lett. 47 (4): 473-486. http://dx.doi.org/10.4014/mbl.1907.07007.

DOI: https://doi.org/10.30564/jms.v3i3.3397

BILINGUAL PUBLISHING CO.
Pioneer of Global Academics Since 1984

Journal of Marine Science
https://ojs.bilpublishing.com/index.php/jms

REVIEW

Dragonflies as an Important Aquatic Predator Insect and Their Potential for Control of Vectors of Different Diseases

Hassan Vatandoost[1,2*]

1. Department of Medical Entomology & Vector Control, School of Public Health, Tehran University of Medical Sciences, Tehran, Iran
2. Institute for Environmental Research, Tehran University of Medical Sciences, Tehran, Iran

ARTICLE INFO

Article history
Received: 21 April 2021
Accepted: 31 May 2021
Published Online: 20 July 2021

Keywords:
Mosquito
Diseases
Predator
Dragonfly

ABSTRACT

Mosquitoes belong to order of Diptera. The main important vectors are genus *Aedes, Culex* and *Anopheles*. They transmit different agents such bacteria, viruses, and parasites. According to the latest information around 7 hundred million people around the world are suffering from mosquito-borne illness resulting over one million deaths. The main important disease transmitted by Anopheles is malaria. Other genus of mosquitoes including *Aedes* and *Culex* species transmit different arboviral disease to human. According to guideline of World Health Organization, the mina control of disease is vectors control. The main important vector control is using different insecticides. Using chemical insecticides for controlling mosquitoes is limited because they develop resistance against these insecticides. So, efforts have been made to control the mosquito vectors by eco-friendly techniques. In this research all, the relevant information regarding the topic of research is research through the internet and used in this paper. An intensive search of scientific literature was done in "PubMed", "Web of Knowledge", "Scopus", "Google Scholar", "SID", etc Results shows that one of important environmental friendly vector control is biological control, using different predators and other microorganisms for vector and pest control. Dragonflies do eat mosquitos and serve as mosquito predators. They feed on mosquitos and reduce their number in outdoor areas. The dragonflies are scary biters, but they are dangerous to mosquitos. Worldwide results showed that dragonflies are able to control *Aedes, Culex* and Anopheles mosquito species. The artificial rearing of these predators and releasing for biological control is an appropriate measure for vector control worldwide.

1. Background

Dragonflies have sharp teeth on the jaws. According to the latest information a total of 7,000 species have been reported. Both nymphs and adult stages are predators of mosquitoes. The adults of dragonflies are scooping the mosquitoes by their legs and eat from them. They fly on sunny and warm days near fresh water (Figure 1). There are some reports indicating that nymph could survive for 5 years. Life span of adult stage varied and depend on species of insects. Dragonflies comprise ten families among which

**Corresponding Author:*
Hassan Vatandoost,
Department of Medical Entomology & Vector Control, School of Public Health, Tehran University of Medical Sciences, Tehran, Iran;
Institute for Environmental Research, Tehran University of Medical Sciences, Tehran, Iran;
Email: hvatandoost1@yahoo.com; vatando@tums.ac.ir

 DOI: https://doi.org/10.30564/jms.v3i3.3121

the Libellulidae, with 140 genera and about 962 species is the largest. This cosmopolitan family, considered to be the family of most recent origin, contains about a quarter of the known species of living Odonata. Dragonflies migrate from different parts of the world to complete the migration. They are known as farthest migrations of all insect species. The dragonfly's speed and agility contribute to its being one of the most effective aerial predators. Dragonflies included several families including Corduliidae, Aeshnidae, Libellulidae, Cordulegastridae, and Gomphidae. The adult dragonflies eat insects especially mosquitos and control their population. Each adult dragonfly feeds upon hundreds of mosquitos within a day. The adult dragonflies can feed on all the insects by using their legs that form the basket to clutch their prey into a slushy mess. These dragonflies then use their mandibles for swallowing the creatures. The adult dragonflies catch the insects during their flight and feed on gnats, mosquitos, mayflies, moths, bees, ants, termites, butterflies and other flying insects. They fly up and down in the air like a helicopter. The mosquitos are the bulk component of their diet. The larger the size of a dragonfly, the larger the prey it will catch. They can consume large prey and eat 15% diet equal to their body weight. The dragonflies eat various mosquitos each day. The nymphs feed on mosquito larvae when in water. The larvae stage of mosquitos is the better predator of mosquitos. The adult dragonflies feed on insects during the daytime when the mosquitos keep hiding in the bushes or timberlines. The adult dragonflies feed on adult mosquitos while basking themselves in sun and sitting on flat rocks.

Nymph usually capture the prey by extending the mouthparts (Figure 2). The nymphal stage is 9-17. Different species of odonate have different nymphal stages. In dry condition they have one generation, while in tropical situation they have multiple generations and those depend on habitat situations. At the nymph stage, they suck the water into their abdomen and then spitting it out. Nymphs usually absorb oxygen by their gills from the water. In the abdomen they draw water in and pump it out again through the anus. The have around 6-15 nymphal stages. Adults which hunt the mosquitos, and midges live about a month. Their legs could catch the mosquitoes and scoop up prey in flight. These insects live in the conditions with stable oxygen levels and clean water. They are considered as bioindicators for environment as well as ecosystem and health. Dragonfly nymph could act as sprawlers, burrowers, hiders, or claspers. Microhabitat they occupy effect on the shape, metabolism, and respiration.

There are some reports indicating that dragonflies fossils belong to the Carboniferous period. They show a wingspans of over one meter and look like a modern hawk (Figure 3).

a

b

c

d

Figure 1. Adults of dragonfly a) Darner Family b) Emerald Family c) Skimmer Family d) Clubtail Family

DOI: https://doi.org/10.30564/jms.v3i3.3121

Figure 2. Nymphal stage of dragonfly a) nymphal stage of different families b) mouthparts of nymph c) eyes of nymph (Google search)

Figure 3. dragonfly fossil (Google search)

 DOI: https://doi.org/10.30564/jms.v3i3.3121

Dragonfly at the adult stage has bristle-like shape. They have large compounds eyes which cover most of the head. They have four membranous wings include veins and cross veins. On the wings they have pigment cell which is important for their identification. Base of hind wing broader than forewing. Their abdomen is long and slender. Their compound eyes are very big and have appropriate and excellent eyesight due to their eye structure. A total of 30,000 facets have been recorded from their compound eyes. Each of facets is a separate light-sensing organ which is called ommatidium. The can see nearly a 360° field of vision (Figure 4).

Males of many of dragonflies are considered as territorial. They have responsibility to defend the territory against other creatures even other species of dragonflies. After laying eggs by females, the males normally set up a territory. The used their good oviposition for defending the breeding places from other males and challenge other dragonfly species and other animals (Figure 5). The mating wheel form is shown in dragonflies when they mate. They have second sexual organ which is located in the second parts of their abdomen. The wheel is formed when the male grasps the female behind the head and the female raises the tip of her abdomen forward to come in contact with the secondary genitalia of the male. Odonates are able to fly in tandem form. The adults dragonfly of dragonflies is around 6 to 8 weeks during the summer. Adults appear to be constantly hunting. Prey is scooped out of the air and consumed in flight. Dragonflies can consume too many and large numbers of mosquitoes. Most dragonflies are regarded as beneficial insects because they feed on small flying insects such as mosquitoes. The main predators of dragonflies are: birds, amphibians, spiders, wasps, lizards, small rodents, other odonata, adults of ceratopogonoidae, carnivorous plants like sundew.

Figures 6-9 show the global distribution of mosquitoes in the world. From these figures it should be concluded

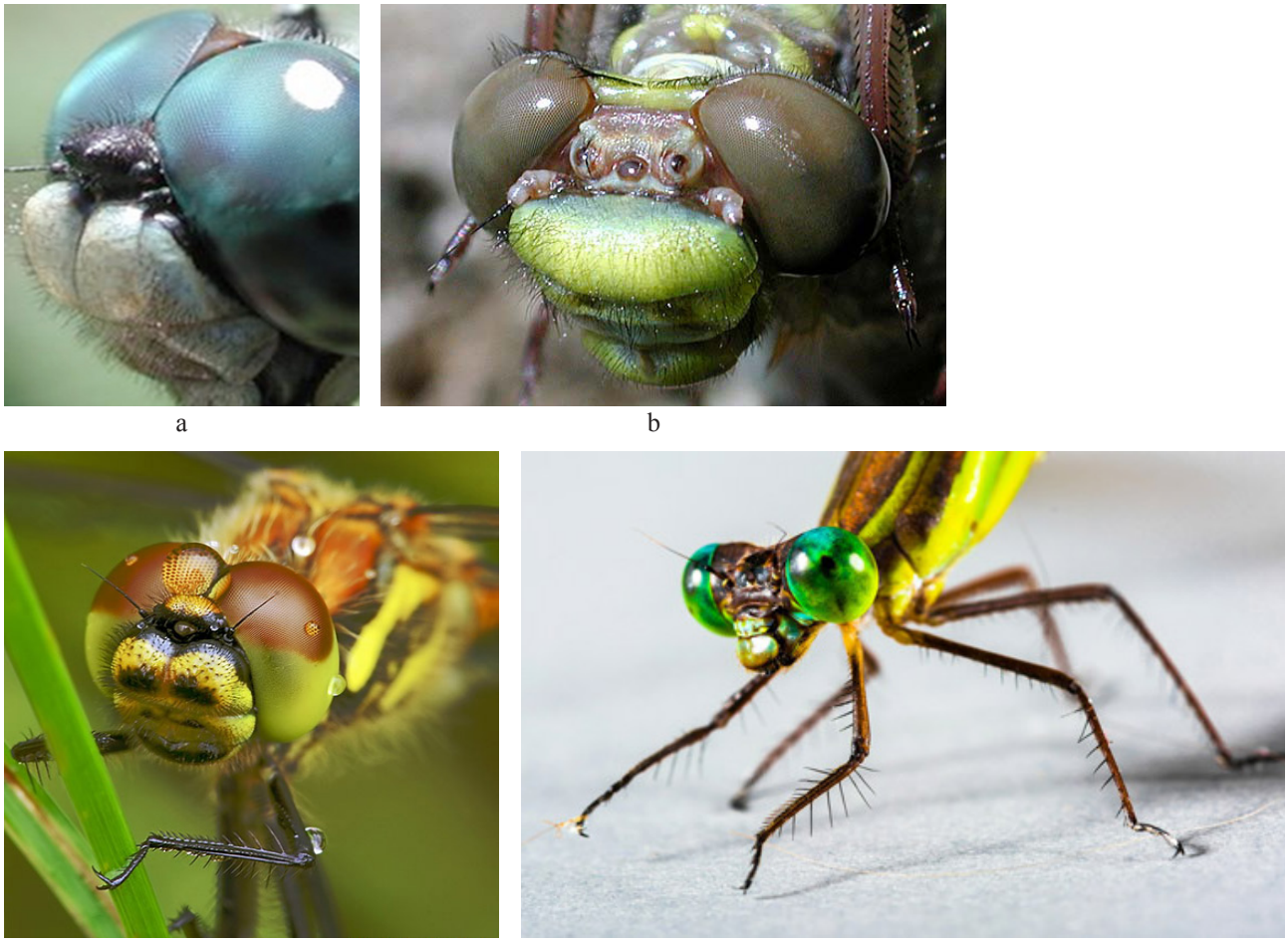

a b

b

Figure 4. Compound eyes of adults of dragonfly a) compound eye, b) ommatidium of compound eye (Google search)

DOI: https://doi.org/10.30564/jms.v3i3.3121

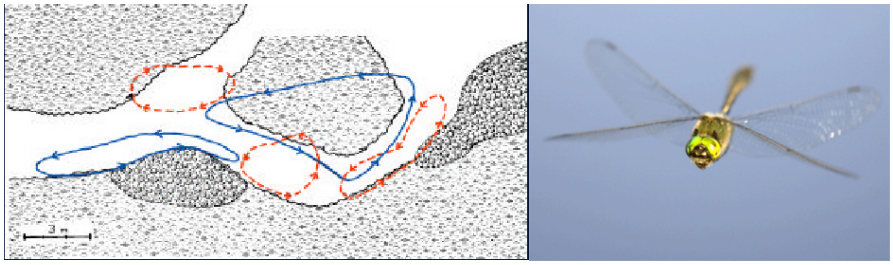

a b

Figure 5. Territory of Male dragonfly to protect the laid eggs by female a) male dragonfly territories over breeding site b) flying of male over territory (Google search)

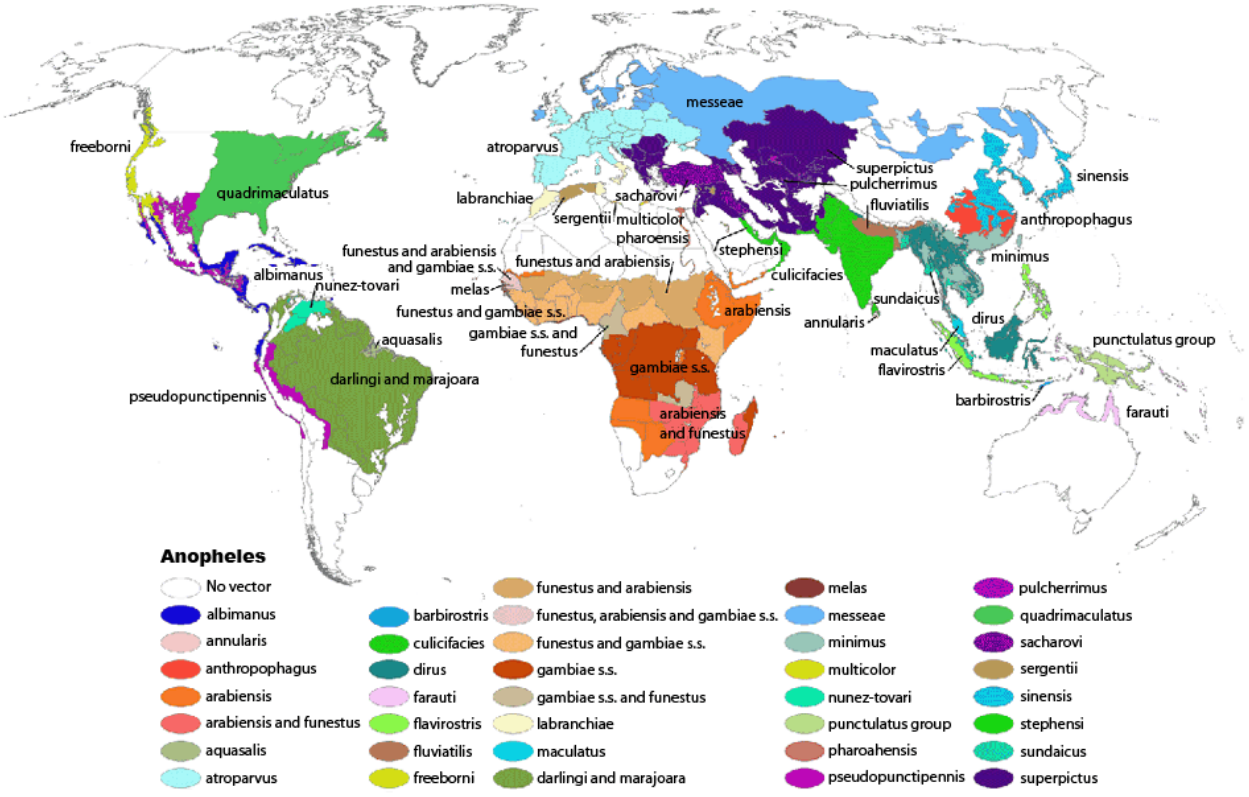

Figure 6. Global map of Anopheles species as the vector of malaria (Google search)

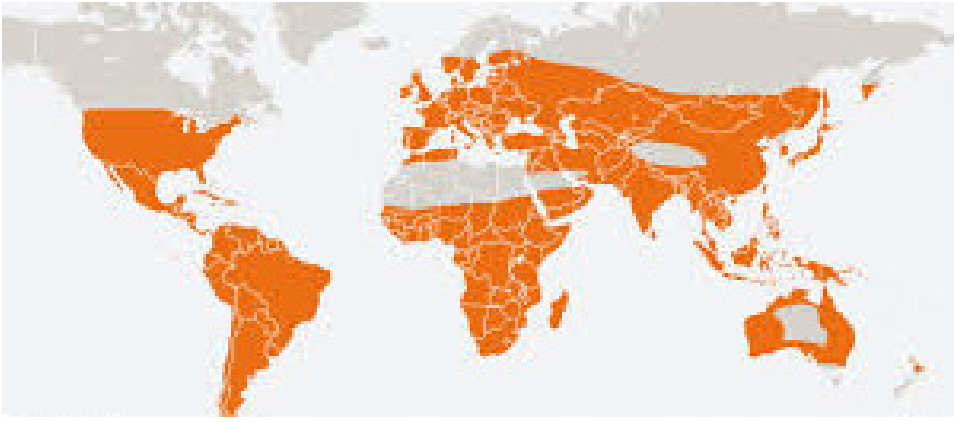

Figure 7. Global distribution of Culex mosquitoes (Google search)

 DOI: https://doi.org/10.30564/jms.v3i3.3121

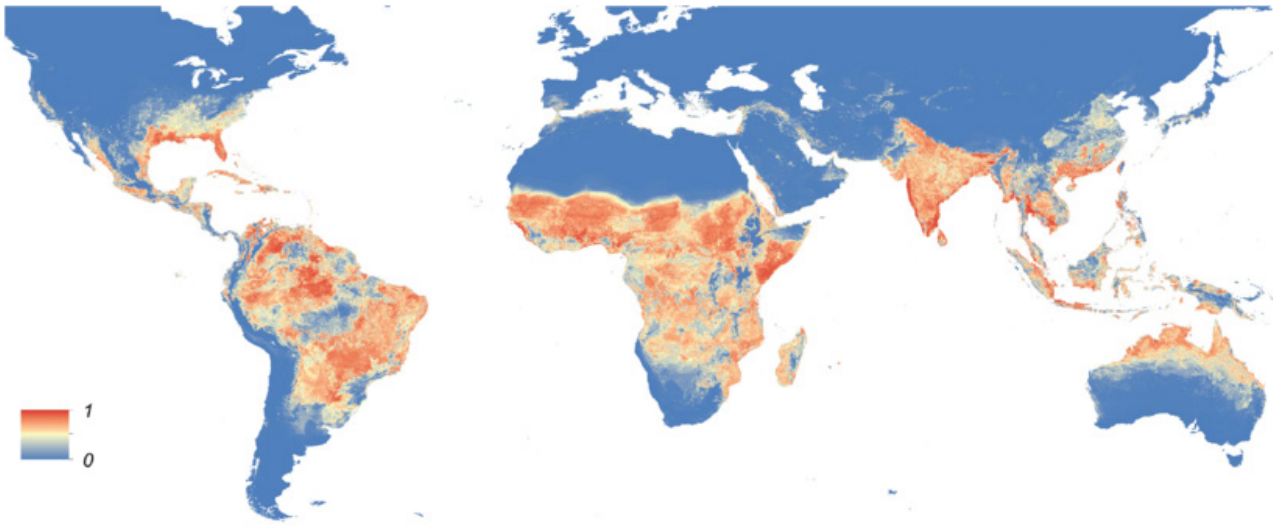

Figure 8. Global distribution of *Aedes aegypti* mosquito (Google search)

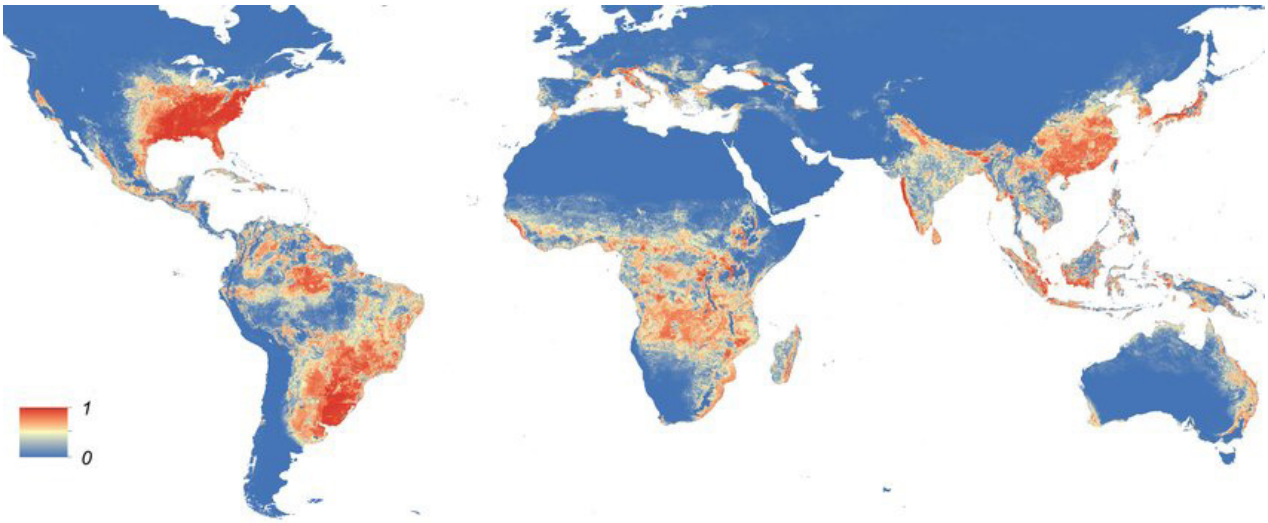

Figure 9. Global distribution of *Aedes albopictus* mosquito(Google search)

that nearly main parts of the world are mainly important breeding places of the mosquito, so that people are at risk of mosquito-borne diseases. According to the report of World Health Organization, more than half populations of the world are at risk of vector-borne diseases.

2. Methods

In this research all, the relevant information regarding the topic of research is research through the internet and used in this paper. An intensive search of scientific literature was done in "PubMed", "Web of Knowledge", "Scopus", "Google Scholar", "SID", etc.

3. Results and Discussion

There are several reports on efficacy of dragonfly for control of mosquitoes [1-15]. In a study odonata nymphs have been releases for control of vector of dengue diseases, *Aedes aegypti.* The release of this dragonfly reduced the mosquito larval production and thereby control dengue epidemics. Due to high longevity of odanata, their predatory habitats, trophic position and laying eggs in mosquito habitats at the immature stages are important factors for biological control of mosquitoes. Mandal *et al*., (2008) [2] used the five Odonate species in semi field conditions. They observed significantly reduction of mosquito larval density after 15 days of introduction. In West Benga. Similarly, the nympha of 5 odonate species *Aeshna flavifrons*, *Coenagrion kashmirum*, *Ischnura forcipata, Rhinocypha ignipennis* and *Sympetrum durum* in were evaluated in West Bengal,

DOI: https://doi.org/10.30564/jms.v3i3.3121

India under the semifield conditions. Results showed, the mosquito density after 15 days of introduction reduced (Mandal et al., 2008). They suggested use of odonate nymph for reducing in the breeding places of mosquitoes reduced the larval population. They could be releases in the temporary pools or larger habitats, where they can be a potential biological resource in regulating the larval population of the vector and pest mosquitoes. In another study, the efficacy of the dragonfly nymphs on dengue vector. *Aedes aegypti* were studied under laboratory and field conditions. The results showed that Nymphs act as predator against larvae and pupae of species *Ae. aegypti*. Complete elimination of immature stage of mosquitoes were achieved between day 4 and 9, depending on density of aquatic stages. In container habitats. Sebastian *et al*. (1980) [15] found that dragonfly nymph calling*, Labellula sp.,* eliminate *all aquatic stage of Ae. aegypti* larvae and pupae in day 4 and 9. They suggested the use of this predators for biological control of *Aedes* mosquitoes. Sebastian *et al*. (1990) [16] conducted a pilot field study. They released nymph of a dragonfly for suppressing *Ae. aegypti* population during the rainy season in Yangon, Myanmar. The results showed reduction of larval population of *Ae. aegypti* in 2 to 3 weeks. The predator suppressed the population of mosquito until the end of trial. The reduction of adult mosquito population was also observed after about 6 weeks. The study was carried out by Chatterjee et al. (2007) [17]. They used dragonflies for control of malaria vector, *Anopheles subpictus* in concrete tanks under field conditions in India. Results showed a significant decrease in *Anopheles subpictus* larval density in dipper samples after 15 days of introduction of dragonfly nymph.

4. Conclusions

More than half populations of the world are at risk of vector-borne diseases. Nearly all parts of the world are favorite breeding places for mosquitoes. According to these results, it is shown that the Odanata species are able to control of *Anopheles, Aedes* and *Culex* species of mosquitoes at the adult and larval stages. These mosquito species are the main important vectors of disease to human. Due to insecticide resistance of the vectors to different insecticides, the using of biological control is an appropriate as Integrated Vector Management program. Therefore, artificial rearing of this predator insects and releasing of them in the mosquito-borne diseases area could reduce the mosquito-borne diseases.

Conflict of interest

The author declare that there is no conflict of interest.

Acknowledgments

This research is partially supported by Ministry of Health and Medical Education of Iran under code number of NIMAD 995633.

References

[1] Jacob, S. Thomas A. Manju, E. (2017), " Bio-control efficiency of Odonata nymphs on *Aedes aegypti* larvae" .*IOSR J. Environ. Sci*.,11, 1-4.

[2] Mandal, S. Ghosh, A. Bhattacharjee, I. Chandra, G. (2008), " Bio-control efficiency of odonate nymphs against larvae of the mosquito,*Culex quinquefasciatus* Say, 1823". *Acta. Trop.,* 106, 109-114.

[3] Shaalan, EA. Canyon, DV. (2009)," Aquatic insect predators and mosquito control". *Trop. Biomed.*,26, 223-261.

[4] Saha, N. Aditya, G. Banerjee, S. Saha, GK. (2012) " Predation potential of odonates on mosquito larvae: Implications for biological control" . *Biol. Control*., 63, 1-8.

[5] Morales, ME. Wesson, DM. Sutherland, IW. Impoinvil DE. Mbogo, CM. Githure, JI. Beier, JC. (2003), " Determination of *Anopheles gambiae* larval DNA in the gut of insectivorous dragonfly (Libellulidae) nymphs by polymerase chain reaction" . *J. Am. Mosq.Control Assoc.,*19, 163-165.

[6] Mary, R. (2013), "Ecology and predatory efficiency of aquatic (odonate) insect over the developmental stages of mosquitoes (Diptera:Culicidae)" .*J. Acad. Ind. Res*.,2, 429.

[7] Norma-Rashid, Y. Saleeza, S. (2014), "Eco-friendly control of three common mosquito larvae species by odonata nymphs. in basic and applied aspects of biopesticides" , 2nd ed.; Sahayaraj, K., Ed.; Springer: New Delhi, India, pp. 235-243.

[8] Akram, W. Ali-Khan, HA. (2016)," Odonate nymphs: Generalist predators and their potential in the management of dengue mosquito,*Aedes aegypti* (Diptera: Culicidae)" .*J. Arthropod. Borne Dis*.,10, 252-260.

[9] Vershini, R. Kanagapan, M. (2014), " Effect of quantity of water on the feeding efficiency of dragonfly nymph-*Bradynopyga geminate* (Rambur): .*J. Entomol. Zool*. *Stud*.,2, 249-252.

[10] Singh, RK. Dhiman, RC. Singh, SP. (2003)," Laboratory Studies on the predatory potential of dragon-fly nymphs on mosquito larvae" . *J. Commun. Dis*., 35, 96-101.

[11] Quiroz-Martínez, H. Rodríguez-Castro, A. (2007)," Aquatic insects as predators of mosquito larvae: . *J. Am. Mosq. Control Assoc*., 23, 110-117.

 DOI: https://doi.org/10.30564/jms.v3i3.3121

[12] Acquah-Lamptey, D. Brandl, R. (2018)," Effect of a dragonfly (Bradinopyga strachani Kirby, 1900) on the density of mosquito larvae in a field experiment using mesocosms". *Web . Ecol*. 18, 81-89.

[13] El Rayah, EA. (1975)," Dragonfly nymphs as active predators of mosquito larvae". *Mosq. News*., 35, 229-230. .

[14] Hedlund J, Ehrnsten E, Hayward C, Lehmann P, Hayward A. (2020)," New records of the Paleotropical migrant *Hemianax ephippiger* in the Caribbean and a review of its status in the Neotropics". *Inter. J. Odonatology*, 23:4,315-325.

[15] Sebastian A, Thu MM, Kyaw M, Sein MM. (1980) ," The use of dragonfly nymphs in the control of *Aedes aegypti". Southeast Asian. J. Trop. Med. Public Health*., 11(1):104-7.

[16] Sebastian, A. Sein, MM. Thu, MM. Corbet, PS (1990)," Suppression of *Aedes aegypti (*Diptera: Culicidae) using augmentative release of dragonfly larvae (Odonata: Libellulidae) with community participation in Yangon, Myanmar". *Bull. Entomol. Res.* 80, 223-232.

[17] Chatterjee, SN. Ghosh, A. Chandra, G. (2007)," Eco-friendly control of mosquito larvae by *Brachytron pratense* nymph". *J. Environment. Health*., 69(8), 44-49.

DOI: https://doi.org/10.30564/jms.v3i3.3121

BILINGUAL PUBLISHING CO.
Pioneer of Global Academics Since 1984

Journal of Marine Science
https://ojs.bilpublishing.com/index.php/jms

ARTICLE

An Overview of Oligocene to Recent Sediments of the Western Pacific Warm Pool (WPWP) (International Ocean Discovery Program-IODP Exp. 363) Using Warm and Cool Foraminiferal Species

Patrícia Pinheiro Beck Eichler[1,2*] Christofer Paul Barker[2] Moab Praxedes Gomes[1] Helenice Vital[1]

1. Programa de Pós-Graduação em Geodinâmica e Geofísica (PPGG), Universidade Federal do Rio Grande do Norte (UFRN), Campus Universitário, Lagoa Nova, 59072-970 - Natal, RN, Brazil
2. Ecologic Project, Boulder Creek, California, United States

ARTICLE INFO

Article history
Received: 4 August 2021
Accepted: 12 August 2021
Published Online: 13 August 2021

Keywords:
Miocene
Population dynamics
Climate change
Tolerance
Temporal
Spatial

ABSTRACT

We use the excellent sediment recovery of International Ocean Discovery Program (IODP) Exp. 363, in the Western Pacific Warm Pool (WPWP) to assess down-core variations in the abundance of warm versus cool benthic foraminiferal species through a warm benthic foraminifers (WBF) curve. The total percentage of the "warm" shallower species group (*Laticarinina pauperata, Cibicidoides kullenbergi, C. robertsonianus, Cibicidoides sp., Hoeglundina elegans*, and *Bulimina aculeata*) and of the "cool" species group from deep waters (*Pyrgo murrhina, Planulina wuellerstorfi, Uvigerina peregrina,* and *Globobulimina hoeglundi, Hopkinsina pacifica*) at all sites is used to assess paleo temporal and spatial variations in preservation and marine temperature. Our study sites span water depths ranging from 875 m to 3421 m and our results indicate that well-preserved living and fossil foraminifera characterize mudline and core sediments at all water depths attesting the wide environmental tolerance of these species to temperature and pressure. Using magneto-and biostratigraphy datum, these sediments are of Oligocene age. Our low-resolution study showed that with the exception of core 1486B which the linear tendency of warmer species is toward cool sediments in old times, all of them show that older sediments indicate warmer periods than today, which is expected from Miocene to Recent. Our results provide evidence for the preservation potential of deeply buried sediments, which has implications on climate reconstructions based on the population dynamics of calcareous benthic foraminifera.

1. Introduction

Benthic foraminifera have been used to reconstruct environmental conditions in all marine and transitional environments, from hypersaline lagoons [1] and coral reefs [2-4] along the coast to deep sea [5]. Relative abundances of foraminiferal species and assemblages have been calibrating recent environmental characteristics of marine environments in mangrove and estuaries [6-9] and

**Corresponding Author:*
Patrícia Pinheiro Beck Eichler,
Programa de Pós-Graduação em Geodinâmica e Geofísica (PPGG), Universidade Federal do Rio Grande do Norte (UFRN), Campus Universitário, Lagoa Nova, 59072-970 - Natal, RN, Brazil; Ecologic Project, Boulder Creek, California, United States;
Email: patriciaeichler@gmail.com

 DOI: https://doi.org/10.30564/jms.v3i3.3516

in upwelling in continental shelves [10,11]. In the Atlantic restricted environments of Delaware inland Bays, USA, [8] traced East-West gradient salinity using *Ammonia* and *Elphidium* species, and have resolved both temperature and salinity variations in Rehoboth Bay. These recent studies show balance of thermohaline features and productivity of shelf-water masses using the stable isotopic composition of benthic foraminiferal. Three major assemblages of benthic foraminiferal from slopes of Ashmore Trough (Gulf of Papua) provided information about the paleo environmental history of modern tropical mixed siliciclastic-carbonate system, in the last ~83 kyr, which, is likely to be linked to sea level-driven changes in the amount of siliciclastic, carbonate, organic matter, and bottom water oxygen concentrations [12].

Here we deal with faunal fluctuations related to cool or warm phases, in the same faunal groups proposed by Lutze in 1977. In these studies [13,14] uses total percentages proportion of "warm" benthic species (*Laticarinina pauperata, Cibicidoides kullenbergi, C. robertsonianus, Cibicidoides* sp., *Hoeglundina elegans,* and *Bulimina aculeata*) and of "cool" species group (*Pyrgo murrhina, Planulina wuellerstorfi, Uvigerina peregrina, Globobulimina hoeglundi,* and *H. pacifica*) while percentages of all other species were ignored, resulting in the warm benthic foraminifera (WBF) curve". Relative abundance of above mentioned warm species and cool species collected in the Expedition 363 sites in the Western Pacific Warm Pool (WPWP) from the continental slope of northwestern Australia and of Papua New Guinea by the International Ocean Discovery Program (IODP) provides insights on the WBF curve and preservation state. These data track reconstruction of temporal and spatial variations from late Oligocene (~24 mya) to Recent in water depths ranging from 875 to 3421 m, and in sediment columns (at least up to 550 m) allowing convenient comparison. Our data reflect past interglacial and glacial cycles in the last 23 Myr tracking paleoclimate variations with well preserved material.

2. Study Area

We investigated the mudlines and cores of nine sites drilled during Exp. 363 (Figure 1, Table 1).

Two of the sites U1482A (Lat. 15°03.3227'S, Long. 120°26.1049'E) and U1483A (Lat. 13°05.2382'S, Long. 121°48.2424'E) are located at 1467.70 and 1732.93 m water depth off northwestern Australia at the southern part of the WPWP. Four sites lie in the Manus basin on the northern border of Papua New Guinea: U1484A at 1030.93 m water depth (Lat. 03°07.9228'S, Long. 142°46.9699'E); U1485A at 1144.75 m (Lat. 03°06.1585'S, Long. 142°47.5750'E); U1486B at 1333.83 m (Lat. 02°22.3368'S, Long. 144°36.0794'E), and U1487A at 873.93 m (Lat. 02°19.9979'S, Long. 144°49.1627'E). Three further sites

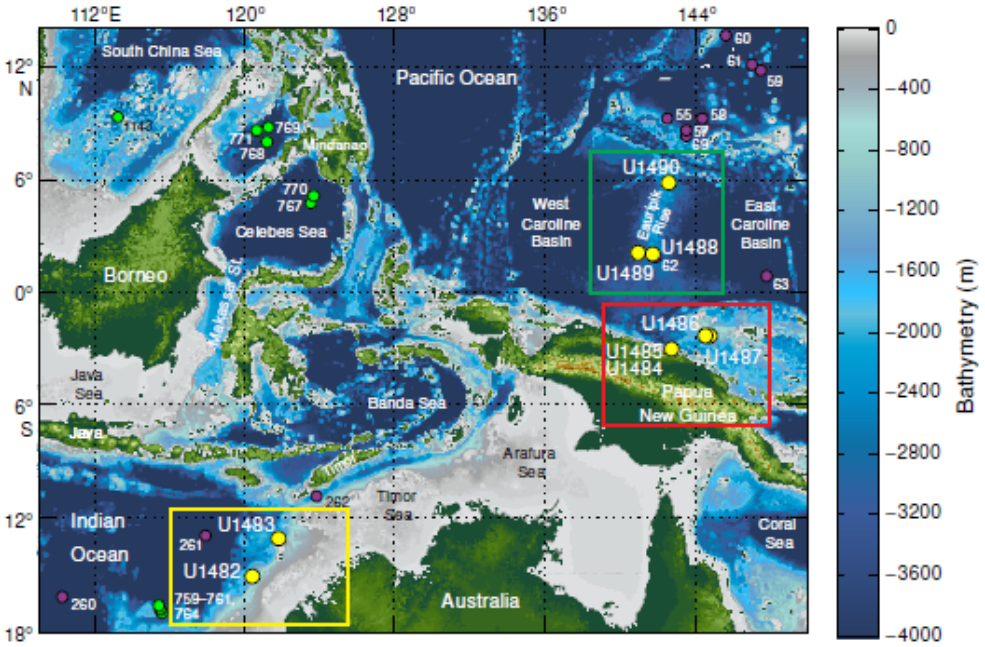

Figure 1. Bathymetric map with three areas cored in the IODP WPWP Exp. 363: Northwestern Australian shelf, Papua New Guinea/Manus Basin, Eauripik Rise.

Yellow circles = Expedition 363 sites, purple and green circles = earlier on cored DSDP and ODP sites. Source and analysis from Amante and Eakins (2009).

DOI: https://doi.org/10.30564/jms.v3i3.3516

Table 1. Expedition 363 Hole summary DSF=drilling depth below seafloor.

Hole	Latitude	Longitude	Water depth (m)	Penetration (m DSF)	Cored interval (m)	Recovered length (m)	Recovery (%)	Drilled interval (m)	Drilled interval (N)	Total cores (N)	APC cores (N)	HLAPC cores (N)	XCB cores (N)	Date started (2016)	Time started (h UTC)	Date finished (2016)	Time finished (h UTC)	Time on hole (days)
U1482A	15°3.3227'S	120°26.1049'E	1467.70	490.0	490.0	505.88	103.24	0.0	0	58	37	8	13	16 Oct	0730	19 Oct	0810	3.03
U1482B	15°3.3142'S	120°26.0988'E	1464.49	366.6	349.1	365.82	104.79	17.5	5	40	35	5	0	19 Oct	0810	20 Oct	1600	1.33
U1482C	15°3.3298'S	120°26.1135'E	1465.19	534.1	517.1	535.86	103.63	17.0	4	56	34	0	22	20 Oct	1600	24 Oct	1500	3.96
U1482D	15°3.3305'S	120°26.0920'E	1466.13	213.0	80.4	82.77	102.95	132.6	1	9	9	0	0	24 Oct	1500	25 Oct	1000	0.79
U1483A	13°05.2382'S	121°48.2424'E	1732.93	293.3	293.3	308.58	105.21	0.0	0	31	31	0	0	25 Oct	2230	27 Oct	1650	1.76
U1483B	13°05.2371'S	121°48.2538'E	1734.01	287.0	287.0	301.62	105.09	0.0	0	31	31	0	0	27 Oct	1650	28 Oct	1810	1.06
U1483C	13°05.2479'S	121°48.2537'E	1731.19	284.8	281.8	292.42	103.77	3.0	1	30	30	0	0	28 Oct	1810	30 Oct	0000	1.24
U1484A	03°07.9228'S	142°46.9699'E	1030.93	223.2	223.2	220.60	98.84	0.0	0	27	21	6	0	6 Nov	1245	7 Nov	1755	1.22
U1484B	03°07.9223'S	142°46.9809'E	1030.48	222.9	220.9	220.51	99.82	2.0	1	30	17	13	0	7 Nov	1755	8 Nov	2250	1.2
U1484C	03°07.9335'S	142°46.9822'E	1030.77	221.4	219.4	225.46	102.76	2.0	1	31	17	14	0	8 Nov	2250	9 Nov	2345	1.04
U1485A	03°06.1585'S	142°47.5750'E	1144.75	300.8	300.8	312.36	103.84	0.0	0	44	20	24	0	9 Nov	2345	11 Nov	1210	1.52
U1485B	03°06.1584'S	142°47.5854'E	1145.34	297.7	295.7	291.18	98.47	2.0	1	46	20	26	0	11 Nov	1210	12 Nov	2125	1.39
U1485C	03°06.1574'S	142°47.5991'E	1145.83	27.5	27.5	29.35	106.73	0.0	0	3	3	0	0	12 Nov	2125	13 Nov	0255	0.23
U1485D	03°06.1574'S	142°47.5867'E	1144.43	63.9	62.9	68.22	108.46	1.0	1	7	7	0	0	13 Nov	0255	13 Nov	1330	0.44
U1486A	02°22.3375'S	144°36.0796'E	1330.33	9.5	9.5	9.95	104.74	0.0	0	1	1	0	0	13 Nov	2321	14 Nov	0600	0.28
U1486B	02°22.3368'S	144°36.0794'E	1333.83	211.2	211.2	215.49	102.03	0.0	0	23	23	0	0	14 Nov	0600	15 Nov	0250	0.87
U1486C	02°22.3478'S	144°36.0798'E	1334.50	201.3	197.3	172.70	87.53	4.0	2	21	21	0	0	15 Nov	0250	16 Nov	0010	0.89
U1486D	02°22.3484'S	144°36.0690'E	1334.10	186.5	162.7	166.53	102.35	23.8	1	18	18	0	0	16 Nov	0010	17 Nov	0018	1.01
U1487A	02°19.9979'S	144°49.1627'E	873.93	144.2	144.2	146.43	101.55	0.0	0	16	16	0	0	17 Nov	0145	17 Nov	2040	0.79
U1487B	02°19.9975'S	144°49.1746'E	873.63	144.3	144.3	148.73	103.07	0.0	0	18	14	4	0	17 Nov	2040	18 Nov	1215	0.65
U1488A	02°02.5891'N	141°45.2864'E	2603.40	314.5	314.5	327.20	104.04	0.0	0	35	32	3	0	19 Nov	1800	21 Nov	1520	1.89
U1488B	02°02.5901'N	141°45.2966'E	2604.40	304.9	304.9	315.77	103.57	0.0	0	33	33	0	0	21 Nov	1520	23 Nov	0140	1.43
U1488C	02°02.5793'N	141°45.2974'E	2604.00	159.3	159.3	153.60	96.42	0.0	0	17	17	0	0	23 Nov	0140	24 Nov	0030	0.95
U1489A	02°07.1976'N	141°01.6654'E	3419.80	9.5	9.5	9.53	100.32	0.0	0	1	1	0	0	24 Nov	0442	24 Nov	1515	0.44
U1489B	02°07.1984'N	141°01.6757'E	3419.50	129.2	129.2	120.66	93.39	0.0	0	14	14	0	0	24 Nov	1515	25 Nov	1355	0.94
U1489C	02°07.1772'N	141°01.6746'E	3423.68	385.6	385.6	376.35	97.60	0.0	0	42	29	2	11	25 Nov	1355	27 Nov	1900	2.21
U1489D	02°07.1761'N	141°01.6651'E	3421.55	385.6	238.8	229.24	96.00	146.8	1	26	14	0	12	27 Nov	1900	29 Nov	1612	1.88
U1490A	05°48.9492'N	142°39.2599'E	2341.03	382.8	382.8	367.35	95.96	0.0	0	44	27	4	13	30 Nov	1400	2 Dec	1655	2.12
U1490B	05°48.9507'N	142°39.2698'E	2339.72	262.9	258.9	267.60	103.36	4.0	2	31	24	7	0	2 Dec	1655	4 Dec	0040	1.32
U1490C	05°48.9385'N	142°39.2690'E	2341.27	170.0	164.0	168.24	102.59	6.0	2	18	18	0	0	4 Dec	0040	5 Dec	1942	1.79
			Totals:	7227.5	6865.8	6956.00		361.7	23	801	614	116	71					

APC= advanced piston corer, HLAPC = half-lengh APC, XCB=extended core barrel

lie on the Eauripik Rise in the heart of the WPWP U1488A at 2603.40 m (Lat. 02°02.5891'S, Long. 144°45.2864'E), U1489B at 3419.80 m (Lat. 02°07.1976'S, Long. 141°01.6654'E), and U1490A at 2341.03 m water depth (Lat. 05°48.9492'S, Long. 142°39.2599'E).

Together these sites span a wide spatial and bathymetric range that will allow us to compare sediment cores in the largest source of water vapor to the atmosphere, the Western Pacific Warm Pool (WPWP). Variations in the strength of convection in the WPWP, therefore alter heat and moisture delivery to extra-tropical regions and may amplify changes in global climate [15,16]. Today WPWP hydrological cycle variability is dominated by (1) the seasonal relocation of the Intertropical Convergence Zone (ITCZ) and subsequent interactions related to the Asian-Australian monsoon and (2) the El Nino Southern Oscillation [17]. The sedimentary sequences of these sites capture the past 23 Myr at varying burial depths due to differing sedimentation rates allowing us to compare spatial and temporal environmental changes and potential effects of diagenesis on foraminiferal test preservation.

3. Methods

3.1 Sediment Processing

Mudline and core catcher samples from the nine study sites were examined for benthic foraminiferal assemblages. Samples from mudline were sampled by unloading the matter from the top of each core into a bucket, washed with water through a 63-µm wire mesh sieve. One gram of Rose Bengal diluted in one liter of alcohol was applied to stain living organisms in the mudline samples.

From each core, a catcher of 20-30 cm^3 of sediment was washed with water over a 63-µm wire mesh sieve and were looked at for the presence of organisms. Consolidated sediments were immersed in a 3% hydrogen peroxide (H_2O_2) solution, with little amount of Borax, prior to washing, to aid disaggregate hard material. Samples were dried in filter paper in low-temperature oven at ~50°C, and picked up with a fine brush under a binocular stereomicroscope. To prevent mixing of organisms between samples, sieve was cleaned, set into a sonicator for 15 minutes, and inspected for organisms. Species picking and identification were made on the >150 µm size fractions.

3.2 Foraminiferal Counts

Total benthic foraminiferal assemblage composition was built on counts of around 100 specimens. The distribution of lower bathyal and upper abyssal species is set apart into two different groups. Foraminifera belonging to the high carbon flux (>3.5 g C m−2 year−1), 'warm' (>3.5°C) group are *Bolivina robusta, Hoeglundina elegans*, *Globobulimina pacifica, Laticarinina pauperata, Bulimina aculeate*, and *Cibicidoides pachyderma*; and the lower carbon flux, 'cold' group includes *Oridorsalis umbontus*, *Uvigerina bifurcata*, and *Planulina wuellerstorfi* [18]. We counted the relative abundance of "warm" water species and "cool" water species and

 DOI: https://doi.org/10.30564/jms.v3i3.3516

calculated the warm benthic foraminifers (WBF) curve. All abundances of other species was counted but is not part of the interpretations.

Figure 2 (a -j) shows preservation status of benthic foraminifera was assessed and classified as: VG = Very Good (zero evidence of abrasion, dissolution, overgrowth); G = Good (low evidence of abrasion, dissolution, or overgrowth); M = Moderate (abrasion, dissolution, overgrowth were common but insignificant); P = poor (considerable abrasion, dissolution, overgrowth, and many fragments).

The illustration shows representative SEM images of the different preservation states at the nine sites. The colors on the back panel of the foraminiferal species (left panel, A) are to visually assign them to different down-core settings (right panel, B). Pictures were taken from the following samples a.1 HCC (0-2mbsf) U1483A; b. 12HCC (100-104mbsf) U1490A; c. 13HCC (104-108 mbsf) U1482A; d. 22HCC (191-195 mbsf) U1490A; e. 43XCC (379-380.1119 mbsf) U1490A; f. 1 HCC (0-2mbsf) U1482A; g. 1HCC (0-2mbsf) U1482A; h. 22HCC (198-202 mbsf) U1486B; i. 35HCC (310 -314.5) U1488A; and j 22HCC (198-202 mbsf) U1490A.

4. Results

4.1 Sedimentological Setting and Microfossil Preservation

U1482A

The core measures ~535 m going to upper Miocene to Pleistocene, rates of sedimentation averaging 5.9 cm/kyr in the upper Miocene, lessening to ~3.3 cm/kyr in the lower Pliocene. Pleistocene has more elevated sediment rates of ~7.0 cm/kyr [19]. The sediment of this site is composed of nannofossil ooze and chalk with assorted amounts of foraminiferal bathyal forms in a clayed environment. Calcareous species (*Pyrgo spp., Laevidentalina spp., Uvigerina spp., Planulina wuellerstorfi*, and *Hoeglundina elegans*) dominates with lower number of agglutinated forms, the latter representing <5% of the benthic foraminifer assemblages. Diversity ranges from 10 to 26 among studied samples. Sample 26H-CC (240.92 mbsf) shows the highest species diversity and the lowest diversity is from Sample 57X-CC (515.88 mbsf). Paleo depth established from the benthic foraminifer genera and species found in this core, rate as a bathyal bathymetric zone [20]. Shells are very well preserved and rare evidence of mineral overgrowth, abraded tests, and recrystallization was noted (Figure 2a).

U1483A

The sedimentation rate at this site is ~9.0 cm/kyr [21] almost double the rate of Site U1482A, and its location is ~264 km northeast of Site U1482A. This site is composed of nannofossil ooze with different quantities of foraminifers, clay, and diatoms and radiolarians. Calcareous species with lower numbers of agglutinated species (<5% of the assemblages) dominate the assemblages. The most dominant genera and species are *Hoeglundina elegans, Pyrgo* spp., *Uvigerina* spp.,

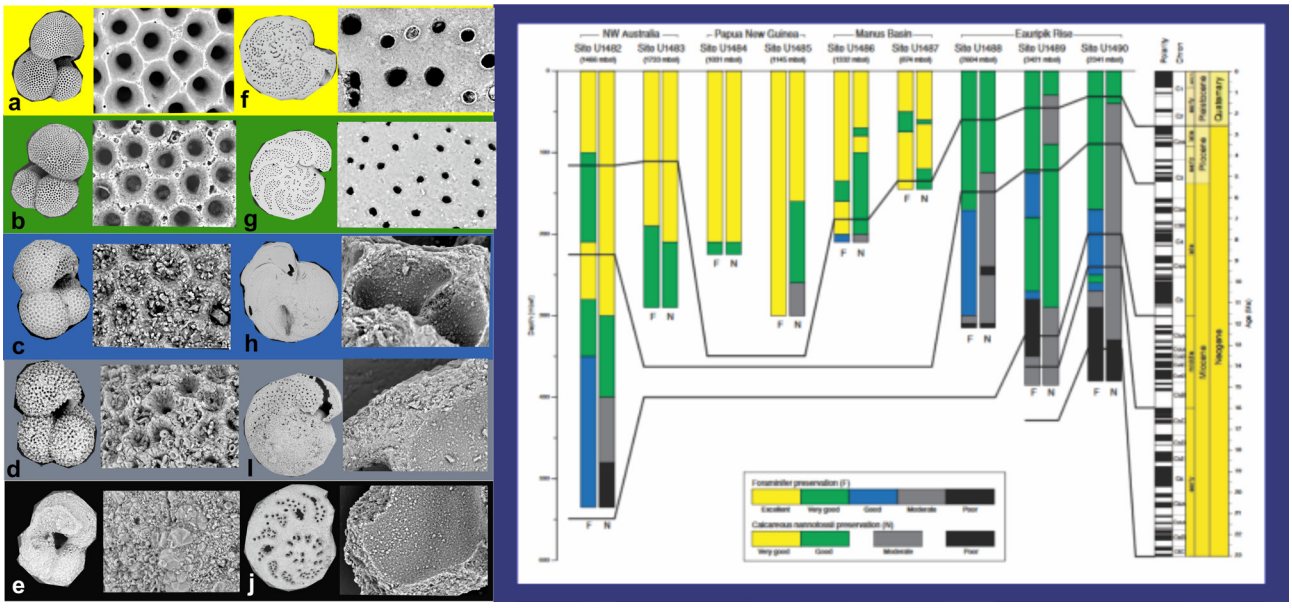

Figure 2 (a - j). Foraminiferal preservation as a function of sediment depth based on visual inspection of planktonic (*Globigerinoides ruber*) and benthic (*Planulina wuellerstrofi*) foraminiferal and nannofossil species (not illustrated) (modified figure from Exp.363 Preliminary report).

DOI: https://doi.org/10.30564/jms.v3i3.3516

Laevidentalina spp., *Planulina wuellerstorfi*. Diversity ranges from 10 to 26 within samples. Sample 10H-CC (94.60 mbsf) shows the highest species diversity and the lowest diversity found in Sample 20H-CC (189.57 mbsf). Paleo depth estimates a bathyal bathymetric zone with shells very well preserved with scarce or with no evidence of abraded shells (Figure 2b).

U1484A

The core presents ~224 m of middle Pleistocene to Recent terrigenous, hemipelagic sediment, containing well-preserved nannofossils, benthic and planktonic foraminifers and it differs from the two previous sites (U1482A and U1483A) because instead of having a deep benthic foraminifera fauna we can see habitats transition in down core catchers samples. This site also differs from previous sites due to the increased abundance and diversity of benthic foraminifera. Benthic foraminifers between Samples U1484A-7H-CC and 17H-CC (62.27-156.48 mbsf) are more dominant than other parts of the hole, and the ratio between benthic foraminifer to planktonic reaches 70:30. Alterations in benthic assemblages are observed downhole, which deeper water benthic foraminifers dominate upper and lower parts of the core; and shallow water benthic foraminifers including reef-dwelling taxa mixed up with deep, dominate the middle section. Alterations in the constitution of the assemblages are described in detail below. Samples U1484A-1H-CC to 6H-CC (5.00-52.95 mbsf) and 17H-CC to 27F-CC (156.48-223.62 mbsf) are mainly constitute of deep-water species: *Cibicidoides pachyderma, Bolivina robusta, Uvigerina prosbocidea, U. hispida, Bolivinita quadrilateral*, identified as bathyal forms, from depths down to 3500 m [20,22]. Samples 7H-CC to 9H-CC (62.27-81.21 mbsf) and 15H-CC to 17H-CC (138.62-156.48), are constituted of deep-water species mixed up with the shallow water species *Rotalinoides compressiusculus*, from water depths of 4-70 m [22]. Reef-dwelling benthic foraminifers as *Operculina complanata* and rare specimens of *Amphisorus hemprichii, Coscinospira arietina,* and *Peneroplis planatus* are noted between Samples 10H-CC and 15H-CC (90.58-138.62 mbsf). These species, which are mostly found at water depths <45 m [22] were probably carried to this specific site with other debris. This transition will be detailed below. The assemblage changed downhole, with deeper water taxa dominating in the upper and lower parts of the sediment core, while middle sections present deep and shallow-water benthic foraminifers mixed with reef-dwelling forms. Preservation is excellent with no calcification or abrasion (Figure 2c).

U1485A

The core length is ~300 m from middle Pleistocene to recent terrigenous and hemipelagic sediment. The upper ~225 mbsf of this site is very similar to Site U1484A, located ~3.2 km distant. Site U1485A contains well-preserved benthic and planktonic foraminifers, and calcareous nannofossils (Figure 2d). Sediment is composed of clay rich foram nanno ooze, sand, and silt. Assemblages are alike to Site U1484A, with less influence from downslope transport. Sandy shallow-water and reef dwelling benthic foraminifers are less frequent at this site comparing to Site U1484A, whereas wood and shells pieces are far more frequent. Hardly any intervals present the shallow-water species *Rotalinoides compressiusculus*, while typical bathyal forms dominate the bulk of the assemblage. Planktonic/benthic foraminifer ratios at this site are around 99:1. Assemblages differ from those at Site U1484A by the presence of deep-water forms without any large contribution from shallower water or reef faunas. A high abundance of volcanic ash in some samples increases the composition of the cool benthic foraminifer assemblage.

U1486B

Sequence of ~211 m of upper Pliocene to recent volcanogenic sediment, authigenic minerals, and biogenic sediment. The sedimentary sequence is signed as late Pliocene linking ages of 2.49 and 3.33 Ma. The sediment core at this site contains benthic and planktonic foraminifers, and nannofossils in extreme excellent preservation, with few foraminifera fragments and cementation or yet incipient recrystallization. Generally, there is no change in the state of shell's preservation with depth (Figure 2e). The assemblage indicates upper bathyal depths all over the core, and ratios around 99:1. It is worthy to mention that the remarkable amount of volcanic ashes a tephra in the sediments below ~130 mbsf most likely influence the diversity and number of foraminifer species.

U1487A

Sequence of ~144 m from upper Pliocene to Recent volcanogenic, biogenic and authigenic sediment, similar to Site U1486B, located 25 km distant. The sedimentary sequence cored shows affinity to Site U1486B. The two sites show the past ~2.7 Myr with reduction in volcanogenic input through time. The sediment core recuperated shows affinity to Site U1486B. The two sites show a decrease in volcanogenic activity through time. A deep-water bathyal environment with a planktonic/benthic

 DOI: https://doi.org/10.30564/jms.v3i3.3516

ratio of 99:1, and shell preservation is excellent to very good (Figure 2f) along the core.

Even with sedimentology similarities between the two sites, there are important differences between Site U1487A and Site U1486B, which are lower sedimentation rates, coarser grain size (with different oozes foraminifer versus nannofossil), intensified reworking and bioturbation, with thicker tephra layers and huge fragments.

U1488A

A sequence of~315 m of upper Miocene to recent, and bio stratigraphic and magnetostratigraphic horizons indicate pelagic sediment from the last ~10 Myr. A foraminifer-rich nannofossil to foraminifer-nannofossil ooze with different proportions of clay in an intermediate to deep bathyal depths [20,22]. Shell preservation at this site shows recrystallization (foraminifers) and fragmentation, overgrowth (foraminifers and nannofossils) and etching throughout the core (Figure 2g).

U1489B

A sequence of ~386 m of lower Miocene to Recent consists of nannofossil ooze, chalk, and different proportions of clay. Radiolarians are a large composition in the lowermost part of the core. This site show similar increase in recrystallization, fragmentation, etching, and overgrowth seen in site U1488A (Figure 2h).

U1490A

A ~380 m of upper Oligocene to Recent based primarily on downhole variations in biosilica, clay minerals, ashes and tephra. Siliceous microfossils (diatoms, sponge spicules, and radiolarians), calcareous microfossils (nannofossils and foraminifers), clay minerals, and volcanic ashes and tephra dominate this site. Planktonic foraminifers and calcareous nanofossils are present throughout the whole sequence. Benthic foraminifera species show evidence of a deep-water environment, and the planktonic/benthic foraminifer ratio is <99:1 throughout the sequence. The increase in recrystallization (foraminifers), fragmentation, etching, and overgrowth, and the assemblage in general seen downhole are alike to that from Eauripik Rise sites (U1488A and U1489B) (Figure 2h).

4.2. Warm and Cool Benthic Foraminiferal Apecies

In our low-resolution study of WBF curve it was possible to notice that with the exception of core 1486B, all of them show that older sediments indicate warmer periods than today, a tendency of what is expected from Miocene to Recent (Figure 3A to 3P, Supplementary Tables 1 to 9 shows abundance of foraminifera species and are available upon request).

Graphs show core catchers samples numbers versus abundance through time.

U1482A

The fauna inversions (cool to warm and vice versa) recorded on Figure 3 shows that upper Miocene (23 to 5.3 Ma) warmer sediments with warm foraminiferal species in rich chalk (Figure 3A) are replaced by cooler foraminifera species in the Pliocene (5.3 to 2.6 Ma) in clay rich nano ooze (Figure 3B). During this time climate became cooler and drier, seasonally similar to modern climate. Towards the end of early Pliocene (3 Ma), a warm foraminifera species rich nano ooze substitute the clay rich nano ooze (with cool foraminifera species) showing fauna inversion. The average temperature in the world during the mid-Pliocene (3.3 Ma-3 Ma) was 2 to 3 °C higher than now and sea level rise of 25 m. In the Northern Hemisphere ice sheet was short-lived before the extensive glaciation over Greenland that took place in the late Pliocene (around 3 Ma) detected by a warm-cool species fauna inversion (Figure 3C). During the early to late Pliocene from 3.6 to 2.2 Ma, the Arctic was warmer than today (with summer temperatures 8 °C warmer than today in the 3.6-3.4 Ma). This is of extreme importance because it is a late Cenozoic marine-based sedimentary record. Later on, in the early to middle Pleistocene (2.5 Ma to 11.7 ka), a nanofossil ooze with cooler foraminifera species is again replaced by warmer species rich nano ooze (Figure 3D).

U1483A

The same fauna inversion in the end of early Pliocene 3.6 to 2.2 Ma when the Arctic was much warmer than today (with summer temperatures 8 °C warmer than today in the 3.6-3.4 Ma, same as U1482A) was recorded on this core (Figure 3A). A fauna inversion on the late Pliocene show the beginning of the extensive glaciation over Greenland that occurred around 3 Ma, and then a clay foram rich nano ooze is changed to diatom foraminifera rich nanno ooze with warmer foraminifera species, same as U1482A (Figure 3B). This epoch is marked by an Arctic ice cap formation noted by a sudden alteration in oxygen isotope ratios and ice-rafted cobbles in the North Atlantic and Pacific Ocean beds, and Mid-latitude glaciation was likely occurring before the end of this Pliocene. The global cooling that happened during the Pliocene may have decreased forests and increase

DOI: https://doi.org/10.30564/jms.v3i3.3516

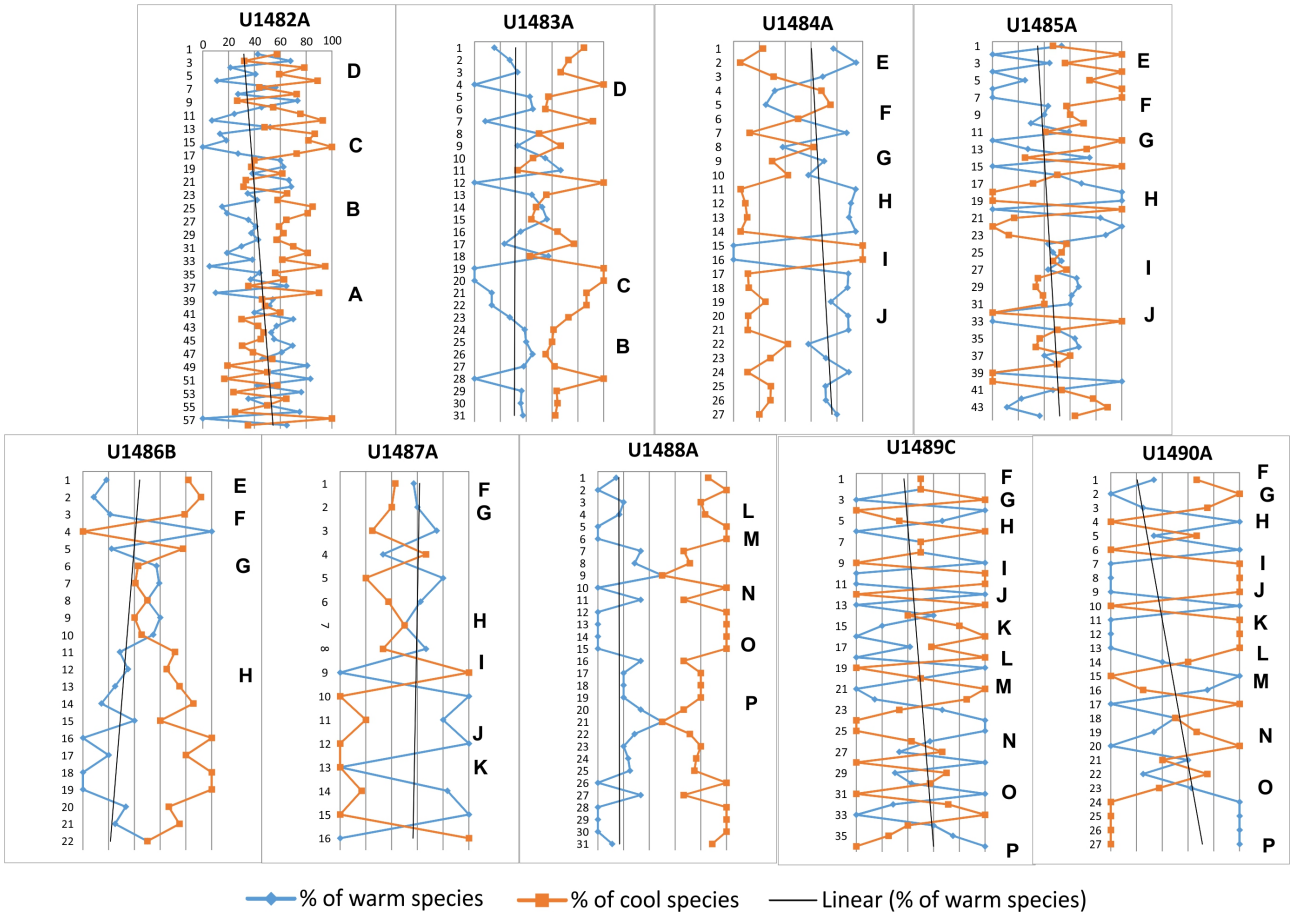

Figure 3 (A - P). Data on spatial abundance (e.g., within each depth transect) of warm and cool species plotted against temporal scale and geological events of sites from Expedition 363 (Stages A to P). Graphs show core catchers samples numbers versus abundance through time.

the spread of grasslands and savannas and a cooler foraminiferal fauna shows it. The Early Pleistocene (=Lower Pleistocene) reaches the time between 2.588 ± 0.005 Ma and 0.781 ± 0.005 Ma (Figure 3C). The base of the Gelasian is designated as the Matuyama (C2r) chronozone (the Gauss-Matuyama magnetostratigraphic boundary, isotopic stage 103). Ice sheets in the Northern Hemisphere started to grow during the Gelasian, in the beginning of the Quaternary glacial stage. The Middle Pleistocene, known as the Ionian stage, from 781 to 126 ka succeeds the Calabrian Stage (the Brunhes-Matuyama reversal) which in turn shows from the beginning of the last interglacial (Marine isotopic stage- MIS 5) to the base of the Holocene (~10.5 ka) and it was verified by the faunal shift from cool to warmer species (Figure 3D).

U1484A

At least two inter glacial and two glacial cycles were recognized on U1484A based on the increase of warm foraminiferal species, and ten major volcanic ash horizons coinciding with climatic cooling and increase of cool species in this middle-late Pleistocene core. They are therefore representative of cold (glacial) and warm (interglacial) past periods.

The top part of the core in the Late Pleistocene is associated with Tarantian stage, and the age is the end of the Pleistocene epoch or glacial stage (Figure 3E). Sediment is composed of clay rich foraminifer's nanno ooze, and sand, silt and clay. Before that, it is possible to see that the last maximum glacial ends with the cold period, known as the Younger Dryas sub stage which sediment is composed by sand, silt, clay and cool foraminiferal species at 12.900 to 11.700 ka (Figure 3F).

The starting of the stage is the Eemian interglacial phase (Figure 3G) prior to the final glacial episode in the Pleistocene at 126.000 ka (Figure 3H). The Eemian (also called the last interglacial) was the interglacial period, which started around 130.000 ka and ended about 115.000 ka. It corresponds to Marine Isotope Stage 5e and it shows increase of warm foraminiferal species in sediment composed by sand, silt, and clay with periods of clay rich

 DOI: https://doi.org/10.30564/jms.v3i3.3516

Foraminifera nanno ooze. Before the Holocene, the last interglacial period has temperatures at at the minimum 2°C warmer, mean sea level of 4-6 m higher than today, with decreases in the Greenland ice sheet. Microfossil and fossil reef proxies indicate mean sea level fluctuations of up to 10 m. This information are important to understand current climate, because mean temperatures around the world during MIS-5e were close to the projected climate change nowadays. The oldest sediments are upper part of middle Pleistocene, in the Ionian stage, reaching a period of geologic time of 0.29 Ma. (Figure 3I). This stage happens after a series of volcanic ash horizons and foraminiferal fauna is colonized by cool species in sand and silt sediments (Figure 3J). It is important to notice that after volcanic ash episodes cool foraminiferal species tend to colonize.

U1485A

Even though U1485A sedimentation rate is twice higher than 1484A, the inter glacial and glacial cycles were similar and based on the increase of warm foraminiferal species, and the seventeen major volcanic ash horizons recorded coincides with climatic cooling and increase of cool species in this middle-late Pleistocene core. The top part of the core in the Late Pleistocene is associated with Tarantian stage, representing the end of the Pleistocene epoch or glacial stage.

In U1486B the Early-Middle Pleistocene transition (c. 1.2-0.5 Ma), or the 'mid-Pleistocene revolution', is a vital episode in the history of Earth. Low-amplitude 41-ka obliquity-forced climate cycles of the earlier Pleistocene were substituted in the later Pleistocene by high-amplitude 100-kyr cycles suggestive of ice build-up slowly (increase of global ice volume at 940 ka) with following rapid melting. These climate alterations, especially the increasing severity and duration of cold stages, had a huge consequence on the biota and landscape in the Northern Hemisphere (Figure 3E) The Matuyama-Brunhes palaeomagnetic Chron border (mid-point at 773 ka) is view as Early-Middle Pleistocene Subseries boundary with warm species (Figure 3F). In terms of foraminiferal fauna, there is an inversion of cool-warm-cool species (Figure 3G). Eemian interglacial phase began about 130,000 ka and ended about 115,000 ka, and it corresponds to Marine Isotope Stage 5e, showing increase of warm foraminiferal species in sediment composed by sand, silt, and clay, rich foraminifera and Nano ooze with ash. Figure 3H shows Calabrian, in the Pleistocene, established as ~1.8 Ma—781,000 ka ± 5,000 years supporting cool foraminiferal species. The last magnetic pole reversal (781 ± 5 Ka) is the end of this stage diving into a glacial and drying stage around the world, which is probably colder and drier than the late Miocene (Messinian) in the Zanclean (early Pliocene) cold period. It has become the second geologic age in the Early Pleistocene.

U1487A

Climate alterations, especially the increasing gravity and duration of cold stages had a profound effect on the microfossils of this site. The same events from U1486 are observed: Figure 3 (E), (F), (G), and (H). Besides that, it is also possible to observe that the bottom of this site exhibits more events such as the Gelasian Stage (Figure 3I), first of four stages of the Pleistocene Series, enclosing deposits during the Gelasian Age (2.588,000 to 1.806,000 ka) of the Pleistocene in the Quaternary Period with warm species (Figure 3J). The Piacenzian is the latest age of the Pliocene, and it reaches the time between 3.6 ± 0.005 Ma and 2.588 ± 0.005 Ma (Figure 3K). Climate of the Piacenzian is wet, moist, and warm period in North America colonized by warm foraminiferal species, occurring after a small chilling period of the Zanclean, which cool species dominating fauna, is similar to sites U1482A and U1483A.

The more recent events from Figure 3F to K are observed at the upper part of the U1488A. This core also shows other events: The Early Pliocene warmth (Figure 3L), at about 4 to 5 Ma, earth had a warm, temperate climate, when the Artic was 8°C warmer than today in a permanent El Nino state and increase of warmer species. The cooling conducted to the setting of temperature patterns of the present, responding to a reduction in atmospheric CO_2 concentration, (100 parts per million) of preindustrial values. The early Pliocene climate had lower austral and zonal temperature gradients but alike maximum ocean temperatures [23]. During the Zanclean flood (Figure 3M), a hypothetically one to have refilled the Mediterranean Sea at 5.33 Ma, ended the Messinian salinity crisis, and marked the beginning of Zanclean age. Sea-level rise may have reached rates at times greater than 10 m per day. In the Pliocene (5.3 Ma to 2.6 Ma) climate set off drier and cooler, and seasonal, similar to today´s climate. The mean temperature in the mid-Pliocene (3.3 Ma-3.0 Ma) was 2-3 °C elevated than today, sea level rise 25 m, and the Northern Hemisphere ice sheet was short lived prior the beginning of the major glaciation above Greenland during the late Pliocene around 3 Ma. The formation of the Arctic ice cap occurs by an abrupt change in oxygen isotope ratios and ice-rafted cobble in the North Atlantic and Pacific Ocean beds. The global cooling that happened in the Pliocene may have stimulated the disappearance of wet forests and the spread of grasslands

DOI: https://doi.org/10.30564/jms.v3i3.3516

and savannas. The equatorial Pacific Ocean sea surface temperature gradient was lower than the present day, and the sea surface temperature in the East were warmer than nowadays but alike in the west. This condition has been described as a permanent El Niño state. The Alps in Europe halt outward expansion suitable to the increase in erosional flux and as a response to the climatic shift to wetter conditions in Europe during the Mediterranean desiccation at the end of the Miocene (Figure 3N). Zone M13 show Bio horizon base with *Pulleniatina primalis* (6.6 Ma) (Figure 3O). The Tortonian age of the Miocene (11.6-7.25 Ma) present changes in the vegetation compared to modern natural (Figure 3P). Warm and temperate forests covered much of Europe, coastal North America and South-East Asia at this time. Our findings show evidences of the dryness spread in the savanna in central USA, the Middle East and on the Tibetan Plateau. The tropical forests in South America were reduced, however enlarged in the Indian sub-continent and East Africa. Mean annual temperature around the world is probably as much as 4.5 °C higher than today with many sites undergoing higher than modern quantity of precipitation. The foraminiferal assemblages are from intermediate to deep bathyal depths, and both cores U1489B and U1490A show evidence of the same phases (Figures 3F to P) evidenced in U1488A.

5. Discussion

Paleo environmental reconstructions found on down-core variations in the geochemistry of foraminifera depend on the availability of pristine samples. Recrystallization in the sediments tends to homogenize the original geochemical signature affecting, in particular, down-core surface temperature reconstructions [24]. The reconstructions of the deep ocean are less affected by this diagenetic effect because the calcification temperature of benthic foraminifera is closer to the recrystallization temperature in the sediments. However, limiting reconstructions to clay-rich sediments would severely limit the spatial coverage of geochemistry-based reconstructions of surface ocean properties. Thus, other indicators of the state of foraminiferal preservation are important contributor to paleo climatic and paleoceanographic reconstructions. Therefore, if preservation of foraminiferal species is good, these data are accurate tool to understand both natural and geomorphologic evolution and changes. The excellent preservation and the remarkable physical tolerance of the species to higher physical pressure in water and in sediment provided data on at least 11 glacial and interglacial cycles from different cores. These cycles correlated well in all depths from late Oligocene (~24 Mya) to Recent were evidenced by WBF fluctuations recorded by shallower "warm" benthic species (*Bulimina aculeate, Laticarinina pauperata, Hoeglundina elegans, Cibicidoides kullenbergi, C. robertsonianus, Cibicidoides sp.,*) and deeper "cool" species *(Pyrgo murrhina, Globobulimina hoeglundi, Uvigerina peregrina Planulina wuellerstorfi*) (Figures 4, 5, 6 and 7).

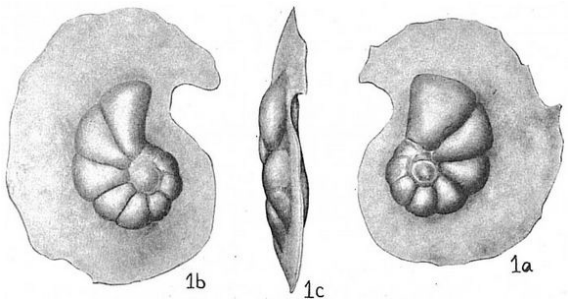

Figure 4. Views of *Laticarinina pauperata.*
1a. Spiral view; 1b. Umbilical view; 1c. Side view (Retired from Cushman, 1931).

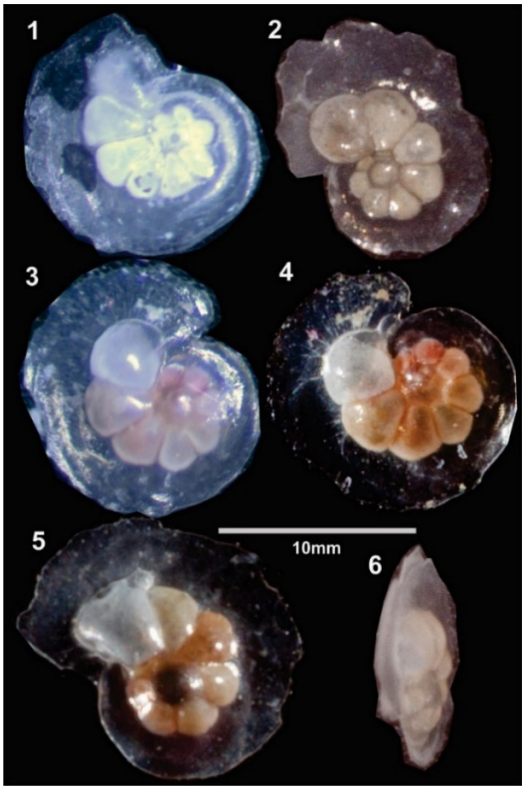

Figure 5. Different views of *Laticarinina pauperata*.
1. Spiral view of a Miocene form of *L. pauperata* found in 23 Mya. 2. Umbilical view of a modern dead specimen found in 1022.77 m depth. 3. Umbilical view of modern living specimen in 1022.77 m. 4. Umbilical view of modern living specimen in 3421 m depth. 5. Spiral view of a modern living specimen in 3421 m depth. 6. Side view of the modern dead specimen found in 3421 m depth.

 DOI: https://doi.org/10.30564/jms.v3i3.3516

Figure 6. Deep-water foraminiferal species

1. Planulina wuellerstorfi (Schwager, 1866) 363-U1482A-1Hcc; *2. Ceratobulimina jonesiana* (Brady 1881) 363-U1482A-1Hcc; *3. Oridorsalis umbonata* (Reuss, 1851) ventral view 363-U1482A-6Hcc; *4. Oridorsalis umbunata* (Reuss, 1851) 363-U1482A-6Hcc; *5. Gyroidinoides soldanii* (d'Orbigny 1826) 363-U1482A-7Hcc; *6. Pleurostomella brevis* (Schwager, 1866) 363-U1482A-7Hcc; *7. Uvigerina aculeata* (d'Orbigny 1839) 363-U1482A-7Hcc; *8. Uvigerina auberiana* (d'Orbigny 1839) 363-U1482A-7Hcc; *9. Rectuvigerina multicostata* (Cushman and Jarvis, 1929) 363-U1482A-15Hcc; 10. *Fissurina lacunata* (Burrows and Holland 1895) 363-U1482A-13Hcc; 11. *Pyrgo lucernula* (Schwager, 1866) 363-U1482A-15Hcc; 12. *Osangularia bengalensis* (Schwager, 1866) 363-U1482A-11Hcc

DOI: https://doi.org/10.30564/jms.v3i3.3516

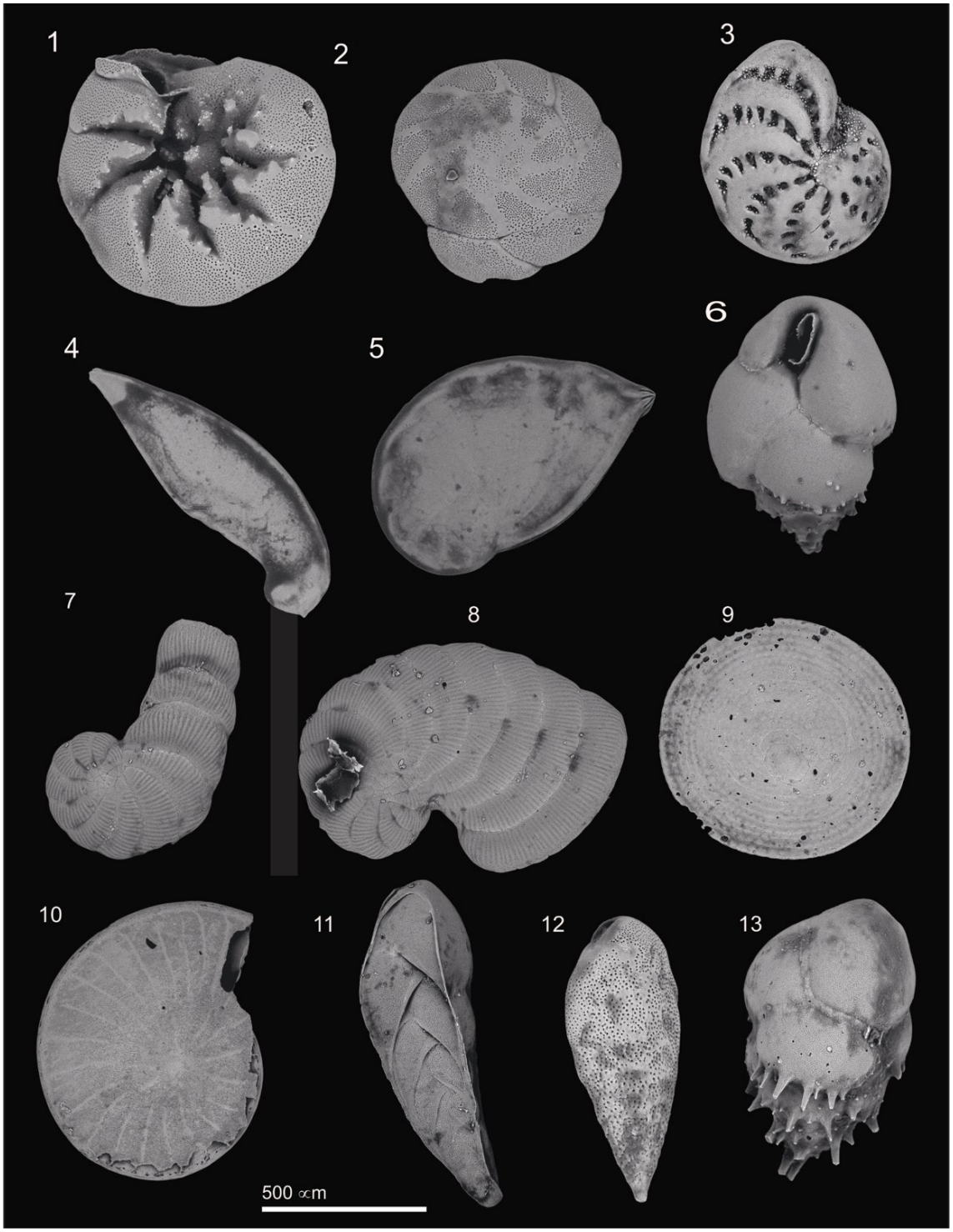

Figure 7. Shallow and reef-dwelling foraminiferal species

1. Rotalinoides compressiusculus (Brady 1884) (ventral view) 363-U1484A-15HCC; 2. *Rotalinoides compressiusculus* (dorsal view) 363-U1484A-15HCC; 3. *Elphidium advenum* (Cushman 1922) 363-U1484A-5HCC; 4. *Planularia australis* (Chapman 1915) 363-U1484A-8HCC; 5. *Planularia australis* (Chapman 1915) 363-U1484A-8HCC; 6. *Bulimina marginata* (D' Orbigny 1826) 363-U1484A-11HCC; 7. *Peneroplis planatus* (Fichtel and Moll 1798) 363-U1484A-15HCC; 8. *Coscinospira arietina* (Batsch 1791) 363-U1484A-15HCC; 9. *Amphisorus hemprichii* (Ehrenberg 1839) 363-U1484A-15HCC; 10. *Operculina complanata* (Defrance 1822) 363-U1484A-15HCC; *11. Bolivinita quadrilatera* (Schwager 1866) 363-U1484A-4HCC; *12. Bolivina robusta* (Brady 1881) 363-U1484A-4HCC; *13. Bulimina aculeata* (D' Orbigny 1826) 363-U1484A-3HCC

 DOI: https://doi.org/10.30564/jms.v3i3.3516

Sites 1482A and 1483A are in the hydrographic transition that divides the warm tropical water of the Indian-Pacific Western warm pool (IPWP) from the Subtropical water masses. They are located in an area affected by the oceanographic front between cool, nutrient-rich water transfer towards North in the Eastern Indian Ocean by the West Australian Current, and warm, oligotrophic Leeuwin Current waters, resulting in a steep north-south SST gradient. Together, these two sites located along the route of the Indian Through Flow (ITF) as it exits into the Indian Ocean through the Timor Strait between northwestern Australia and Java allow reconstruction of the southwestern extent of the IPWP since early late Miocene. The Timor Strait is one of the main exits of the ITF to the Eastern Indian Ocean [25]. Thus, U1482A and U1483A are easily located to facilitate monitoring changes in the intensity and thermal structure of ITF water masses entering the Eastern Indian Ocean [26].

In the southern reefal area of Abrolhos (BA, Brazil) [27] found *Laticarinina pauperata* in 1.100 m of water depth, and [28] used benthic foraminiferal biotas to track changes in the strength and seasonality of the monsoons. During the dry boreal winter monsoon with northeasterly winds, low biological productivity in the Indian Ocean provides low food to deep-sea fauna. As opposed to the intense, wet, southwesterly winds of the southwest (boreal summer) monsoon cause widespread upwelling and high surface productivity [29,30], and therefore a high supply of organic particles to the seafloor. This monsoon-linked productivity is large in the Arabian Sea, and in the Bengal Bay, as seen in satellite images collected by the Coastal Zone Color Scanner and SeaWIFS (http://bluefin.gsfc.nasa.gov/chi/level3.pl). Deep-sea benthic foraminifera are responsive to total export flux of food to the seafloor and seasonality [31-34].

Laticarinina pauperata is from cool, strongly pulsed high seasonality, low to intermediate organic flux sites [28]. In according to the Encyclopedia of life, its chronostratigraphic ranges from Mioceno to Recent; its evolution and systematics show first appearance for older bound is at 28.1 Mya (Chattiano Age), and the first appearance for younger bound is 23.03 Mya (Aquitaniano Age). The last appearance (older bound) is at 3.6 Mya (Piacenziano Age), and the last appearance (younger bound) is at 2.59 Mya (Gelasiano Age). This species lives in all mudlines of the nine cores and it has defined limits of appearances in the past. The environmental ranges for modern habitat are wide for depth (m): 0 - 3100, temperature (°C): -1.260 - 29.191, nitrate (umol/L): 0.038 - 42.384, salinity (PSU): 31.836 - 36.672, oxygen (ml/l): 0.206 - 7.696, phosphate (umol/l): 0.047 - 3.105, and silicate (umol/l): 1.067 - 125.649 showing species' tolerance.

Among the benthic indicator species studied, *Laticarinina pauperata* [35] is unique by its beautiful appearance, cosmopolitan, calcareous epifaunal foraminifera species [36] with biconvex trochospiral form being common in bioturbated horizons [37]. The presence of these specimens under this huge physical pressure is amazing. Can you imagine 3000 m of water plus 500 m of sediment? Can you imagine the sum of perpendicular force put in to the surface of this species per area? The pressure a liquid applies depends on its depth. This pressure in open conditions is approximated as in "static" or non-moving conditions (even in the moving ocean), because the currents and waves generate only insignificant changes in the pressure. Besides that, foraminiferal tests can suffer taphonomic process known as diagenesis, where sediments are compacted and buried under layers of sediment and stick to minerals that precipitate.

Here we show that preserved foraminifera were able to contribute to paleoceanographic reconstructions of at least 11 glacial and interglacial cycles correlated with depths from late Oligocene to Recent showing that foraminiferal fluctuations track tropical and subtropical fronts, in the Miocene, and that besides the delicate *Laticarinina pauperata* morphology it has great tolerance to physical pressure and is a remarkable paleo indicator.

6. Conclusions

Excellent preserved microfossils with scarce evidence of mineral overgrowth, recrystallization and abraded shells, show that the sedimentological setting with varying amounts of facies and foraminiferal forms from different paleo depth are very suitable for this research. Sites composed of nannofossil ooze with different amounts of siliceous microfossils (diatoms and radiolarians), and clay ranging from the Miocene to Recent day, are dominated by foraminifers calcareous species and less than 5% of the assemblages is composed by agglutinated forms. A mixed fauna shows alterations in the middle Pleistocene to Recent present terrigenous and hemi pelagic sediment with well-preserved calcareous nannofossils, benthic and planktonic foraminifers which unravels habitat transition in down core catchers' samples. The habitat change observed downhole show that deeper water benthic foraminifers inhabits upper and lower parts of the core; while middle part of the core consists of a mix of deep and shallow water benthic foraminifers, including reef-dwelling species in a 1000 m deep, including *Operculina complanata, Amphisorus hemprichii, Coscinospira arietina,* and *Peneroplis planatus*. These species are

DOI: https://doi.org/10.30564/jms.v3i3.3516

characteristic of water depths shallower than 45 m, and probably were carried to this site with other debris.

The presence of deep-water and cool forms without any large contribution from shallower water or reef faunas in a high abundant volcanic ash environment is also a new finding. Our low-resolution study of the relation of WBF shows that with the exception of core 1486B, all of them show that older sediments indicate warmer periods than today, a tendency of what is expected from Miocene to Recent.

The excellent preservation and the remarkable physical tolerance that species present to higher physical pressure from water column and sediment provided data on at least 11 glacial and interglacial cycles from different cores. These cycles correlated well in all depths with occurrence from late Oligocene (~24 million years ago) to Recent were evidenced by WBF fluctuations recorded by the shallower warm benthic species (*Cibicidoides* sp.*, Laticarinina pauperata, Cibicidoides kullenbergi, C. robertsonianus, Bulimina aculeata, Hoeglundina elegans*) and deep-water cool species (*Uvigerina peregrina, Pyrgo murrhina, Globobulimina hoeglundi, Planulina wuellerstorfi*). *Laticarinina pauperata* is unique by its beautiful and delicate appearance, but it is also an excellent calcareous epifaunal foraminifer from strongly pulsed, high seasonality, cool, low to intermediate organic flux, ranging from Mioceno to Recent. It is also living these days in all mudlines of the nine cores that we collected and we show that this form is common in bioturbated horizons and tolerant to high physical pressure. In addition, taphonomic process known as diagenesis can prevent the studies by destroying the tests through time, and our findings were able to unravel many interesting information because of the tolerance and preservation of the shells.

Acknowledgements

This article used samples collected by the Ocean Drilling Program (ODP) and provided by the International Ocean Discovery Program (IODP), sponsored by the U.S. National Science Foundation (NSF) and participating countries. We are thankful for the Project Geohazards and Tectonics (CAPES Grant 88887.091714/2014-01, IODP Program). Research was also supported by IODP/CAPES Brazil fellowship granted to PE to go aboard the Research Vessel Joides Resolution in 2016. This research would not have been conduct without funding from Ciências do Mar II (CAPES Coordenação de Aperfeiçoamento de Pessoal de Nível Superior) through the Project Processos oceanográficos na quebra da plataforma continental do nordeste brasileiro: fundamentos científicos para o planejamento espacial marinho (n°43/2013, 23038.004320/2014-11) through for the Post-Doc Fellowship for Eichler at the Moss Landing Marine Laboratories of the San Jose State University (MLML/SJSU), and at the Ocean Sciences Department of the University of California at Santa Cruz (UCSC) (grants Nº88887.305531/2018-00, Nº88881.188496/2018-01). We are also grateful for the International Ocean Discovery Program (IODP) in the Texas A&M University (USA) (Grant Nº9999.000098/2017-05) and to the Technical Support to Strengthen National Palaeontology (Apoio Técnico para Fortalecimento da Paleontologia Nacional, Ministério da Ciência e Tecnologia MCTI/National Research Council CNPq Nº 23/2011, Nº 552976/2011-3) for funding opportunity. We are grateful for the EcoLogicProject for the manuscript detailed editing.

References

[1] Debenay, J.P., Geslin, E., Eichler, B.B., Duleba, W., Sylvestre, F. and Eichler, P., (2001). Foraminiferal assemblages in a hypersaline lagoon, Araruama (RJ) Brazil. The Journal of Foraminiferal Research, 31(2), pp.133-151.

[2] Hallock, P., 1984. Distribution of selected species of living algal symbiont-bearing foraminifera on two Pacific coral reefs. The Journal of Foraminiferal Research, 14(4), pp.250-261.

[3] Hallock, P., 2000. Larger foraminifera as indicators of coral-reef vitality. In Environmental micropaleontology (pp. 121-150). Springer, Boston, MA.

[4] A'ziz, A.N.A., Minhat, F.I., Pan, H.J., Shaari, H., Saelan, W.N.W., Azmi, N., Manaf, O.A.R.A. and Ismail, M.N., 2021. Reef foraminifera as bioindicators of coral reef health in southern South China Sea. Scientific Reports, 11(1), pp.1-13.

[5] Murray,J. 2006. Ecology and Applications of Benthic Foraminifera. xi + 426 pp. Cambridge, New York, Melbourne: Cambridge University Press.

[6] Allen, S. 2010. Environmental controls and distributions of surface foraminifera from the Otter estuary salt marsh, UK: their potential use as sea level indicators. Plymouth Student Scientist 4, 293-324.

[7] Eichler, P.P.B., Eichler, B.B., de Miranda, L.B. and Rodrigues, A.R., 2007. Modern foraminiferal facies in a subtropical estuarine channel, Bertioga, São Paulo, Brazil. The Journal of Foraminiferal Research, 37(3), pp.234-247.

[8] Eichler, P.P., Billups, K. and Cardona, C.C.V., 2010. Investigating faunal and geochemical methods for tracing salinity in an Atlantic coastal lagoon, Delaware, USA. The Journal of Foraminiferal Research, 40(1), pp.16-35.

 DOI: https://doi.org/10.30564/jms.v3i3.3516

[9] Horton, B.P. and Murray, J.W., 2007. The roles of elevation and salinity as primary controls on living foraminiferal distributions: Cowpen Marsh, Tees Estuary, UK. Marine Micropaleontology, 63(3-4), pp.169-186.

[10] Eichler, P.P., Billups, K., Vital, H. and De Moraes, J.A., 2014. Tracing thermohaline properties and productivity of shelf-water masses using the stable isotopic composition of benthic foraminifera. The Journal of Foraminiferal Research, 44(4), pp.352-364.

[11] Martins, M.V.A., Moreno, J.C., Miller, P.I., Miranda, P., Laut, L., Pinheiro, A.E.P., Yamashita, C., Terroso, D.L., Rocha, F., Bernardes, C., 2017. Biocenoses of benthic foraminifera of the Aveiro Continental Shelf (Portugal): influence of the upwelling events and other shelf processes. Journal of Sedimentary Environments, 2 (1): 9-34.

[12] Carson, B. E., Francis, J. M., R. M. Leckie, A. W. Droxler, G. R. Dickens, S. J. Jorry, S. J. Bentley, L. C. Peterson, and B. N. Opdyke, 2008. Benthic foraminiferal response to sea level change in the mixed siliciclastic-carbonate system of southern Ashmore Trough (Gulf of Papua), J. Geophys. Res., 113, F01S20.
DOI: 10.1029/2006JF000629.

[13] Lutze, G. F., 1977. Neogene benthonic foraminifera from Site 369, Leg 41. In Lancelot, Y., Seibold, E., et al., Initial Reports of the Deep Sea Drilling Project, v. 41: Washing-ton (U.S. Government Printing Office), p. 659-666.

[14] Lutze, G.F. 2007. Benthic Foraminifers at Site 397: Faunal Fluctuations and Ranges in the Quaternary. doi:10.2973/dsdp.proc.47-1.111.1979DSDP Volume XLVII Part 1.

[15] Fedorov A.V., Philander, S.G. 2000. Is El Nino Changing? Science, 288: 1997-2002.Rasmusson, E.M., and Arkin, P.A., 1993. A global view of large-scale precipitation variability. Journal of Climate, 6(8):1495-1522.

[16] Pierrehumbert, 2000. Climate change and the tropical Pacific: the sleeping dragon wakes, Proc. Natl. Acad. Sci. U.S.A., 97(4): 1355-1358.

[17] Rasmussen, E.M., and Arkin, P.A., 1993. A global view of large-scale precipitation variability. Journal of Climate, 6(8):1495-1522.

[18] Billups, K. Eichler, P. P. B., Vital H. 2020. Sensitivity of Benthic Foraminifera to Carbon Flux in the Western Tropical Pacific Ocean. Journal of Foraminiferal Research; 50 (2): 235-247.
DOI: https://doi.org/10.2113/gsjfr.50.2.235.

[19] Rosenthal, Y., Holbourn, A., Kulhanek, D.K., and the Expedition 363 Scientists, 2017. Expedition 363 Preliminary Report: Western Pacific Warm Pool. International Ocean Discovery Program. http://dx.doi.org/10.14379/iodp.pr.363.2017.

[20] Morkhoven, F.P.C.M. Van, Berggren, W.A. and Edwards, A.S. 1986. Cenozoic cosmopolitan deep-water benthic foraminifera, Bulletin des Centres de Recherches Exploration-Production Elf-Aquitaine. Mémoire., v.11, p.421.

[21] Holbourn, A., Kuhnt, W., Schulz, M. and Erlenkeuser, H., 2005. Impacts of orbital forcing and atmospheric carbon dioxide on Miocene ice-sheet expansion. Nature, 438(7067), pp.483-487.

[22] Jones, R.W. 1994. The Challenger Foraminifera. Oxford University. Press, Oxford, ix+149pp.

[23] Fedorov, A.V., Brierley, C.M., Lawrence, K.T., Liu, Z., Dekens, P.S., Ravelo, A.C. 2013. Patterns and mechanisms of early Pliocene warmth. Nature: 496(7443): 43-49.
DOI: 10.1038/nature12003.

[24] Pearson, P.N., Ditchfield, P.W., Singano, J. and Harcourt-Brown, K.G., 2001. Warm tropical sea surface temperatures in the Late Cretaceous and Eocene epochs. Nature, 413(6855), p.481.

[25] Vranes, K. and Gordon, A.L., 2005. Comparison of Indonesian throughflow transport observations, Makassar Strait to eastern Indian Ocean. *Geophysical Research Letters, 32*(10).

[26] Xu, J., Holbourn, A., Kuhnt, W., Jian, Z. and Kawamura, H., 2008. Changes in the thermocline structure of the Indonesian outflow during Terminations I and II. Earth and Planetary Science Letters, 273(1-2), pp.152-162.

[27] Oliveira-Silva, P., Barbosa, C. F. and Soares-Gomes, A. "Distribution of macrobenthic foraminifera on brazilian Continental margin between 18ºS-23ºS." Revista Brasileira de Geociências 35.2 (2016): 209-216.

[28] Gupta, A. K., and Thomas, E. 2003. Initiation of Northern Hemisphere glaciation and strengthening of the northeast Indian monsoon: Ocean Drilling Program Site 758, eastern equatorial Indian Ocean. *Geology* 31.1 (): 47-50.

[29] Banse, K. and English, D.C., 1994. Seasonality of coastal zone color scanner phytoplankton pigment in the offshore oceans. Journal of Geophysical Research: Oceans, 99(C4), pp.7323-7345.

[30] Gregg, W.W. and Conkright, M.E., 2002. Decadal changes in global ocean chlorophyll. Geophysical Research Letters, 29(15), pp.20-1.

[31] Murray, J.W. and Smart, C.W., 1994. Distribution of

  DOI: https://doi.org/10.30564/jms.v3i3.3516

smaller benthic foraminifera in the Chagos Archipelago, Indian Ocean. Journal of micropalaeontology, 13(1), pp.47-53.

[32] Jannink, N.T., Zachariasse, W.J. and Van der Zwaan, G.J., 1998. Living (Rose Bengal stained) benthic foraminifera from the Pakistan continental margin (northern Arabian Sea). Deep Sea Research Part I: Oceanographic Research Papers, 45(9), pp.1483-1513.

[33] Loubere, P. and Fariduddin, M., 1999. Benthic foraminifera and the flux of organic carbon to the seabed. In Modern foraminifera (pp. 181-199). Springer, Dordrecht.

[34] Ohkushi, K.I., Nemoto, N., Murayama, M., Nakamura, T. and Tsukawaki, S., 2000. Paleoceanography of the Oyashio Area during the Last 20, 000 Years Based on Benthic Foraminifera. The Quaternary Research (Daiyonki-kenkyu), 39(5), pp.427-438.

[35] Parker, K.W. and Jones, R.T., 1865. VI. On some foraminifera from the North Atlantic and Arctic Oceans, including Davis Straits and Baffin's Bay. Philosophical transactions of the Royal Society of London, (155), pp.325-441.

[36] Corliss, B.H. and Chen, C., 1988. Morphotype patterns of Norwegian Sea deep-sea benthic foraminifera and ecological implications. Geology, 16(8), pp.716-719.

[37] King, S.C., Kemp, A.E., Murray, J.W., 1995. Benthic foraminifer assemblages in Neogene laminated diatom ooze deposits in the eastern equatorial Pacific Ocean (Site 844). In: Mayer, L.A., Pisias, N.G., Janecek, T.R., Palmer-Julson, A., van Andel, T.H. (Eds.), Proc. Ocean Drill. Prog, Sci. Results vol. 138, 665 - 673.

 DOI: https://doi.org/10.30564/jms.v3i3.3516

BILINGUAL PUBLISHING CO.
Pioneer of Global Academics Since 1984

Journal of Marine Science
https://ojs.bilpublishing.com/index.php/jms

ARTICLE

Hydrogeological and Hydrochemical Characterization of Coastal Aquifers with Special Reference to Submarine Groundwater Discharge in Uttara Kannada, Karnataka, India

B. K Purandara[1*] Sudhir Kumar[2] N Varadarajan[1] Sumit Kant[1] J V Tyagi[2]

1. National Institute of Hydrology, HRRC, VV nagar, Belagavi, Karnataka, India
2. National Institute of Hydrology, Jal Vigyan Bhavan, Roorkee, Uttarakhand, India

ARTICLE INFO

Article history
Received: 19 July 2021
Accepted: 9 August 2021
Published Online: 10 August 2021

Keywords:
Groundwater recharge
Submarine groundwater recharge
Aquifers
Hydraulic properties
Hydrochemistry

ABSTRACT

In coastal areas of our country, in spite of having excess rainfall (more than 3000 mm), groundwater become a rare commodity during summer. Number of researchers have discussed the issues related to water scarcity of coastal areas where there is a huge pressure on environment due to increased population, tourism, agriculture and industrial growth. Fast depletion of groundwater is also reported in coastal districts due to continuous discharge of direct runoff and also through subterranean flow which is termed as Submarine Groundwater Discharges (SGD). Large quantity of contaminants enter the ocean system through runoff. This necessitated a detailed investigation to understand the hydrological processes involved and the source of contaminants. The present investigation is an attempt to make quantitative and qualitative assessment of SGD based on hydrological, hydrogeological and hydrochemical components. Accordingly, water balance components were evaluated based on hydrological and hydrogeological investigations. Hydrochemical parameters were also evaluated to understand the impact of seawater intrusion in pre and post-monsoon of 2019. Study revealed that, there are signatures of considerable quantity of submarine groundwater discharge in parts of Honnavara, Kumta, Ankola and Karwar talukas. The influence of seawater in coastal aquifers is quite rare all along the coast of Uttara kannada district which is attributed to high groundwater recharge (15-20%) occurring in catchment areas.

1. Introduction

Management of water along the coastal zone of India, has been a matter of great concern to the administrators and policy makers, in spite of having some of the most potential aquifer systems in the region. However, major part of the aquifers particularly the Tertiary to Recent ones are highly exploited and needs well defined scientific approach to resolve the issues related to overexploitation and pollution of water bodies. The problems associated are primarily due to rapid urbanization, industrialization, infrastructure development and climatic uncertainties that seriously affects the spatio-temporal distribution of water. Along the coastal tracts, there is a continuous interaction between groundwater and seawater either leading to seawater intrusion or submarine groundwater

**Corresponding Author:*
B. K Purandara,
National Institute of Hydrology, HRRC, VV nagar, Belagavi, Karnataka, India;
Email: purandarabekal@gmail.com

DOI: https://doi.org/10.30564/jms.v3i3.3476

discharge [1]. Surface water inputs are through rivers and streams and discharge a large quantity of water received from the catchment and hence, the contribution of surface water discharge to the ocean, its hydrodynamics, geochemical cycles of elements and its influence on the ocean ecosystem has been well recognised [2]. On the contrary, groundwater discharge typically has a smaller water flow rate compared to river flow and hence not well demarcated.

Most of the studies conducted in the coastal region are focused on water quality aspects and radon concentration and for some of the studies in East coast, barium and strontium were also applied [3-5]. A detailed study was conducted using hydrogeological modelling to quantify SGD from the coastal aquifers of Vizhinjam (Kerala) [6]. According to the various studies conducted in India and elsewhere, the primary factors that influence the discharge of groundwater into adjoining oceans is due to water table fluctuations resulting from variations in recharge, pumping rate, tidal surges and transmissivity of the aquifers.

2. Methodology

2.1 Study Area

The coastal district of Uttara Kannada lies between north latitudes, 13^0 55' 02" to 15°31' 01" and east longitudes 74°00´35" to 75°10´23" (Figure 1). Study area is mainly covered by lateritic soils with underlying geological formation which include Pre-cambrians (Dharwar Super group) dominated by granitic gneisses, schists, greywackes and phyllites. There are basically two types of aquifers encountered in the study area, namely confined and unconfined aquifers. Ground water occurs under unconfined condition in alluvium, laterite soil cover and weathered crystalline rocks like granites, basic rocks and Deccan traps. Confined layers located at deeper depth which includes shear zones, fractured and jointed crystalline rocks, iron ore and chert, kankar, sand and gravel.

In the present investigation, the following methodologies were adopted.

2.2 Estimation of Hydrological Components Using Soil and Water Assessment Tool (SWAT Model)

SWAT is a physically based, semi distributed river basin or watershed scale model [7,8] was applied to estimate the hydrological components such as Runoff, Evapotranspiration (ET) and Groundwater recharge.

2.3 In-situ Determination of Soil Hydraulic Properties

In-situ infiltration rate and saturated hydraulic conductivity (Ks) of the soils were determined by using

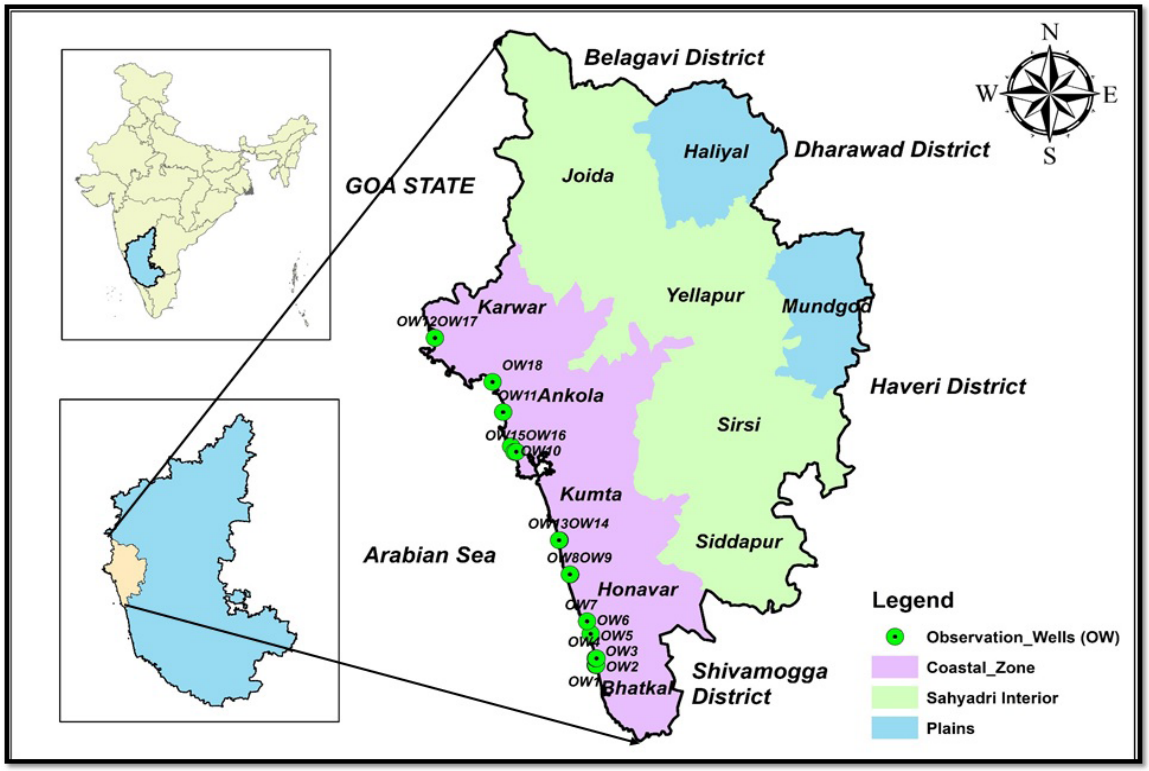

Figure 1. Uttara Kannada district

 DOI: https://doi.org/10.30564/jms.v3i3.3476

disc permeameter. Soil hydraulic parameters such as infiltration, sorptivity and saturated hydraulic conductivity were derived by the method developed by [9,10].

2.4 Geophysical Investigation

In the current study, using resistivity meter, VES (Vertical Electrical Sounding) soundings were taken in selected locations. Apparent resistivity were calculated by multiplying apparent resistance and geometric factor [11]. A log-log plot was drawn between apparent resistivity and half current electrode separation (AB/2). Curve-matching technique was applied (Schlumberger array master curve and auxiliary curves) to determine the layer resistivity values and thicknesses.

RESIST software was applied to estimate true geological section of the study area. The logged depths were compared with VES data using linear regression analysis.

2.5 Estimation of Groundwater Recharge by Empirical Methods

Groundwater Recharge was calculated using the following formula:

a) Chaturvedhi [12] derived an empirical equation to calculate groundwater recharge as.

$$Rg = 2(P-15)^{0.4} \quad (1)$$

Where, Rg is the Groundwater recharge and P is the annual precipitation.

(b) Krishna Rao [13] developed an empirical relation to calculate groundwater recharge based on climatic conditions.

$$Rg = K\,(P-X) \quad (2)$$

Where, Rg = groundwater recharge, K is constant (based on climatic homogeneity), P is annual precipitation (in mm), X is normal annual average rainfall zones, accordingly, the following equation was adopted. Rainfall recharge (Rr) = 0.35(P-600) for areas with rainfall more than 600 mm.

Physical parameters such as electrical conductivity, temperature and pH were measured using a handheld pH and Electrical conductivity meter (HANNA HI—9828, USA). Major anions such as bicarbonate, chloride, calcium, magnesium sodium and potassium were determined by the methods suggested by [14].

3. Results

3.1 Soil Characteristics

Soil profile investigations have been carried out in selected locations along the coast of Uttara kannada. Major soil types identified in the study area are leguminous laterites underlain by hard sandy clay to medium dense sandy layer. In some of the areas slightly weathered granites are the basement rocks. The soil types across the profile play a significant role in holding moisture content as well as it influences the groundwater recharge. Textural analysis of the soil showed that the soils between Murudeshwar and Honnavara are relatively more permeable than the adjoining northern taluks of Uttara kannada. Typical soil profile (approximate thickness of each layer is given in meters, m) observed along the Uttara kannada coast is presented in Figure 2.

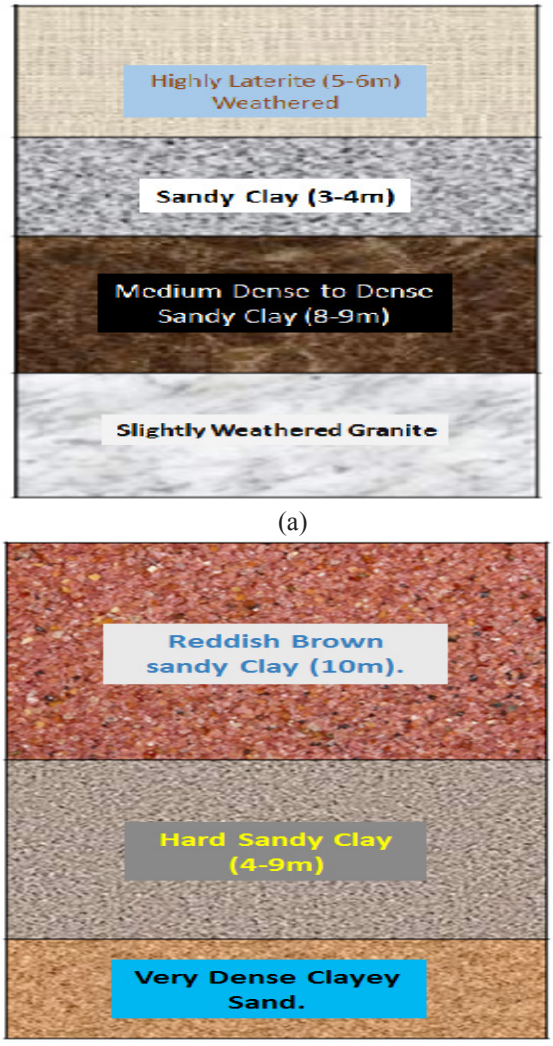

Figure 2. Soil Profile observed at Murudeshwar and Honnavara

Infiltration, sorptivity and saturated hydraulic conductivity were determined with reference to soil type and land use/land cover change. Rate of infiltration is significantly high in lateritic area covered with forests and

DOI: https://doi.org/10.30564/jms.v3i3.3476

acacia plantation. Highly weathered laterites were found in parts of Kumta and Ankola taluks. In Hattikeri, laterite cover exhibited very high infiltration rate and hydraulic conductivity (Table 1). This could be attributed to the land cover such as forest and acacia plantation which open up the top soil layers and influence the development of preferential flow paths leading to high groundwater recharge and pipe flow [15].

Three sets of resistivity data obtained through field investigations were plotted on log-log graph (Figure 3) for three different sections of the study area representing Q, H and K type curves.

Table 1. Range of Field determined Hydraulic properties of different soils along the coast of Uttara kannada

Sl No	Soil type along the coast	Infiltration rate mm/hr	Sorptivity mm/hr$^{-1/2}$	Saturated Hydraulic conductivity mm/hr
1	Laterite in forest catchment (Honnavar)	60 -192	**30-120**	**70-80**
2	Laterite in acacia plantation	120-175	**80-120**	**40-50**
3	Barren land (laterite cover)	12-24	**6-8**	**6-12**
4	Laterite (Hattikeri)	25-245	**10-130**	**85-120**
5	Beach sand with plantation (transitional zone between beach and land area)	70-280	**20-60**	**60-180**
6	Shrubs	28-76	**12-40**	**8-18**
7	Leguminous laterites	22-88	**0-4**	**6-14**
8	Clay dominated laterites	2 -18	**1-15**	**1-9**

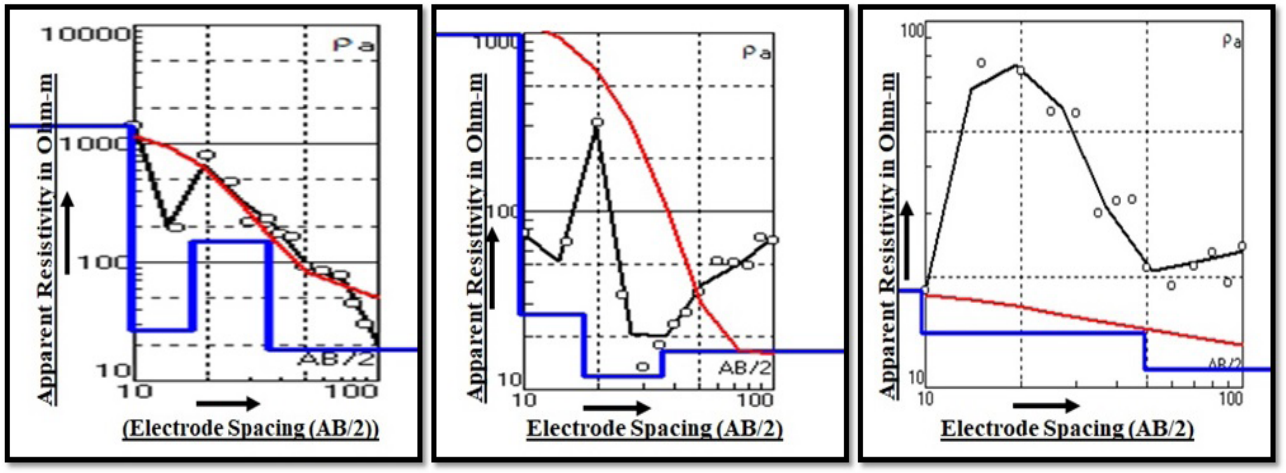

(a) (b) (c)

Figure 3. Typical Resistivity curves of the study area

a. Q Type (p1> p2> p3)

Figure 3a shows the cross-section of the coastal zone with varying apparent resistivity. This is the most common section found in hard lateritic terrain occupying the top layer.

b. H Type(p1> p2 <p3)

Figure 3b indicate the H-type curve with initial fluctuation and having relatively high resistivity at the top which is followed by a water saturated and weathered layers of low resistivity and then a compact hard rock of high resistivity at the bottom.

c. K-Type (p1> p2 >p3)

Though these types of curves (Figure 3c) are common in basaltic area, and in the present case, it indicates the fresh water zone between clay layer and saline zone.

The resistivity data were converted to 2D images and presented in Figures 4a, b & C. Comparison of the ERT image and field observations indicated reasonably good agreement. The profile up to 5m depth with a very low resistivity in range of 0.2 to more than 4000 Ωm has been observed which indicate the presence of the top soil and sand within the clay formation. The high resistivity values could be attributed to the extension of lateritic plateau in the deeper layer.

 DOI: https://doi.org/10.30564/jms.v3i3.3476

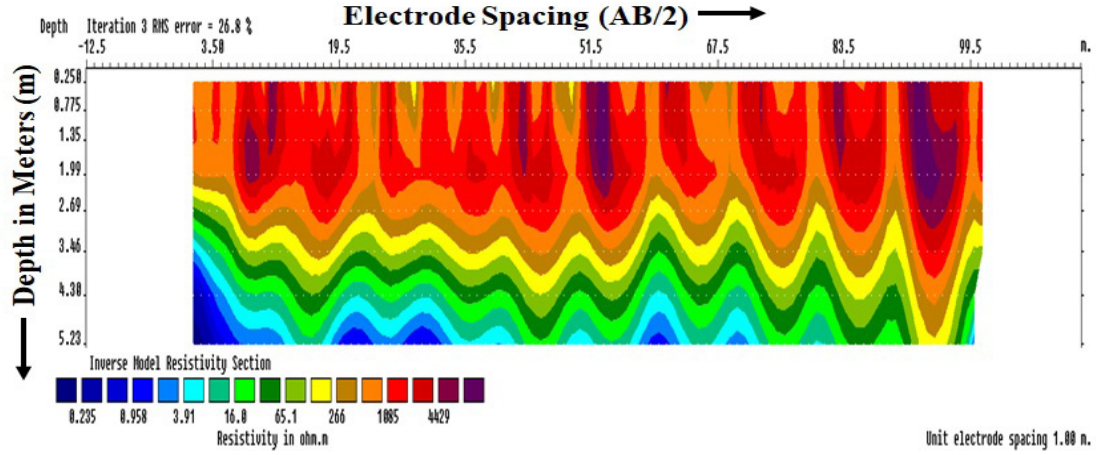

Figure 4a. ERT profile of Q -type curve

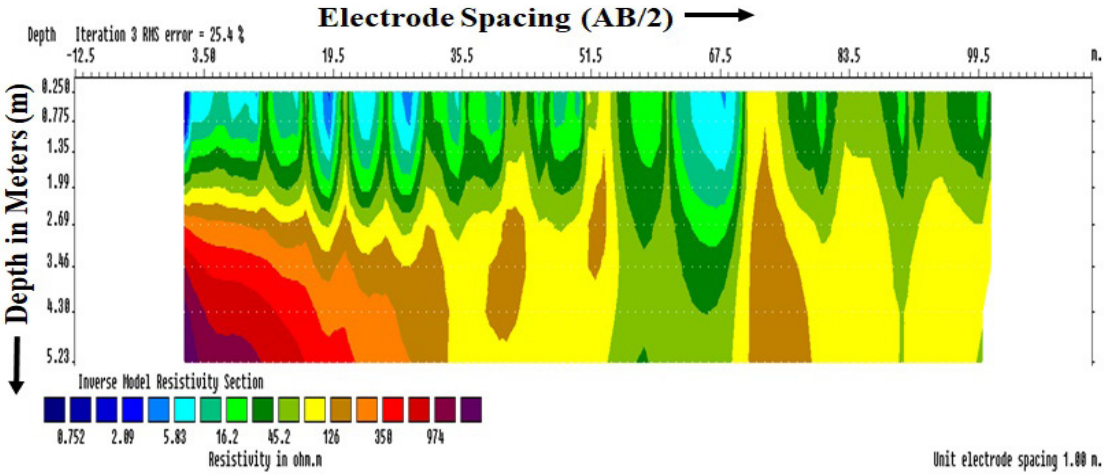

Figure 4b. ERT profile of H -type curve

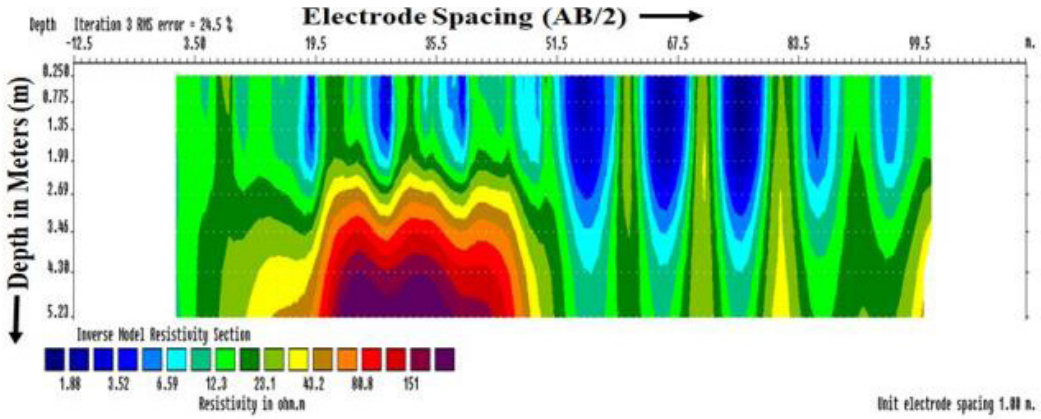

Figure 4c. ERT profile of K type curves

The occurrence of groundwater in the study area is found to vary with the depth of weathered layer and thickness of over burden. In major part of the district, well depth varied from 16 m to 47 m. Lithologically, the zone consists of fine to medium sand with alternative layers of silt and clay. Groundwater level data of thirty three wells monitored by Central Ground Water Board (CGWB) were analysed and found that the depths range from 89 to 200 meters with an effective porosity of about 1-3%. The transmissivity of aquifer material in general range from 2.09 to 24.41 m^2/day. The yield of the wells ranges between 1.88 and 2.25 lpm (litres per minute) and drawdown reported was 1.6 to 10.39 meters.

DOI: https://doi.org/10.30564/jms.v3i3.3476

Groundwater levels in the pre monsoon vary between 5 and 10 mbgl (metres below ground level) in 2017 and 2018. Low water table (less than 2 mbgl) was observed around Karwar town and towards southern part (Kumta and Ankola), water table showed fluctuation between 2 m and 5 m. In the coastal zone, groundwater levels range between -0.19 and 13.03 m. The maximum recorded was 13.15 m in Honnavar and negative fluctuation of -0.19 m was found in Murudeshwara.

Water balance components were estimated by using calibrated SWAT model (Table 2). Model was run for a representative watershed available in each taluka. It is observed that, the runoff estimated is higher for Kumta region whereas minimum was observed in Ankola. Groundwater recharge (shallow) was also found to be maximum in Ankola and Karwar tauka in comparison to other three talukas (Bhatkal, Honnavara and Kumta). Variation in runoff and recharge could be presumed due to increased deforestation followed by urbanization and conversion of forest land to agriculture (however, to conclude specific investigation is required). In all watershed of each taluka showed high lateral flow which is attributed to highly porous lateritic soils below moderately weathered laterites.

Table 2. Water Balance Components Estimated using SWAT Model

Water Balance Components	Bhatkal	Honnavar	Kumta	Ankola	Karwar
Surface Water	45.170	45.996	46.849	37.749	39.758
Groundwater	18.218	18.680	17.862	23.536	23.956
Lateral flow Q	4.503	3.917	3.471	4.128	4.513
Evapotranspiration (ET)	29.405	29.415	28.858	28.894	28.706

Recharge values estimated by SWAT model was also compared with that obtained from using empirical methods. Chaturvedi and Krishna Rao formulae showed a significant correlation between each other (Table 3).

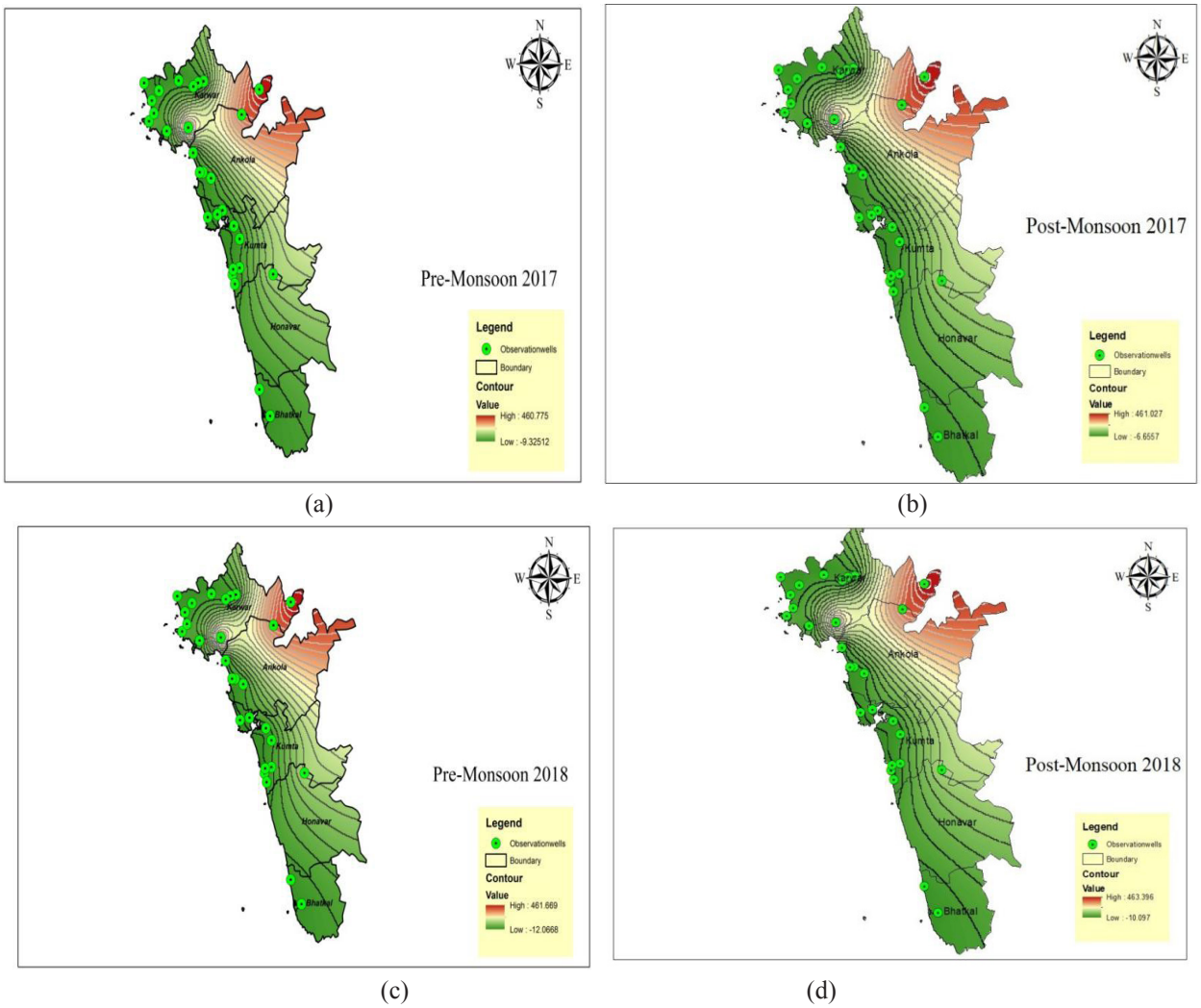

Figure 5(a to d). Groundwater levels of Uttara Kannada district

 DOI: https://doi.org/10.30564/jms.v3i3.3476

Table 3. Comparison of Estimated Ground Water Recharge using SWAT with Conventional methods

Year	Rainfall in mm	% Recharge By SWAT model	% Recharge (Chaturvedi)	% Recharge (Krishna Rao)
2002	2361.1	19.37	18.17	18.07
2003	2688.30	18.28	15.76	19.53
2004	2607.7	17.48	17.24	19.74
2005	3223.30	18.55	19.22	22.01
2006	3410.7	19.28	15.94	21.86
2007	3657.50	13.55	23.22	15.90
2008	3271.5	20.02	19.86	22.46
2009	3694.0	16.43	14.83	20.75
2010	4668.8	19.39	19.57	18.28
2011	4236	19.65	17.57	22.65
2012	3886.88	17.34	16.90	19.27

The above estimated recharge values demonstrate the applicability of SWAT model to the present study area.

3.4 Groundwater Quality Evaluation

Groundwater samples were collected during pre-monsoon and post-monsoon seasons of year 2019. Sixty two sites have been identified for water sampling and tested for physical parameters. Among the collected samples, based on the site characteristics, detailed analysis for both major anions and cations were carried out.

3.4.1 pH

pH is a primary indicator of water quality status of a surface or groundwater body. The pH in coastal aquifers of Uttara kannada, vary between 6.49m and 7.70m in premonsoon and 6.50m to 7.53m during post-monsoon. Acidic water is a characteristic of lateritic cover and alkaline water shows the human impact on water quality.

3.4.2 Electrical Conductivity and TDS

The EC values varied between 54.7 µmhos/cm and 5060 µmhos/cm during the pre-monsoon and 32 µmhos/cm to 3025 µmhos/cm during the post-monsoon (Figure 6 a & b). According to the classification of EC, 94% of the total groundwater samples fall under type I (low enrichment of salts) and the remaining 6% were grouped as type III indicating high enrichment of salts. Similar classification was adopted by [16].

Total dissolved solids showed a significant correlation with Electrical conductivity. TDS values varied from 31.6 mg/l to 2430 mg/l (pre-monsoon) and 17 mg/l to 1739 mg/l during post-monsoon. From the analysis it is evident that all water samples have low TDS which demonstrated the influence of rock-water interaction in relation to recharge

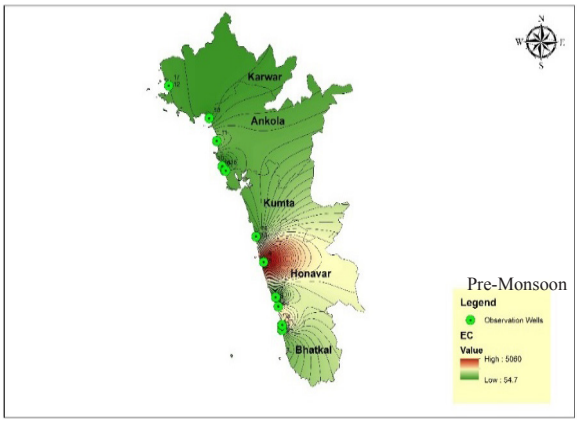

(a)

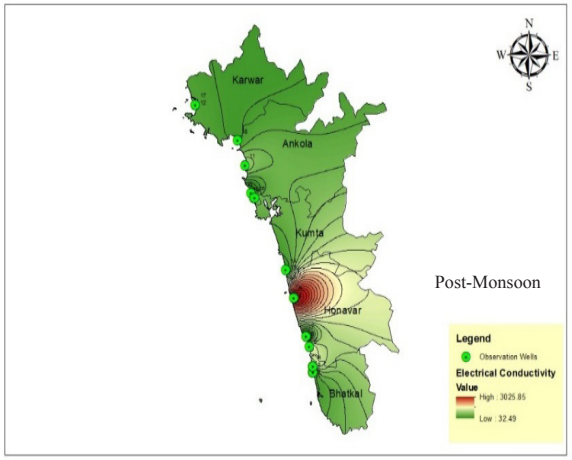

(b)

Figure 6 (a) & (b). Spatial Variation of EC during pre-monsoon and post-monsoon

water except for one well. The concentration of bicarbonate is observed from 70 to 520 mg/l during pre-monsoon and 46 to 414 mg/l during post-monsoon (Figure 7 a & b).

3.4.3. Chloride

The chloride content is found to vary between 19 and 1116 mg/l in pre-monsoon and 19 to 700 mg/l during post-monsoon (Figure 8 a & b). 83.3 % of the groundwater samples lie within the permissible limit whereas remaining 16.6 % were exceeding the permissible limits.

The concentration of Ca is between 17 mg/l and 244 mg/l, and Mg varied from 5 mg/l to 56 mg/l during pre-monsoon. In the post monsoon, Ca content vary between 10 mg/L and 166 mg/l, and concentration of Mg varied from 6 mg/l to 25 mg/l. Majority of the water samples collected from the study area fall under moderately hard to hard category during both pre and post-monsoon. The hardness values range from 22 mg/l to 260 mg/l with an average value of 157.1 mg/l during pre-monsoon. Similarly during post-monsoon the hardness values range from 16 mg/l to 186 mg/l with an average value

DOI: https://doi.org/10.30564/jms.v3i3.3476

of 117.7 mg/l. The concentration of Na varied from 3.09 to 85.5 mg/l during pre-monsoon (Figure 9a) and 0 to 81 mg/l during post-monsoon (Figure 9b). Na is the dominant ion among the cations and is present in most of the natural waters, which contribute approximately 53 to 69 % of the total cations.

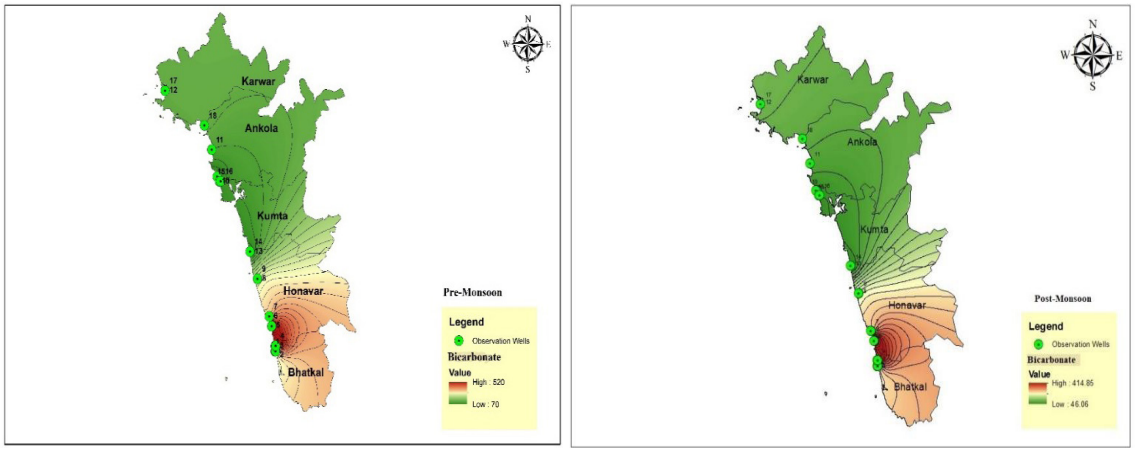

(a) (b)

Figure 7(a) & (b). Spatial variation of HCO_3 (pre and post monsoon)

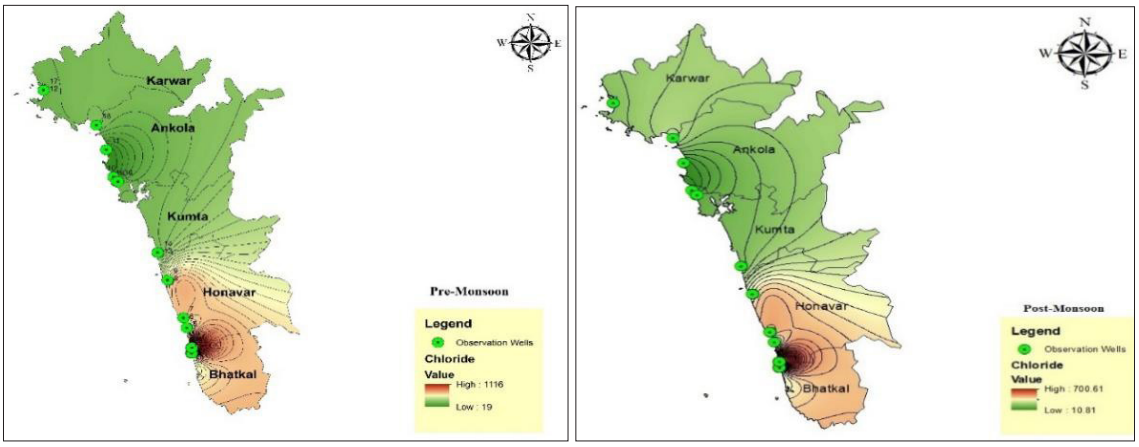

(a) (b)

Figure 8(a) & (b). Spatial variation of Chloride (pre and post-monsoon)

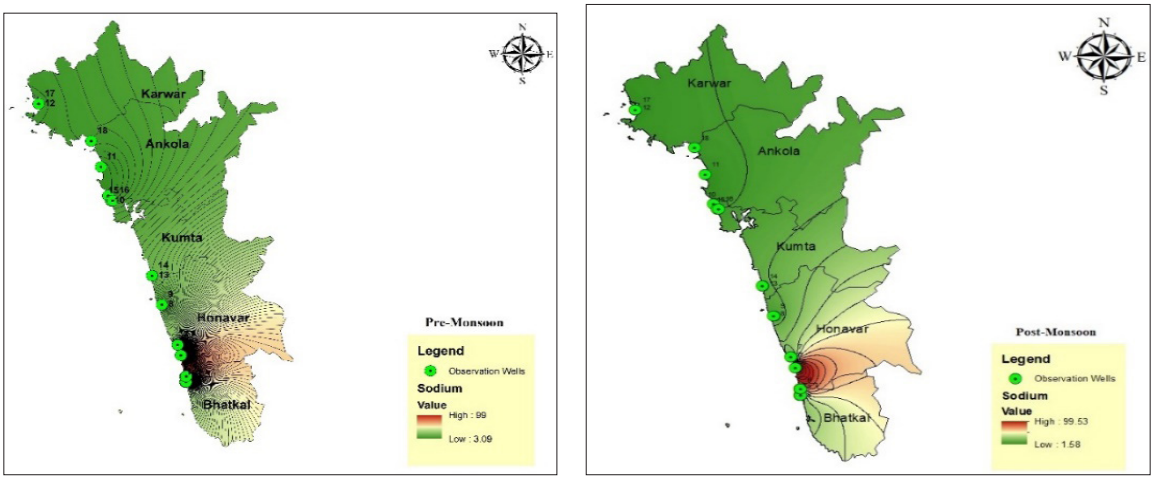

(a) (b)

Figure 9(a) & (b). Spatial Variation of Na during pre-monsoon and post-monsoon

 DOI: https://doi.org/10.30564/jms.v3i3.3476

3.4.4 Phosphorous

The phosphorous content observed during pre-monsoon varied between 0.46 mg/l and 1.82 mg/l. Analysis of post-monsoon water quality data showed that the concentration of P, vary from 0.37 mg/l to 1.60 mg/l.

3.4.5 Salinity

Salinity is the total amount of inorganic solid material dissolved in any natural water, and water salinization relates to an increase in TDS and overall chemical content of water. The salinity concentration in the study area ranges between 0.02 and 2.48 mg/l during pre-monsoon and 0.03 to 1.65mg/l during post-monsoon.

3.4.6 Sodium Adsorption Ratio

The analytical data plotted on the US salinity diagram [17] suggest that groundwater samples grouped in the domain of C1S1, C2S1, indicate water of low-medium salinity and low sodium, which can be utilized for irrigation in all types of soils. Few samples fall in the C3S2 domain with one sample exhibiting C4S2 type. At the outset, the study area can be classified as of good to moderate category irrespective of the rainfall seasons.

3.4.7 Permeability Index

In the present study, water suitability classification for irrigation developed by [18] has been adopted. The PI values vary from 18.65 to 345.92 (pre-monsoon) and in the post monsoon, PI values varied between 25.28 and 253.672. Accordingly, 88.88 % of the samples fall under the class 1 (PI >75) and 11.11 % of the samples fall under class 3 (PI< 25 %) during pre-monsoon period. However considerable variation was observed in post monsoon 2019. It was observed that 33.33 % of the samples fall under class 3 (PI >75) and 66.66 % belong to class 2 (PI ranged between 25 and 75 %).

A ratio namely index of magnesium hazard was developed by [19]. Magnesium hazard values fall in the range of 9.75 to 49.41 (pre-monsoon) and from 11.65 to 49.72 (post monsoon). All the samples showed MH ratio <50 % (suitable for irrigation) during pre-monsoon and post monsoon. The variation of Mg content is shown in Figure 10a & 10b.

3.4.8 Kelley Ratio

KR more than one is a sign of an excess level of sodium in waters and less than one, is an indication of suitability of water for irrigation. During both pre-monsoon and post-monsoon, KR values were less than one, indicating water is suitable for irrigation.

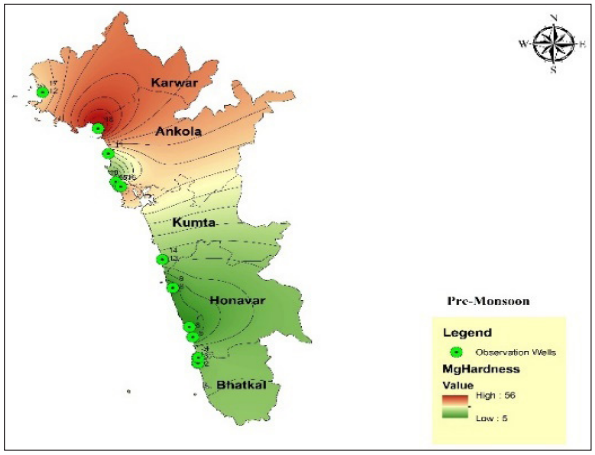

(a)

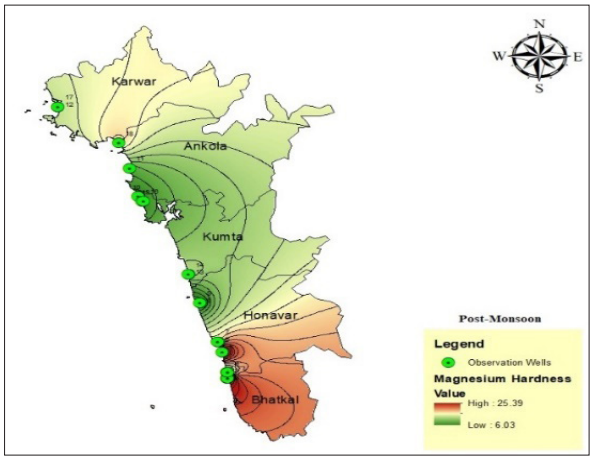

(b)

Figure 10(a) & (b). Spatial Variation of Mg during pre-monsoon and post-monsoon

3.4.9 Ionic Ratios

According to [20], EC alone cannot determine the salinity status of aquifers. Ionic ratios were used [21,22] to identify the source and nature of the salinity present. In the present study, $Cl/(HCO_3+CO_3)$, Kelly's ratio and permeability indices were used to understand the impact of seawater intrusion. $Cl/(HCO_3+CO_3)$ ratio which is also known as Simpson's ratio classify the groundwater into five category-good quality (< 0.5); slightly contaminated (0.5 - 1.3); moderately contaminated (1.3 - 2.8); highly contaminated (2.8 - 6.6); and extremely contaminated (6.6 - 15.5). Majority of the samples were found to be under good category except two samples which grouped as extremely contaminated during pre-monsoon and post-monsoon seasons.

4. Conclusions

Hydrogeological investigations have shown that the

DOI: https://doi.org/10.30564/jms.v3i3.3476

coastal aquifers of Uttara kannada do not show any signature of seawater intrusion as observed during the study period. From the study, it is understood that the recharge to groundwater is very high (15-20% of annual rainfall) due to which, the possibility of seawater intrusion become rare. However, there are chances of temporary phenomena which occur mainly due to advancement of sea towards the land during heavy monsoon causing enormous losses due to coastal erosion and fishery resources.

River flow characteristics of some of the rivers have been analysed based on the discharge data. Base-flow estimated indicate that, submarine groundwater discharge occurs during dry seasons mainly due to high rainfall (average rainfall more than 3000 mm) and high groundwater recharge. The estimated saturated hydraulic conductivity showed that the soils are highly permeable in lateritic areas, particularly below the top soil due to which the infiltrated water flows to sea continuously. From the present study, a rough estimate of about 0.15% to 0.18% of rainfall quantity enter the sea as submarine ground discharge from March to May. This is mainly based on monthly moisture trend which were observed at three sites and found a reasonably high moisture content in three locations namely, Murudeshwar, Kumta and north of Karwar taluks. Groundwater quality investigations carried out in more than thirty wells all along the coast also demonstrated that, the coastal aquifers are safe for drinking, irrigation and domestic purposes.

Acknowledgement

Authors are highly grateful to Ministry of Earth Sciences, New Delhi, Director (N-CESS, Thiruvananthapuram), and also to Dr. Suresh Babu, Scientist F and Head, Hydrological Sciences, N-CESS for their continuous support for carrying out the study. Central Ground Water Board is gratefully acknowledged for providing supporting data. Dr. B Venkatesh, Head, NIH, Hard Rock Regional Center, Belagavi is acknowledged for his encouragement. Mr. Ujval Utagi and Smt Vidya Arjun are thanked for their kind assistance provided at each stage.

References

[1] Burnett, W. C., Bokuniewicz, H., Huettel, M., Moore, W. S., and Taniguchi, M. Groundwater and pore water inputs to the coastal zone. *Biogeochemistry* 66 (2003) 3-33.
DOI: 10.1023/B:BIOG.0000006066.21240.53.

[2] Mulligan, A. E & Charette, M. A. Inter-comparison of submarine groundwater discharge estimates from a sandy unconfined aquifer. *J. Hydrol*. 327(2006) 411-425.
DOI: 10.1016/j.jhydrol.2005.11.056.

[3] Gopal Krishan, Someshwar Rao. M., Kumar, C P., Sudhir Kumar , Ravi Anand Rao, M. A study on identification of submarine ground water discharge in northern east coast of India Sci dir aquatic procedia 3-10 (2015).

[4] Moore, W. S. The effects of groundwater input at the mouth of the Ganges-Brahmaputra Rivers on barium and radium fluxes to the Bay of Bengal. Earth Planet. Sci. Lett. 150:141-50(1997).

[5] Taniguchi, M., Burnett, W. C., Cable, J. E., and Turner, J. V. Investigation of submarine groundwater discharge. *Hydrol. Process*. 16 (2002), 2115-2129.
DOI: 10.1002/hyp.1145.

[6] Suresh Babu, D.S., Anish, M., Vivekanandan, K. L., Ramanujam, N., Murugan, K.N., & Ravindran, A. A. An account of submarine groundwater discharge from the SW Indian coastal zone. Journal of Coastal Research, 25(1) (2009), 91-104. West Palm Beach (Florida), ISSN 0749-0208.

[7] Arnold, J. G., Srinivasan, R. Muttiah, S & Williams, J. R. Large-area hydrologic modeling and assessment: Part I. Model development. J. American Water Resour. Assoc. 34(1) (1998) 73-89.

[8] SWAT, Soil and Water Assessment Tool: SWAT model. College Station, Texas: Tex. A&M University. Available at: www.brc.tamus.edu/swat/soft_model.html. Accessed 21 February 2007.

[9] Perroux, K. M. and White, I. Designs for Disc permeameters. Soil Sci. Soc. Am. J., 52 (1988) 1205-1214.

[10] White, I. and Perroux, K. M. Use of sorptivity to determine field soil hydraulic properties. Soil Sci. Soc. Am. J., 51(1987) 1093-1101.

[11] Sharma, P. V. *Environmental and Engineering Geophysics*. Cambridge University Press. Cambridge. U.K. 474p (1997).

[12] Chaturvedi, R. S. A Note on the Investigation of Ground Water Resources in Western Districts of Uttar Pradesh. *Annual Report, U.P. Irrigation Research Institute, India (1973)*.

[13] Krishna Rao. Hydrometeorological aspects of estimating ground water potential. Seminar on ground water potential in hard rock areas, Bangalore. Geological Society of India., 1(1) (1970) 99.1-18.

[14] American Public Health Association. *Standard Methods for the Examination of Water and Wastewater*, American Public Health Association, Washington, D (2012).

[15] Putty, M R Y, VSRK and Ramaswamy, R. A study on

 DOI: https://doi.org/10.30564/jms.v3i3.3476

rainfall intensity pattern in Western Ghats, Karnataka. *In: proceedings of workshop on watershed development in Western Ghats*, February 2000. CWRDM, Kozhikode, Kerala, pp.44-55.

[16] Sarath Prasanth, S. V., Magesh, N. S., Jitheshlal, K. V., Chandrasekar, N. & Gangadhar, . 2012. Evaluation of groundwater quality and its suitability for drinking and agricultural use in the coastal stretch of Alappuzha District, Kerala, India, Applied Water Sciences, Vol. 2, pp:165-175.

[17] Richards, L.A. *Diagnosis and Improvement of Saline Alkali Soils, Agriculture, 160, Handbook 60.* US Department of Agriculture, Washington DC (1954).

[18] Doneen, L. D. Notes on water quality in agriculture. *In: Published in water science and engineering.* University of California, Davis (1964).

[19] Paliwal, K. V. Irrigation with saline water. *In: Monogram no. 2 (new series). IARI*, New Delhi (1972) pp 198.

[20] Revelle. Criteria for recognition of seawater in groundwater; Trans. Am. Geophys. Union 22 (1941) 593-597.

[21] Kim, J. H., Kim, R. H. & Chang, H. W. Hydrogeochemical characterization of major factors affecting the quality of shallow groundwater in the coastal area at Kimje in South Korea; Environ. Geol. 44 (2003) 478-489.

[22] Moujabber E L M, Bousamra B, Darwish T and Atallah T. Comparison of different indicators for groundwater contamination by seawater intrusion on the Lebanese coast; J. Water Resour. Manag. 20 (2006) 161-180.

DOI: https://doi.org/10.30564/jms.v3i3.3476

BILINGUAL PUBLISHING CO.
Pioneer of Global Academics Since 1984

Journal of Marine Science
https://ojs.bilpublishing.com/index.php/jms

EDITORIAL

Journal of Marine Science: An Open Framework Dedicated to the Presentation of the Discoveries and Insights in Marine Science Research

Eugen Rusu[1,2*]

1. Editor in Chief, Journal of Marine Science
2. Faculty of Engineering, "Dunărea de Jos" University of Galati, 800201, Galati, Romania

ARTICLE INFO

Article history
Received: 3 August 2021
Accepted: 4 August 2021
Published Online: 5 August 2021

Marine environment represents a very important and actual topic. Water bodies cover more than two thirds of the earth's surface and even after thousands of years, scientists have yet to fully uncover their mysteries. At the same time climate, change has visible effects with a growing dynamics in the last decades and the marine environment is very sensitive to these changes. In order to mitigate the effects of the climate change there is an increasing need of reducing the CO_2 emissions and from this perspective the marine environment represents an important source of clean renewable energy. In this respect, the *Journal of Marine Science* represented even from the beginning an open framework dedicated to the presentation of the discoveries and insights in marine science research.

If we refer only to this year, we can notice that in 2021 several valuable works have been published in Volume 3 of *Journal of Marine Science*. Thus, in the first issue, based on the incompressible RANS equation, the first work [1] presents a ship's resistance field's numerical simulation. The bare hull (calm water resistance and wave resistance) and hull-propeller rudder models are studied and compared with the values of the Hydrostatic resistance test. In the hull-propeller-rudder system's performance analysis, the body force method is used to replace the real propeller model. The new calculation domain is set for the hull-propeller-rudder system model and meshed again to obtain the highly reliable numerical simulation results. Further on, in [2] having as target the semi-enclosed basin of the Black Sea, the objective of the paper is to present an overview of its extensive physical features and circulation patterns. To achieve this goal, more than five decades of data analysis - from 1960 to 2015 - were taken into consideration and the results were validated against acknowledged data, both from satellite data over the last two decades and in-

**Corresponding Author:*
Eugen Rusu,
Editor in Chief, Journal of Marine Science; Faculty of Engineering, "Dunărea de Jos" University of Galati, 800201, Galati, Romania;
Email: eugen.rusu@ugal.ro

 DOI: https://doi.org/10.30564/jms.v3i3.3511

situ measurements from the first decades. Based on the perspective of marine tourism, in [3] various types of marine pollution are discussed as well as high-quality development solutions and future extension directions of marine tourism. Through the research, it is found that the main culprits of marine pollution mainly include the following seven points: human activities produce garbage; white pollution; ship pollution; exploration of marine oil and gas resources and mineral pollution highlighted. The causes of marine pollution and countermeasures are also discussed. Starting from the facts that red tides are a major public hazard in the global oceans and that the coast of the East China Sea is the sea area where red tide disasters are the most frequent and serious in China, [4] deals with these aspects. Thus, in order to accurately grasp the occurrence of red tides in the coastal waters of the East China Sea, and to understand the microbial communities in the waters during the occurrence of red tides in the East China Sea, a special survey of red tides in the coastal waters of Zhejiang, China which was carried out in June 2018 is described. Finally, the last paper of this issue, [5] presents a mass spectrometry-based sequencing of venom peptides (conotoxins) from vermivorous cone snail, conus loroisii. Conus loroisii is a marine vermivorous snail found profusely in the southern seas of India. They harbor several toxic peptide components commonly called as 'conotoxins'. In this study, the authors have identified and sequenced five conotoxins using proteome based tandem mass spectrometry analysis through Data analysis 4.1 software.

The second issue of Volume 3 contains also very interesting works. Thus, [6] presents a study related to thermal front variability during the El Nino Southern Oscillation (ENSO) in the Banda Sea using remotely sensed data. The Banda Sea is one of the routes of global ocean currents that move from the Pacific Ocean to the Indian Ocean. This flow is known as Indonesian Through Flow (ITF). The Banda Sea is an area where warm and cold water masses meet, so it has the potential for a thermal front. This study aims to understand the variability of thermal front in the Banda Sea during the El Nino Southern Oscillation period. Southern Oscillation Index (SOI) and sea surface temperature (SST) data in 2010, 2012 and 2015 were used in this study. Further on, [7] presents a study of the coastal vulnerability in Indramayu Regency, Indonesia. Coastal vulnerability is a condition of a coastal community or society that leads to or causes an inability to face the threat of danger. The level of vulnerability can be viewed from the physical (infrastructure), social, demographic, and economic vulnerabilities. Physical vulnerability (infrastructure) describes a physical condition (infrastructure) that is prone to certain hazardous factors. The coastal vulnerability areas can also be interpreted as a condition where there is an increase in the process of damage in the coastal area which is caused by various factors such as human activities and factors from the nature. This research aims to determine the level of coastal vulnerability in Indramayu coastal Regency with a Coastal Vulnerability Assessment (CVA) analysis approach and a Geographic Information System (GIS). Mapping the status of the vulnerability level of the Indramayu coastal area using the CVA method where the index range generated from the calculation of the four physical parameters mentioned above is between 2.887-3.651 or are in moderate vulnerability. In order to solve the technical problems of autonomous berthing of the Unmanned Surface Vehicle (USV), in [8] is presented a research that has met the requirements of manoeuvrability berthing under different conditions by effectively using the bow and stern thrusters, which is a technological breakthrough in actual production and life. Based on the MMG model, the manoeuvrability mathematical model of the USV with bow and stern thruster was established. And the motion simulation of USV manoeuvring was carried out through the numerical simulation calculation. Then the berthing plan was designed based on the manoeuvrability analysis of the USV low-speed motion, and the simulation of automatic berthing for USV was carried out. The research results of this paper can be of certain practical significance for the USV based on the support of the bow and stern thruster in the berthing. At the same time, it also provides a certain theoretical reference for the handling of the USV automatic berthing. [9] describes a hydrocarbon detection based on phase decomposition in Chaoshan Depression, Northern South China Sea. Located in the northern South China Sea, Chaoshan Depression is mainly a residual Mesozoic depression, with a construction of Meso-Cenozoic strata over 7000m thick and good hydrocarbon accumulation conditions. Amplitude attribute of -90°phase component derived by phase decomposition is employed to detect Hydrocarbon in the zone of interest (ZOI) in Chaoshan Depression. And it is found that there are evident amplitude anomalies occurring around ZOI. Phase decomposition is applied to forward modeling results of the ZOI, and high amplitudes occur on the -90°phase component more or less when ZOI is charged with hydrocarbon, which shows that the amplitude abnormality in ZOI is probably caused by oil and gas accumulation. Finally, in the last paper of this second issue, [10] a simulation of deep water wave climate for the Indian Seas is presented.

Finally, issue 3, which is still open for submissions,

DOI: https://doi.org/10.30564/jms.v3i3.3511

presents for now two interesting works. Thus starting from the fact that surfaces submerged in seawater are colonized by various microorganisms, resulting in the formation of heterogenic marine biofilms, [11] aims to evaluate the biofilm formation by Cobetia marina alex and doing a comparative study between this promising strain with the two bacterial strains isolated previously from the Mediterranean seawater, Alexandria, Egypt. Three strains; Cobetia marina alex, Pseudoalteromonas sp. alex, and Pseudoalteromonas prydzensis alex were screened for biofilm formation using the crystal violet (CV) quantification method in a single culture. The values of biofilm formed were OD600= 3.0, 2.7, and 2.6, respectively leading to their selection for further evaluation. However, factors affecting biofilm formation by C. marina alex were investigated. Biofilm formation was evaluated in single and multispecies consortia. Synergistic and antagonistic interactions proved in this work lead to the belief that these bacteria have the capability to produce some interesting signal molecules N-acyl Homoserine Lactones (AHLs). Finally, in [12] a study is presented about dragonflies as an important aquatic predator insect and their potential for control of vectors of different diseases.

The above mentioned articles constituting volume 3 made various analyses related to marine science issues. Finally, we strongly believe that the works included in this volume are useful for many scientists, researchers and industries working on marine issues. At this final point, it has to be also highlighted that the topics targeting marine sciences remain very actual, especially if we take into account the great expectations from the marine environment in short and medium term, expectations requiring very rapid scientific and technical advances while at the same time significant challenges have to be faced.

References

[1] Xie, H., Zhang B., 2021, Numerical Simulation of Resistance Field of Hull-Propeller-Rudder Coupling, *Journal of Marine Science*, Vol 3 (1), https://doi.org/10.30564/jms.v3i1.2506.

[2] Girleanu, A., Rusu, E., 2021, An Evaluation of the Main Physical Features and Circulation Patterns in the Black Sea Basin, *Journal of Marine Science*, Vol 3 (1), https://doi.org/10.30564/jms.v3i1.2552.

[3] Zheng, Y., Liu, D., 2021, Research on Marine Pollution Problems and Solutions in China from the Perspective of Marine Tourism, *Journal of Marine Science*, Vol 3 (1), https://doi.org/10.30564/jms.v3i1.2599.

[4] Huang, B., Wei, N., Hu, Y., Mao, H., 2021 Microbial Communities in Water during Red Tides along the Coast of China-A Case Study of Prorocentrum Donghaiense Red Tide in the East China Sea, *Journal of Marine Science*, Vol 3 (1), https://doi.org/10.30564/jms.v3i1.2622.

[5] Saleh Syed, H., Arun Kumar R., Masilamani Selvam, J. M., Rajesh R. P., Mass Spectrometry-based Sequencing of Venom Peptides (Conotoxins) from Vermivorous Cone Snail, Conus Loroisii: Toxicity of its Natural Venom, *Journal of Marine Science*, Vol 3 (1), https://doi.org/10.30564/jms.v3i1.2416.

[6] Fachruddin Syah, A., Sholehah, S., 2021, Thermal Front Variability during the El Nino Southern Oscillation (ENSO) in the Banda Sea Using Remotely Sensed Data, *Journal of Marine Science*, Vol 3 (2), https://doi.org/10.30564/jms.v3i2.2741.

[7] Waluyo, W., Fitrina Devi, A., Arifin, T., 2021, Study of the Coastal Vulnerability in Indramayu Regency, Indonesia, *Journal of Marine Science*, Vol 3 (2), https://doi.org/10.30564/jms.v3i2.2859.

[8] Wu, G., Zhao, X., Wang, L., 2021, Modeling and Simulation of Automatic Berthing based on Bow and Stern Thruster Assist for Unmanned Surface Vehicle, Journal of Marine Science, Vol 3 (2), https://doi.org/10.30564/jms.v3i2.2962.

[9] Zhong, G., Jiang, R., Yi, H., Wu, J., Feng, C., Zhou, G., Wang, K., Liu, L., Sun, M., 2021, Hydrocarbon Detection Based on Phase Decomposition in Chaoshan Depression, Northern South China Sea, Journal of Marine Science, Vol 3 (2), https://doi.org/10.30564/jms.v3i2.3063.

[10] Swain, J., Umesh, P. A., Baba, M., Murty, A. S. N., 2021, Simulation of Deep Water Wave Climate for the Indian Seas, Journal of Marine Science, Vol 3 (2), https://doi.org/10.30564/jms.v3i2.3126.

[11] Abouelkheir, S. S., Abdelghany, E. A., Sabry, S. A., Ghozlan, H. A., 2021, Biofilm Formation by Marine Cobetia marina alex and Pseudoalteromonas spp: Development and Detection of Quorum Sensing N-Acyl Homoserine Lactones (AHLs) Molecules, Journal of Marine Science, Vol 3 (3), https://doi.org/10.30564/jms.v3i3.3397.

[12] Vatandoost, H., 2021, Dragonflies as an Important Aquatic Predator Insect and Their Potential for Control of Vectors of Different Diseases, Journal of Marine Science, Vol 3 (3), https://doi.org/10.30564/jms.v3i3.3121.

 DOI: https://doi.org/10.30564/jms.v3i3.3511

About the Publisher

Bilingual Publishing Co. (BPC) is an international publisher of online, open access and scholarly peer-reviewed journals covering a wide range of academic disciplines including science, technology, medicine, engineering, education and social science. Reflecting the latest research from a broad sweep of subjects, our content is accessible world-wide——both in print and online.

BPC aims to provide an analytics as well as platform for information exchange and discussion that help organizations and professionals in advancing society for the betterment of mankind. BPC hopes to be indexed by well-known databases in order to expand its reach to the science community, and eventually grow to be a reputable publisher recognized by scholars and researchers around the world.

BPC adopts the Open Journal Systems, see on ojs.bilpublishing.com

Database Inclusion

Asia & Pacific Science Citation Index

Creative Commons

China National Knowledge Infrastructure

Google Scholar

Crossref

MyScienceWork

BILINGUAL
PUBLISHING CO.
Pioneer of Global Academics Since 1984

Tel:+65 65881289
E-mail: contact@bilpublishing.com
Website:ojs.bilpublishing.com

ISSN 2661-3239
03
9 772661 323217